TECHNO-ECONOMIC ANALYSIS OF A REVERSE OSMOSIS DESALINATION PLANT RUN BY PHOTOVOLTAICS FOR METU NCC

A THESIS SUBMITTED TO
THE BOARD OF GRADUATE PROGRAMS
OF
MIDDLE EAST TECHNICAL UNIVERSITY, NORTHERN CYPRUS CAMPUS

BY

IBRAHIM MOHAMED SHAABAN MOHAMED ABOUHASSANIN

IN PARTIAL FULFILLMENT OF THE REQUIREMENTS
FOR
THE DEGREE OF MASTER OF SCIENCE
IN SUSTAINABLE ENVIRONMENT AND ENERGY SYSTEMS PROGRAM

SEPTEMBER 2021

Approval of the Board of Graduate Programs

Prof. Dr Cumali Sabah
Chairperson

I certify that this thesis satisfies all the requirements as a thesis for the degree of Master of Science

Assoc. Prof. Dr. Ceren İnce
Derogar
Program Coordinator

This is to certify that we have read this thesis and that in our opinion it is fully adequate, in scope and quality, as a thesis for the degree of Master of Science.

Asst. Prof. Dr. Bengü Bozkaya Schrotter
Supervisor

Examining Committee Members (first name belongs to the chairperson of the jury and the second name belongs to supervisor)

Assoc. Prof. Dr. Murat Fahrioglu	METU NCC Electrical Engineering
Asst. Prof. Dr. Bengü Bozkaya Schrotter	METU NCC Chemical Engineering
Prof. Dr. Umut Türker	EMU Civil Engineering

I hereby declare that all information in this document has been obtained and presented in accordance with academic rules and ethical conduct. I also declare that, as required by these rules and conduct, I have fully cited and referenced all material and results that are not original to this work.

Name, Last name : Ibrahim Mohamed Shaaban Mohamed, Abouhassanin

Signature :

ABSTRACT

TECHNO-ECONOMIC ANALYSIS OF A REVERSE OSMOSIS DESALINATION PLANT RUN BY PHOTOVOLTAICS FOR METU NCC

Abouhassanin, Ibrahim Mohamed Shaaban Mohamed
Master of Science, Sustainable Environment and Energy Systems Program
Supervisor: Asst. Prof. Dr. Bengü Bozkaya Schrotter

SEPTEMBER 2021, 136 pages

Northern Cyprus has always depended on groundwater as the main source of domestic and irrigation water use. However, aquifers have been depleted faster than they have been recovering, resulting in a challenging water situation in Northern Cyprus. Recently built water pipeline from Turkey to Northern Cyprus has greatly resolved this issue. However, the recent breakdown of the pipeline and its climate-dependent source in Turkey has been the motivation of this study to evaluate other alternative sources for the island. Sea Water Reverse Osmosis (SWRO) is a desalination technology that can help Northern Cyprus solve the water problems it has been facing by making sea water drinkable or suitable for domestic and irrigation purposes in a most sustainable manner. The SWRO plant in this study will be providing 560 m^3/day of water for METU NCC and will be powered by photovoltaic solar panels with an energy recovery unit to improve efficiency by using the hydraulic power of the rejected brine. The model shows the economic feasibility of the SWRO plant by using the water consumption and weather data of METU NCC. The specific energy of desalinated water was found to be between 3.08 and 5.66 kWh/m^3 depending on the configuration. While the price of a cubic meter of produced water was found to be between 1.26 and 1.53 \$/m^3.

Keywords: Seawater desalination, LCOW, PV, TRNC

ÖZ

ODTÜ KKK'DA FOTOVOLTAIK ENERJI ILE ÇALIŞAN TERS OZMOZ TUZSUZLAŞTIRMA SISTEMININ TEKNO-EKONOMIK ANALIZI

Abouhassanin, Ibrhaim Mohamed Shaaban Mohamed
Yüksek Lisans, Sürdürülebilir Çevre ve Enerji Sistemleri
Tez Yöneticisi: Dr. Öğr. Üyesi Bengü Bozkaya Schrotter

Eylül 2021, 136 sayfa

Kuzey Kıbrıs, evsel su ve sulama suyu ihtiyacını çoğu zaman yeraltı suyundan karşılamıştır. Bununla birlikte, akiferler dolması gerektiklerinden daha hızlı tükenmiş ve bu da Kuzey Kıbrıs'ta gerçekten zorlu bir su yoksunluğuna neden olmuştur. Yakın zamanda inşa edilen Türkiye ve Kuzey Kıbrıs arasındaki su boru hattı, su sorununun çözülmesine büyük ölçüde yardımcı olmuştur. Ancak, boru hattının son zamanlarda arızalanması ve Türkiye'deki kaynağın iklime bağlı olarak değişebilecek olması, ada için diğer alternatif kaynakları değerlendirmek amacıyla bu çalışmaya motivasyon bulmuştur. Deniz suyu ters ozmoz (SWRO), Kuzey Kıbrıs'ın deniz suyunu içilebilir veya evsel sulama amaçlı olarak sürdürülebilir bir hale getirmek amacıyla su sorunlarını çözmeye yardımcı olabilecek bir tuzdan arındırma teknolojisidir. Bu projede öngörülen SWRO tesisi, ODTÜ KKK'ya günde 560 m^3 su tedarik etmekteyi amaçlamaktadır. SWRO sisteminin enerjisi PV panelleri ile sağlanacak olup, tesisin verimliliğinin enerji geri kazanım ünitesinin atılan tuzlu suyun hidrolik gücünü alması sayesinde arttırılması planlanmaktadır. Model, ODTÜ KKK'nın su kullanımı ve meteorolojik verilerini kullanarak SWRO tesisinin ekonomik geçerliliğini gösterecektir. Yapılan hesaplamalara göre arıtma prosesi için kullanılan özgül enerji konfigürasyona bağlı olarak 3,08 ile 5,66 kWh/m^3 arasında değişmektedir. Üretilen suyun metreküp fiyatı ise 1,26 ile 1,53 \$/m^3 arasında bulunmuştur.

Anahtar Kelimeler: Deniz suyu ters ozmoz, LCOW, KKTC

To My Parents; Mohamed and Huda

ACKNOWLEDGMENTS

I would like to express my utmost gratitude to my advisor Asst. Prof. Dr. Bengü Bozkaya Schrotter for her support, guidance and encouragement. Thank you for having patience with me, and for all the knowledge you have provided. It has been a great honor having you as my advisor.

I sincerely thank the jury committee, Assoc. Prof. Dr. Murat Fahrioglu, and Prof. Dr. Umut Türker for their engaging and comprehensive discussion during my defense.

I would also like to thank my previous advisor, Assoc. Prof. Dr. Onur Taylan for the help he provided by teaching me the basics of renewable energy systems modeling. And I extend my thanks to Dr. Jean-Christophe “JC” Schrotter for his help and criticism of my desalination plant design.

A special gratitude to my parent, Mohamed and Huda, for their unconditional support and love that have warmed my days. Also, I would like to thank my siblings, Sereen, Yasmeen, Maha, and Yousef for all the support they have provided, and most importantly, for being my best friends in life.

Finally, I would like to convey my gratitude towards my dearest friends, Perihan Yılmaz, Hossam Hamdi, Melissa Altuntaş, Shehab Asar, Zülal Karataş and Batıkan Özkan for their support and friendship they have provided during my studies in the island.

TABLE OF CONTENTS

LIST OF TABLES

TABLES

LIST OF FIGURES

FIGURES

LIST OF ABBREVIATIONS

ABBREVIATIONS

AC	Alternating Current
ACC	Annual Chemical Cost
AFS	Average Feed Salinity
ALC	Annual Labor Cost
AMC	Annual Maintenance Cost
APF	Average Permeate Flux
BWRO	Brackish Water Reverse Osmosis
CAPEX	Capital Expenditure
CF	Capacity Factor
CPF	Concentration Polarization Factor
CRF	Capital Recovery Factor
CSP	Concentrated Solar Power
DAF	Dissolved Air Flotation
DC	Direct Current
DHI	Diffuse Horizontal Irradiance
DNI	Direct Normal Irradiance
DP	Double Pass
DPBP	Discounter Payback Period
ED	Electrodialysis
ERD	Energy Recovery Device
GHG	Greenhouse Gas
GHI	Global Horizontal irradiance
HPP	High Pressure Pump
ISD	Internally Staged Design
LCOE	Levelized Cost of Energy
LCOW	Levelized Cost of Water

MED	Multi-effect Distillation
METU NCC	Middle East Technical University Northern Cyprus Campus
MMF	Multi Media Filtration
MSF	Multi-stage Flash
NDP	Net Driving Pressure
NF	Nanofiltration
NF	Nanofiltration
NOCT	Nominal Operating Cell Temperature
NTU	Nephelometric Turbidity Units
O&M	Operation and Maintenance
OPEX	Operational Expenditure
PR	Performance Ratio
PV	Photovoltaic
RO	Reverse Osmosis
ROI	Return on Investment
SDI	Silt Density Index
SEC	Specific Energy Cost
SP	Single Pass
SR-RO	Solar Rankine-Reverse Osmosis
SWRO	Seawater Reverse Osmosis
TCF	Temperature Correction Factor
TDS	Total Dissolved Solids
TMP	Trans-membrane Pressure
TMY	Typical Meteorological Year
TRNC	Turkish Republic of Northern Cyprus
UF	Ultrafiltration
USD	United States Dollar
VC	Vapor-Compression
WHO	World Health Organization

CHAPTER 1

INTRODUCTION

1.1 Background

One of the issues that Northern Cyprus faces is the increasing shortage in fresh water. Historically, Cyprus' inhabitants were mostly dependent on groundwater. There are 11 main aquifers in TRNC as shown in Figure 1 totaling around 74 million cubic meters of available water, where that accounts for 75.5% of water that is available as a resource in TRNC, excluding the Turkey-TRNC water pipeline [1].

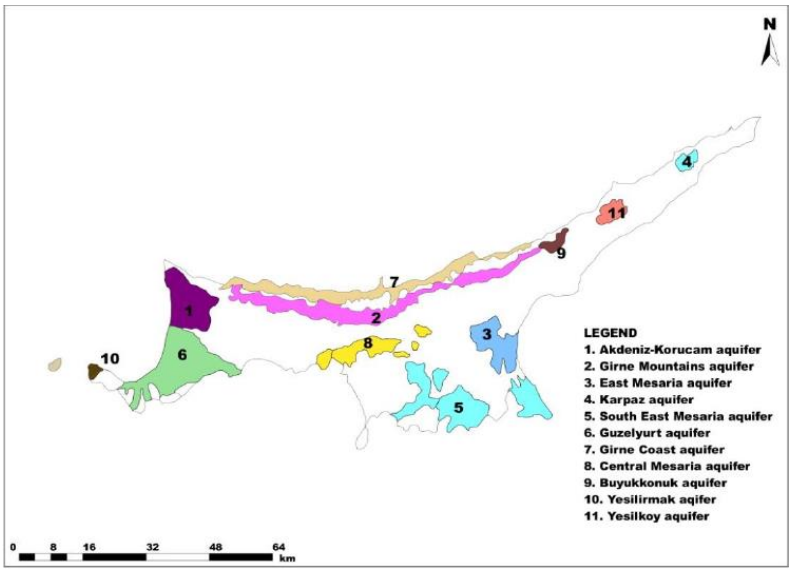

Figure 1. The main aquifers' locations in TRNC [1].

However, due to the increase in population and climate change, TRNC was facing a scarcity in fresh water [2]. The topography of the region causes a considerable amount of rainfall to be lost to evapotranspiration. In addition, the decrease in rainfall due to an ongoing drought, combined with the overuse of groundwater through pumping, caused a depletion of the aquifers and a decrease in the level of the water

in the aquifers. This may have caused saltwater intrusion in some of the coastal aquifers in TRNC such as the Guzelyurt aquifer, due to the aquifer being below sea level, seawater finds a way to get to the aquifer. This exacerbate the water problem of the affected aquifers as the seawater intrusion is considered as a contaminant, rendering water from the affected aquifer unusable. Seawater intrusion can be a problem that persists for decades, even after the aquifer gets replenished [3].

Another major source of water for TRNC historically is surface water in terms of 38 streams, which are non-perennial due to the topography of TRNC, thus making them highly dependent on rainfall and snow melts, in which have seen a gradual decrease over the past few decades. Therefore, the deficit in surface water to supply the demand of water has shifted to groundwater.

Since TRNC have very fertile lands, the agriculture is one of the major industries in the country. Therefore, a considerable amount of water goes for irrigation and livestock [4]. Thus, the water used shall be of a suitable quality for irrigation specially. While some crops are tolerant to saline water, such as asparagus and oats, which can tolerate up to 3500 total dissolved solids (TDS) water, some other crops have no tolerance towards a high TDS, such as strawberries and carrots which requires water of TDS less than 500 [5]. With the low TDS requirement, and the rise in the salinity of the groundwater due to saltwater intrusion, a solution must be implemented by the country to save its agriculture industry [3].

At the end of 2015, a project between Turkey and TRNC was established to set up a pipeline from the Alakopru Dam in Southern Turkey to Gecitkoy Dam in the Girne region in TRNC. The pipeline is submerged at 250 m under sea level and extends around 80 km from Southern Turkey to Northern Cyprus as shown in Figure 2 [6].

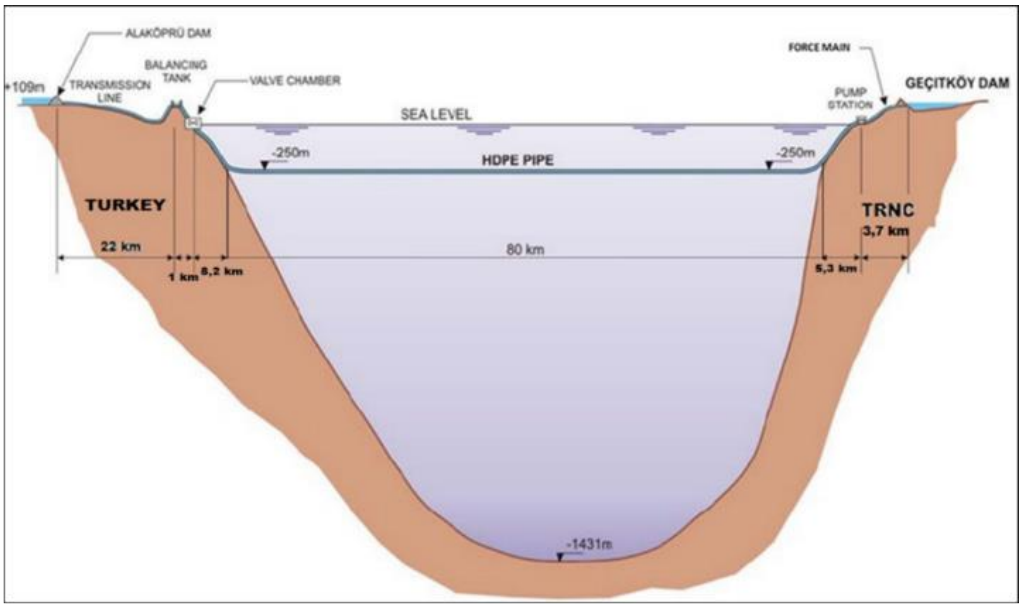

Figure 2. The sectional view of the Turkey-TRNC pipeline [6].

The pipeline is meant to deliver up to 75 million cubic meters of fresh water to TRNC. This pipeline is meant to be a solution for what TRNC facing with its water scarcity. The pipeline is supposed to sufficiently supply all the demand of water in TRNC, whether it is for domestic use or for irrigation. However, the infrastructure of the region does not allow all the demand to be met by the water from Turkey, as only 72% of the total demand is met by the pipeline [4]. Where the rest of the demand is supplied by groundwater wells and desalination plants, accounting for 23% and 5% respectively [4].

CHAPTER 2

THEORY & LITERATURE REVIEW

2.1 Desalination with Renewable Energy Systems

Solar power is abundant during the daytime for most of the countries where people live. It may differ for each location on Earth, but TRNC has a relatively good solar resource. For this reason, a lot of studies in literature focused on taking the advantage of the use of solar energy to provide the thermal or electrical energy to run desalination plants for various desalination technologies. Solar powered desalination can be very similar to conventional desalination technologies, but instead of using fossil fuel or electricity to run thermal or membrane-based technologies, solar technologies use solar power. The reason these solar desalination technologies are sought after is because they tend to be more environmentally friendly, or in some situations cheaper than conventional ones.

The most common ways of coupling solar power with desalination technologies are using the solar energy as the thermal energy provider for thermal based technologies or using the solar energy as electricity energy provider for membrane-based and other electrical energy dependent technologies.

For the thermal based desalination technologies, usually Concentrated Solar Power (CSP) collectors are the providers of thermal energy for the heating element for these technologies. CSP coupled with multiple effect distillation (MED) or multi-stage flash distillation (MSF) seem to be the most common in literature, speaking in terms of common thermal technologies.

Literature also has plenty of studies on using solar energy directly instead of converting it to thermal or electrical energy. These solar desalination systems operate solely on solar energy or with a little help of electrical energy in some cases.

These technologies can be summed into three major solar desalination technologies: solar still, solar chimney, and solar humidification-dehumidification.

As for the membrane-based desalination technologies, Photovoltaics (PV) is the most common technology coupled with. However, there are also studies with solar organic Rankine cycle, where reverse osmosis (RO) is coupled with solar organic Rankine cycle to take advantage of how the technology works well in low temperatures [7]. This works well because the sun provides enough heat to make the working organic fluid (usually propanes) to complete a Rankine cycle to produce electricity [7].

However, it comes without saying, RO can be coupled with any renewable energy sources as well, whether it is wind or geothermal, whatever the renewable technology used to produce electricity, RO can benefit from it, making RO a very flexible technology coupled with renewable energy sources.

2.2 Desalination Technologies

Desalination is a relatively new commercial technology. Most of the development happened in the previous century, beginning with MED in the early 1930s to RO in mid 1960s [8]. In the previous two decades, the desalination technologies saw an increase in efficiency, safety and reduced ecological impact. That advance in technology specially improved the RO technology. This improvement in the technology -not just RO but all the desalination technologies- caused the popularity of desalination to rise as a way to desalinate water for municipal water. Up till February 2020, the global installed capacity was 114.9 million m^3/day up from 95.6 million m^3/day in 2016, a 19% increase in just 4 years [8]. Going further back to the year 1952, the total capacity was around 100,000 m^3/day, that's a significant increase of 114900% in just 68 years [11]. These numbers can clearly show the importance of desalination, as it is being adopted all over the world to overcome water supply shortages.

There are many types of desalination technologies available. But they usually fall under two categories: thermal desalination and membrane desalination. Thermal desalination can be broken down to two subcategories, multistage flash distillation (MSF) and multi effect distillation (MED). While membrane desalination has many subcategories, e.g., reverse osmosis (RO), nanofiltration (NF), and electrodialysis (ED).

There are also non-conventional desalination processes, some of these unconventional desalination processes are called passive desalination processes. Unlike conventional desalination processes, which are also called active desalination processes, passive desalination processes do not need an active energy input generated by humans like thermal in the case of MSF and MED, or electrical as in the case of RO. Instead, it uses the power of nature such as the sun. One example of a passive desalination is using a solar distillatory or a solar pond. However, these technologies are inefficient, and mostly require a huge amount of land to make the process viable, while other technologies need more power from the sun than the sun already gives to the earth [9].

That leaves the choices for the optimum desalination process to be between the two active categories that are mentioned before, i.e., thermal and membrane processes.

From the beginning of the desalination technologies' history, thermal technologies dominated the desalination market. However, over the last two decades, membrane technologies seemed to have an increased popularity as compared to the thermal technologies as can be realized from Figure 3. After the 2000s the number of membrane-based technologies boomed and is increasing at a much higher rate than thermal technologies. This is due to the advancement in membrane-based technologies as compared to the thermal based technologies. Moreover, membrane-based technologies are less energy demanding. And as many countries and regions are not fossil fuel producing countries, the idea of having a less energy intensive technology that requires only electricity to run, puts RO membranes in an attractive position. Moreover, RO membranes have a smaller carbon footprint overall

compared to thermal technologies. And what's even better is that RO can be coupled with renewable energy sources to make it even more environmentally friendly while also being economically viable.

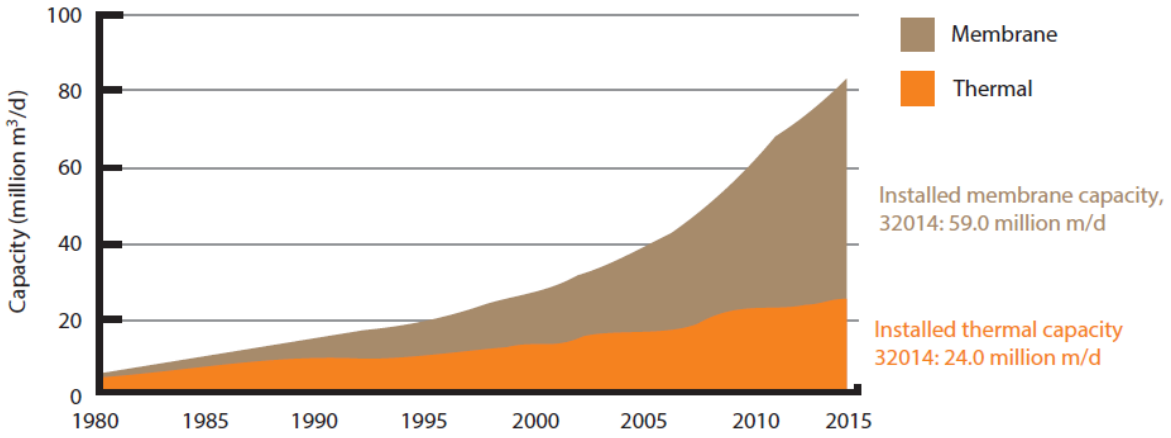

Figure 3. Comparison of the increasing capacity of membrane-based technologies as opposed to thermal based technologies between the years 1980 and the third quarter of 2014 [10].

2.2.1 Thermal Desalination Technologies

Thermal desalination simply put is a case of both the first and second law of thermodynamics. Most of the laws that thermal desalination technologies follow are derived from these two laws of thermodynamics, where mass and energy transfer play the biggest role in these thermal desalination technologies [10]. One thing to keep in mind is that thermal desalination has two energy inputs, thermal and electrical, where the thermal is usually the larger portion of the energy input.

The core of thermal desalination can be drawn out of the name of these technologies, "thermal desalination". Broadly speaking, the technologies depend on heating the brine to be desalinated such as the water, that would reach the boiling point and reaches the gas phase. Afterwards, the steam produced from boiling the water can be condensed to get pure water with no salt concentration at all, at least theoretically.

However, because some saltwater droplets stick with the flowing steam, similar to how smoke particles, solid particles, stick with the produced gas from burning making it visible to the eye [10].

MED and MSF are more common in regions that are rich in oil and gas, as getting the temperature needed by the process is usually done by burning gas or oil. That makes countries in the Middle East like Saudi Arabia or Kuwait to have more MED and MSF desalination plants than other technologies, mostly because fossil fuel is readily available in these countries. Moreover, most of the MED and MSF plants are coupled with power generation plants that run on fossil fuel that takes the fossil fuel heated steam used to run the turbines to heat the feedwater of the MED or MSF plant. Moreover, another reason Gulf countries rely on MSF and MED is that the water in the Gulf Sea and the Red Sea are highly saline, making the use of RO prone to membrane fouling at much quicker intervals than less saline waters from the Mediterranean Sea for example [8].

One of the disadvantages of thermal desalination technologies is that they rely on economies of scale. It would be very uneconomical to have a small-scale MED or MSF plant. Therefore, most of the MED and MSF plants are large scale plants with huge capacities. On the other hand, RO seem to carry a lower price for smaller scale plants as can be seen in Figure 4. While Table 1 shows the average cost of water of common desalination technologies. It should be noted that Figure 4 data may not be an accurate representation of the economy of the desalination technologies, because some of the plants from the study done by Eke et al. are expensive due to the high capital costs in Australia for the case of the XL RO plant (Tugun Gold Coast plant) [8].

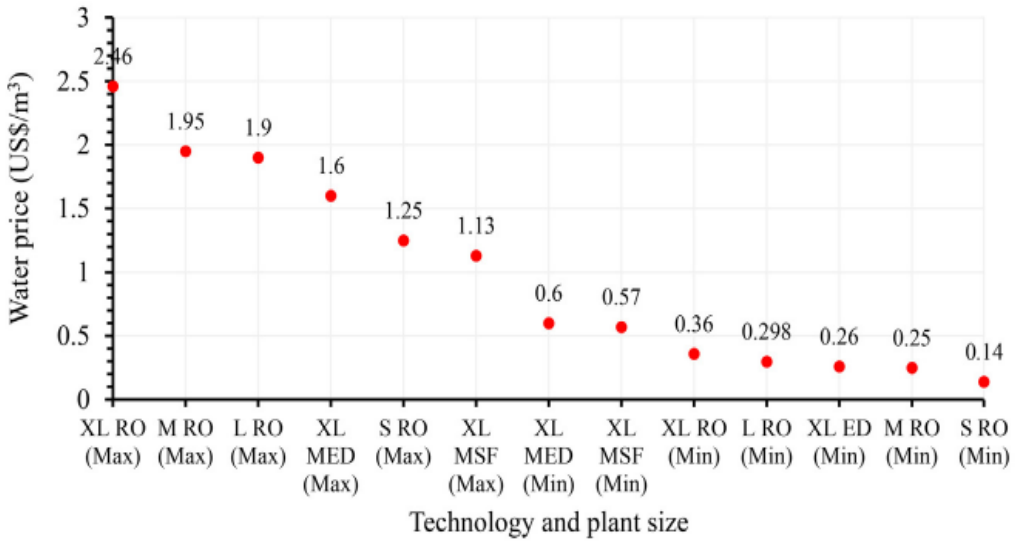

Figure 4. Minimum and maximum water prices of various plants depending on their technology and size [8].

Table 1. Average cost of water per meter cube for different sea water desalination technologies depending on size [11].

	Cost of water by plant size (US$/m^3)			
Desalination Technology	Small	Medium	Large	Extra Large
MSF	-	1.155		
MED	5	1.225	0.765	
RO	1.21	1.05	0.555	
VC	2.3	0.91	-	-
ED	1.05	-	0.6	-

One more important aspect of desalination technologies is their specific energy consumption. It is very crucial to have the minimum amount of energy required to produce fresh water, not just for an increased efficiency, but also to decrease the amount of greenhouse gasses (GHG) emitted to the atmosphere. The most viable energy efficient technology is RO desalination by a relatively good margin compared

to other technologies like MSF and MED as shown in Table 2. It should be noted that the data shown on Table 2 may be outdated to today's technology, as they are SECs for studies and plants that range from the late 1980s to early 2000s [11].

Table 2. The range of SEC of the three major seawater desalination technologies [11].

Desalination Technology	Thermal energy consumption [kWh/m^3]	Electrical energy consumption [kWh/m^3]	Total energy consumption [kWh/m^3]
MSF	15.83-23.5	2.5-5	19.58-27.25
MED	12.2-19.1	2-2.5	14.45-21.35
SWRO	-	4-6*	3-6

*with energy recovery device

2.3 Reverse Osmosis

Reverse osmosis is a technology that is used in many industries, and not just for seawater desalination. Industries where reverse osmosis is utilized are many, some examples include but not limited to pharmaceutical, food and beverages, electronics and most importantly brackish water and seawater desalination. Reverse osmosis is a membrane-based desalination technology, which relies on pressure to drive the feedwater through the membrane to obtain the desalinated water. This pressure requirement is provided by a pump that pressurizes the feedwater, which in most cases, the pump is driven by electricity, as opposed to the thermal desalination processes' need of both electrical and thermal energies, thermal being the bigger portion of the energy need.

Osmosis is a process that occurs in nature and most importantly in biological organisms. It happens in many biological mechanisms ranging from roots of plants to kidneys. Simply put, osmosis is a process where in the presence of a semi-permeable membrane between a dilute solution and a concentrated solution, there

would be movement from the dilute solution to the concentrated solution. This process occurs due to the presence of chemical potential difference between the two sides of the semi-permeable membrane. Because there is a presence of chemical potential difference, and chemical potential difference is thermodynamically unstable, thus water will pass from the region of less salt concentration to the one with greater salt concentration in order to stabilize the difference. The process will happen due to the water moving down the concentration gradient. This movement will cause a pressure difference to occur from the lower concentrate to higher concentrate water. This pressure difference is called the “osmotic pressure” [12].

Reverse osmosis, as the name implies, is the opposite of osmosis, it is the flow of the more concentrated water to the less concentrated water. The occurrence of osmosis happens naturally, without an input in energy, just like how water flows from greater heights to sea level. However, reverse osmosis requires an energy input to move the solute-rich solvent to the less concentrated one. For that to happen, the energy input is in the form of pressure, and the pressure needed is a pressure that exceeds the osmotic pressure between the two sides of the permeable membrane. This is the exact principle that RO desalination plants use to obtain desalinated water.

Most of the RO membranes that are used in the desalination industry are in spiral wound configuration. This configuration wraps multiple membrane sheets with a porous permeate spacer in between two sheets. The stack of sheets of membranes and spacers are sealed from three sides and the 4th side is left unsealed so that permeate is guided towards the permeate tube at the center [13]. Moreover, the spacers are designed to have channels that produces turbulence in the permeate flow in order to reduce concentration polarization [14]. The membranes and the spacers are wound around a plastic tube that allows the flow of permeate into it as shown in Figure 5.

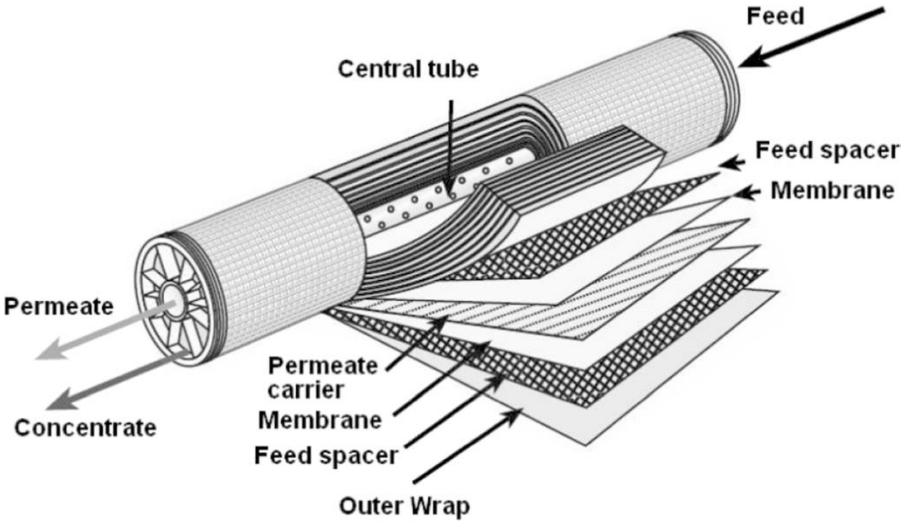

Figure 5. A typical spiral wound RO membrane [15].

The flow in a spiral wound RO membrane is called cross flow. Cross flow is better suited for RO desalination membrane modules. Mostly, because a cross flow causes less fouling on the membrane's surface compared to perpendicular flow as shown in Figure 6. This is due to the cross flow disposing the foulants that accumulates on the membrane's surface with the concentrate flow [14].

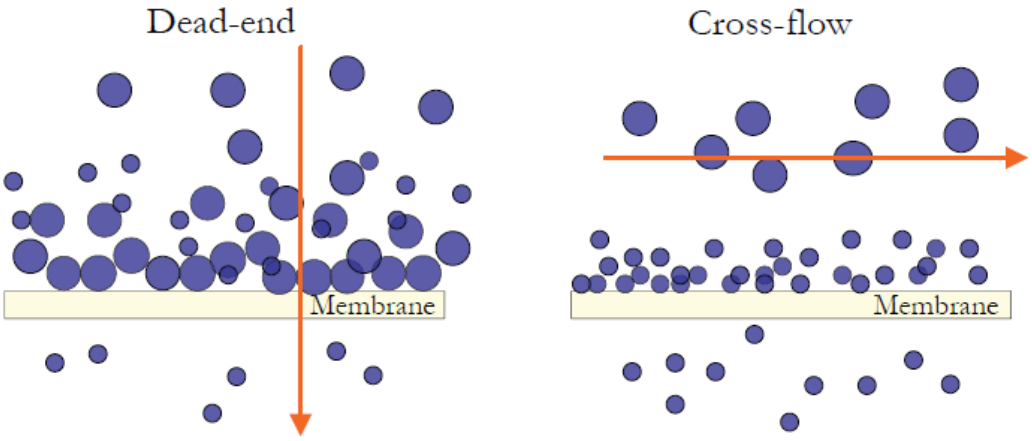

Figure 6. The fouling on the membrane caused by dead-end flow (perpendicular flow) vs cross-flow [14].

The way most RO plants in the industry work is by having trains of pressure vessels containing RO membrane as spiral wounds. Usually, each pressure vessel contains

RO membrane elements of up to 8 elements connected in series [16]. But current industrial SWRO plants usually house between 6-8 membrane elements per pressure vessel.

Once the feedwater enters the pressure vessel, it will pass onto the first RO element, where RO filtration would occur, leaving the reject in the feedwater. This makes the reject mix with the feedwater into what is called concentrate. The concentrate then passes to the second RO element where the same process happens and so on. Therefore, it should be noted that along the pressure vessel's length, the concentration of the feedwater increases. Moreover, within each element, there is a pressure drop that exists. The pressure drop and the concentration gradient causes the membranes further along the pressure vessel to have less recovery. Which means that the first RO element in a pressure vessel will have the highest recovery. Once the water passes by the last RO membrane, its concentrate is discarded as waste.

As for the permeate, the permeate of each RO element passes through its own permeate collection tube. These permeate collection tubes are all connected to each other in series. Therefore, the permeate's TDS is a combination of all the elements' individual permeate's TDS with taking mass conservation into consideration. Once the permeate from the last membrane is collected, it exits the pressure vessel to post-treatment. There is a brine seal that is fitted to each membrane to prevent the permeate from mixing with the concentrate [13].

Currently, the leading RO membrane material in the market is polyamide RO membranes with a market share of 91%. While the next leading RO membrane material is held by asymmetric cellulose acetate membranes that are in the shape of hollow fibers [17]. The difference between the two is that the polyamide usually has higher rejection and higher net driving pressure required. Whereas the asymmetric cellulose acetate membranes offer better chlorine resistance, in which can resist higher doses of chlorine that is injected into raw water with high algal and microorganism activity [17].

Since recovery is one of the most important parameters in RO calculations, it is also expected to be important for the energy production. Since recovery is dependent on pressure, it is expected for the pressure to increase with recovery. However, the specific energy consumption actually decreases to a certain point, usually 55 bars in single stage SWRO, and then goes up again as shown in Figure 7.

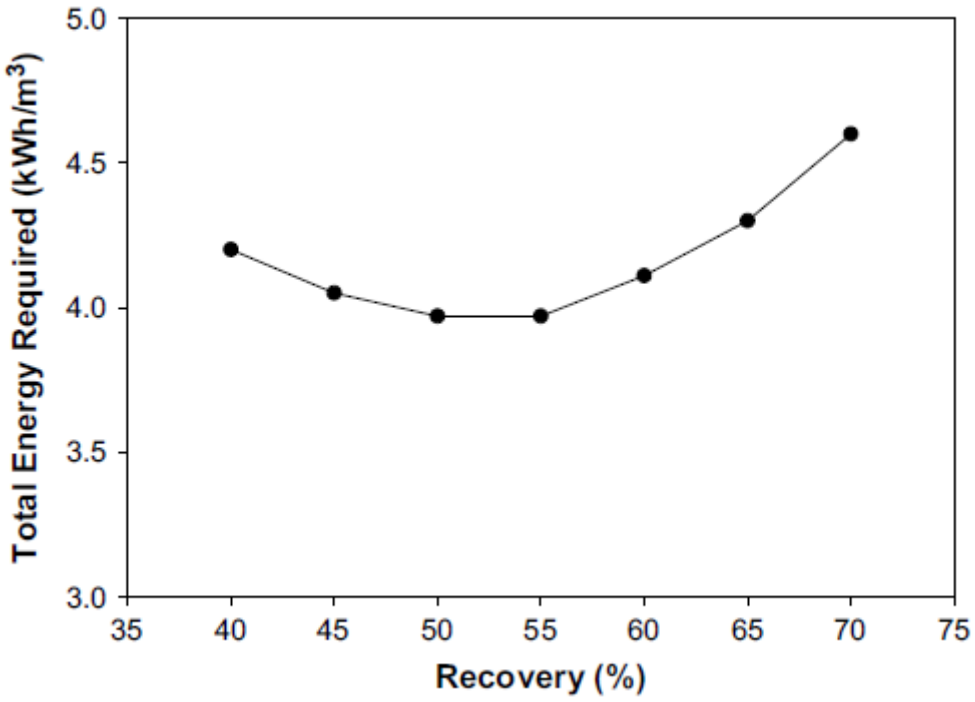

Figure 7. The SEC vs. Recovery for an RO plant with 34,000 TDS feedwater [18].

And as can be seen from Figure 8. The price follows the same trend as the SEC vs recovery as was shown in Figure 7. According to the study, the lower price of the water with higher recovery is due to the feedwater intake system and the smaller pretreatment system.

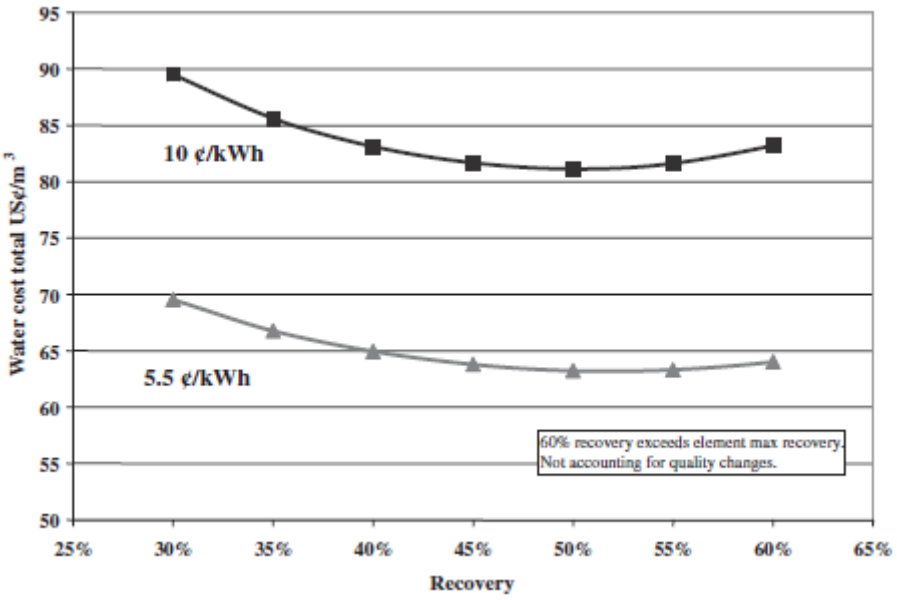

Figure 8. The effect of recovery has on the water cost [19].

RO plants have different flow patterns for different goals and purposes. For example, in order to get more recovery, the concentrate from the first pressure vessel is transferred to another pressure vessel as feedwater. Then it is processed with the RO process through the membranes to create more permeate, therefore increasing the recovery. This flow pattern is called a two stage layout. That means every time the feedwater passes by a pressure vessel of RO membranes, that is called a "stage". Each stage may have many pressure vessels in parallel, it is only when they are connected in series, it becomes another stage. Since the next stage would have a more saline concentrate, it usually requires more energy than the first stage. A 2 stage RO plant layout can be seen in Figure 9.

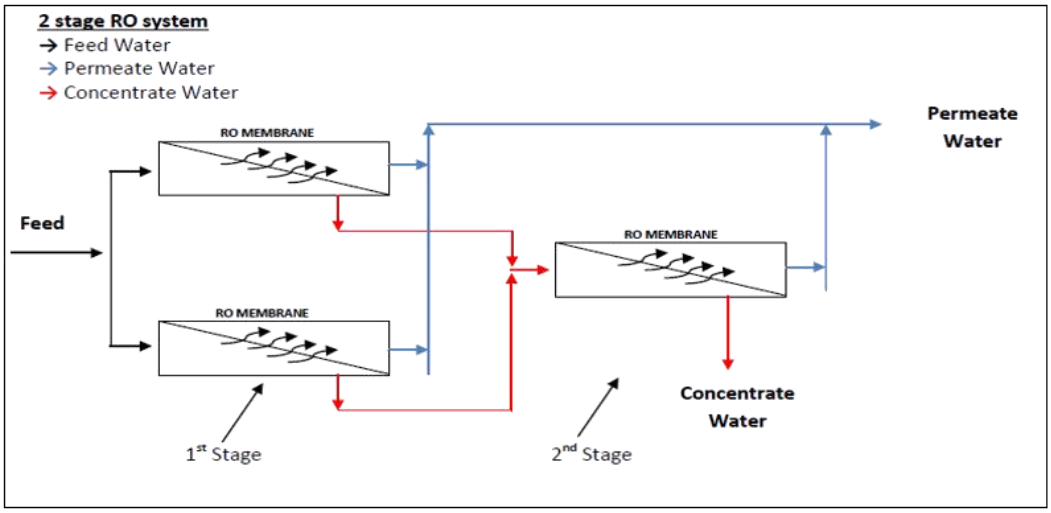

Figure 9. A layout of 2 train first stage with 1 train second stage [20].

Another flow pattern is called a "pass". A pass is characterized by having two pressure vessels connected in series. However, unlike the "stage", the permeate of the previous pressure vessel passes on to the next one. Therefore, the permeate is processed again to obtain much cleaner water. Since the permeate is already with a low TDS due to the first pass, the second pass would require much less energy to produce a permeate with high recovery. The double pass layout is usually used to remove boron from seawater with the second pass being done with brackish water RO membranes, while the first pass is done with seawater RO membranes. It should be noted that the overall recovery reduces in multiple passes RO plant compared to one pass with the same inlet feedwater pressure. A double pass RO layout can be seen in Figure 10.

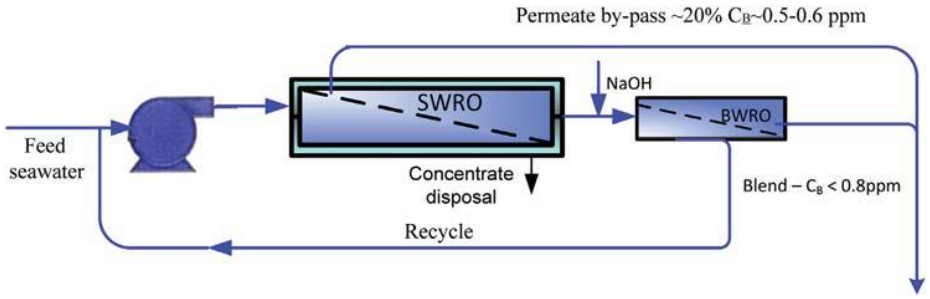

Figure 10. Double pass RO layout with NaOH addition for further boron removal [21].

An RO plant may contain a combination of stages and passes. It can be denoted as "stages:passes". For example, if an RO plant has two stages and one pass, it would be denoted as a "2:1" array. The combination is done to make sure that the plant produces a permeate with the required quantity and quality.

Water temperature has an effect on the RO process. When it increases, it allows more permeate to pass, but it will also allow more salt to pass, therefore offer less rejection. And when the water temperature decreases, it allows less permeate flux and higher salt rejection. The change in the permeate flux is around 3% for each °C increase [22]. The effect of temperature can be seen on Figure 11 and Figure 12.

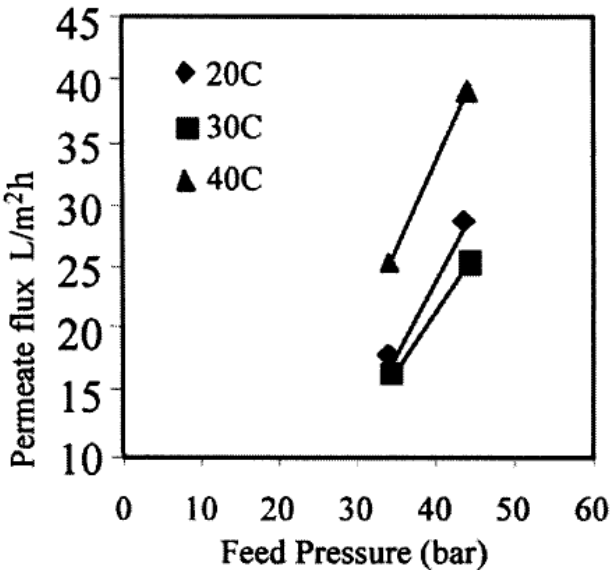

Figure 11. Effect of temperature on permeate flux with certain feed pressures [23].

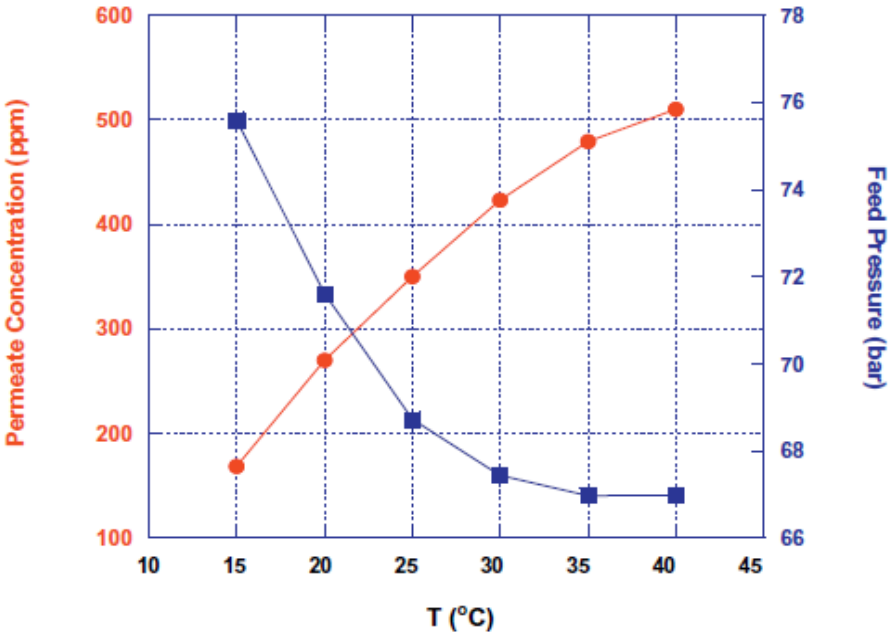

Figure 12. Effect of temperature on permeate concentration and required feed pressure [22].

2.3.1 Pretreatment

The water taken from the sea contains a variety of suspended solids, microorganisms, metals, organics and many other undesirable materials in the water. These undesirables can be directly fed onto the RO membrane, and the membrane would reject them. However, these undesirables would greatly decrease the life of the membrane by damaging it and causing scaling and fouling.

Therefore, an important process that is placed before the RO process called pretreatment is used. Pretreatment would get rid of most of the undesirables in the water so that most of the material in the feed water is just dissolved salts. It is crucial step in improving the feedwater quality entering the RO process. Without it, RO desalination would be highly unfeasible.

There are many types of pretreatment processes that are used in RO desalination plants worldwide. However, in the past few years, some of them gained more

popularity compared to others. Mostly, because of their better outcomes, compactness, and economic advantage.

- Coagulation

One of the first steps of the pretreatment process is coagulation. Coagulation is when a coagulant is added to the feedwater to stick the coagulant that is positively charged, mostly alum, with the negatively charged colloids. Therefore, neutralizing the negatively charged colloids.

- Flocculation

Once the negatively charged colloids are neutralized. They are able to flock, in other words stick with each other forming bigger particles. These bigger particles are produced using mixers of varying stages, each stage slower than the one before. The decrease in the speed of mixing is to not break the bigger particles that form.

- Sedimentation

Once the particles are mixed to form bigger particles. A process called sedimentation is now possible. In this process, the bigger particles start to precipitate with the help of gravity to the bottom zone in which all the sludge of sediments are collected.

- Chlorination

The feedwater usually has so many microorganisms. These would create biofouling on the surface of the RO membrane if left untreated before entering the RO stage. Therefore, the water is usually disinfected before entering the RO stage. One of these disinfection processes is the usage of chlorine to kill the microorganisms in the feedwater. It can be done by adding sodium hypochlorite to the feedwater to get active chlorine in the feedwater, or directly dissolve chlorine gas into the feedwater. Usually, the recommended dose by Lenntech is specified as 3 mg/L of active chlorine. [24]

- Multi Media Filtration

A multi media filtration tank is used to remove solid particles of down to 10 microns in diameter. It takes advantage of multi layers of granules of decreasing diameter. The first layer would be the biggest diameter which is usually consisting of coarse anthracite granules at the top, followed by sand granules, and the last layer having the smallest diameter, is made of fine garnet granules. Each layer has a higher density than the one on top of it. The suspended particles in the raw feedwater would not pass through the pores of the media, if the diameter of the particle is bigger than that of the pores. The multi media filtration tank would be pressurized. The raw feedwater must be pressurized, otherwise the filtration process would be slow if gravity was the only force pulling the water. Sometimes, polymer coagulants are used alongside the multi media filtration process. Where the polymer coagulants would make particles of suspended solids stick together, and that lump would have a bigger diameter than that of the pores in the medium. Thus, the usage of polymer coagulants would increase the efficiency of the multi media filtration process [25].

- Dissolved Air Flotation (DAF)

The DAF process takes the advantage of air bubbles having less density than the water, which would push the bubbles upwards to the surface of the tank. At first, coagulants and flocculants are injected into the feedwater to increase the size of the suspended particles. Another stream of clarified water saturated with air combines with the feedwater. The two streams after combining head to an open tank. In the open tank, air bubbles would form and attach to the suspended particles, pushing them upwards to the surface. Some particles would be very heavy for the air bubbles to carry, those would fall down as sediments at the bottom of the tank. Afterwards, the sludge formed at the surface of the water would be removed by a scraper or by hydraulic means. Usually, a scraper is preferred for its simplicity and effectiveness. For the DAF process to be a significant part of the pretreatment process, it is recommended to have feedwater of turbidity above 5 NTU. If it is below 5 NTU, it would be hard for the particles to coagulate and form bigger particles, and therefore

harder for the bubbles to float these particles. Otherwise, If the feedwater has a turbidity of less than 5 NTU, it is recommended to skip the DAF process [26].

- Cartridge Filter

These filters are made out of thin plastic strings that are wound around a tube to form the cartridge filter. These cartridge filters are usually there to protect the RO membranes from particles that passed the previous pretreatment processes. It can remove particles of sizes between 1-25 microns, where the most common design is for the removal of 5 microns. Cartridge filters are not used to improve the feedwater quality. Therefore, the silt density index (SDI) of the feedwater before and after passing the cartridge filter is almost the same. Otherwise, if the SDI is not the same, that is an indicator that the pretreatment processes before the cartridge filter are incompetent [26]. The SDI is a way of measuring if the water would be fouling for the reverse osmosis membranes, and to what degree.

- Ultrafiltration or Nanofiltration

UF (Ultrafiltration) or NF (Nanofiltration) are membrane-based pretreatment processes. Just like the RO membranes, they have minuscule pores that would allow the water to pass but restrict microbes or algae. But unlike RO membranes, they would not reject salts. Although, NF membranes can offer a low salt rejection [27]. UF would filter microbes but is unable to reject some of the low molecular weight organics. Therefore, some of the microbes that happen to be introduced downstream, can have nutrients to grow on the RO membranes and cause biofouling. To avoid this issue, chlorination is recommended to minimize biofouling. Unlike UF membranes, NF membranes are able to reject these organics, along with color as well [25][26]. Just like RO membranes, UF and NF membranes usually come in spiral elements that allows cross-flow mode. Also, most of the same working principles of RO membranes apply to UF and NF membranes. Therefore, it is expected for the NF membranes to be more energy intensive than UF membranes for the same flux [28].

UF seems to be affected by how much bioactivity that is happening in the feedwater. For example, in the equator or in a tropical climate, there would be high algal blooming. The algae can cause biofouling of the UF membrane. And to prevent this biofouling, coagulants can be used [29]. Otherwise, if the bioactivity is high, DAF can be used before the UF process [26].

Just like RO process, UF process have a recovery, trans-membrane pressure and membrane flux. For the UF these parameters are usually much higher for the recovery and membrane flux. While it depends on the water intake source, the UF process usually have a recovery of 90% to 95%, a membrane flux of 40-80 lmh, and a trans-membrane pressure (TMP) of 0.2 to 1 bar [26]. Most common UF membranes are set in a direct-flow configuration as it is more efficient for UF membranes. Due to that, solids would accumulate on the membrane over time. Therefore, a backwash is necessary, and it is much more frequent in that of RO membrane's maintenance backwash. Usually, UF membranes are backwashed every 20-120 minutes for around 30-60 seconds. And compared to MMF as a pretreatment, the backwashing of UF membranes happen much more frequently compared to the once every 24 hours of backwash that is usually done for MMF [26].

Pretreatment is an essential process in an RO plant. It is essential for protecting the RO membranes from bigger particles like suspended solids or fouling agents such as algae and microorganisms. While the RO membranes require a huge amount of energy to reject the salt from the water, the pretreatment process is not as energy intensive as the RO process. For most RO plants, conventional methods of pretreatment require around 0.06-0.08 kWh/m^3 effluent [30]. However, in some studies done on membrane pretreatments such as MF and UF membranes shows that the specific energy consumption (SEC) of membrane-based pretreatments tend to be higher at around 0.10-0.12 kWh/m^3 effluent [31]. While another study has found that the energy consumption of a UF process accounts for 5% of the total energy consumption of the whole RO desalination plant, which was 3.46 kWh/m^3 [19]. But with the increased quality of the pre-treated water, membrane-based pretreatment can be more protective for the RO membranes. The effluent quality produced by

conventional pretreatment is usually around 2-3 SDI, while membrane-based pretreatments can produce effluent quality of below 1 SDI. Moreover, there will be no need for chlorination or the use of coagulants for membrane-based pretreatments, due to the frequent but quick backwashing.

While there are many pretreatment and post-treatment processes that are used in the industry, a study shows that most conventional RO plants have a 1 kWh/ m^3 SEC for pretreatment and post-treatment processes (including water intake and transportation). This 1 kWh/ m^3 is not affected by factors such as the feedwater condition [32]. While another study has found that the pretreatment energy consumption to be 0.25 kWh/ m^3 including water intake, screening and UF pretreatment process, with 0.11 kWh/ m^3 being consumed by the UF membrane [33].

2.3.2 Posttreatment

After the RO process, the permeate produced by the RO can be acidic or alkaline. Therefore, a pH adjustment is needed to bring that pH to acceptable drinking water levels. Hydrated lime and carbon dioxide are added to do these pH adjustments, while also stabilizing the water during the transportation process. The water would be prone to contamination, and to avoid that, chlorine should be added to disinfect the produced water.

2.4 Energy Recovery Device

Since the energy consumption of RO desalination is high, a way of decreasing that consumption was sought after. In fact, the largest portion of cost in producing a meter cube of water goes to the electrical energy used to pressurize the water as can be seen in Figure 13.

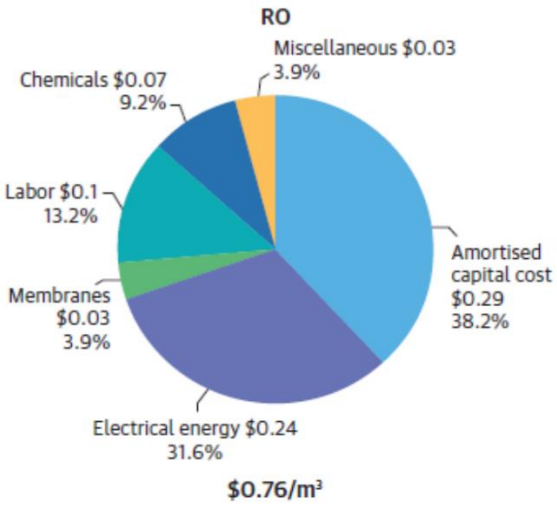

Figure 13. The cost breakdown of water produced by RO desalination [34].

Other than increasing the efficiency of the RO membranes, researchers focused on the implementation of energy recovery devices in RO plants. The concentrate discharge of the RO process usually has high energy in terms of flow and most importantly pressure. Since the concentrate stream has high energy, it is wise to extract that energy in order to optimize the efficiency of the RO process. To do that, an energy recovery device (ERD) may be used. There are a few ways of recovering the energy of the concentrate, but the most important are the Pelton turbine and isobaric energy recovery.

The Pelton turbine works in a simple way. The high-pressure stream is directed to a nozzle, this causes the stream to exit the nozzle in a higher speed than before the nozzle. Once the jet exits the nozzle, it is directed at a spoon shaped portion at the end of a wheel. This wheel has many of these spoon shaped portions. The water would hit the top side of the spoon and be directed to hit the lower side of the spoon, making a “U-turn”. This allows the momentum of the water to be transferred to the wheel. The wheel is of course connected to a turbine that would generate electricity [35]. But mostly, the spoon shaped portions are extensions of the turbine instead of having turbine blades. Otherwise, the rotation energy can be directly used to push a portion of the feedwater using a pump connected to the Pelton turbine. It should be noted that a booster pump may be needed after the Pelton turbine for the pressure to

reach the required value to push the feedwater through the membranes with the needed NDP. Another method is by connecting the Pelton turbine to the main high pressure pump's motor, to offload some of the energy required to run the pump. Otherwise, the Pelton turbine can be added after the high-pressure pump and add pressure to the feedwater before it enters the RO pressure vessels, this method uses a Pelton turbocharger instead.

The other type of energy recovery method is the isobaric energy recovery. It works by exchanging pressures. There are different devices in the market that uses this method. However, they work very similar to each other.

One of these companies have an ERD called DWEER. Where there are two cylinders in parallel that contain a piston each, check valves for each entrance, and a "Linux valve" system. The pressurized brine would be entering from one pressure vessel which is separated from the feedwater by the piston. The higher-pressure brine would push the piston to the feedwater direction, this will transfer the pressure to the feedwater. At the end of that process, the "LinX valve" system redirects the pressurized feedwater towards the RO membranes, while redirecting the lower pressurized feedwater towards the pressure vessel. The lower pressurized feedwater would have a higher pressure than the brine, therefore pushing it back. The check valve would open allowing the brine to be discarded. The two pressure vessels work together in an opposite manner. The cycles are slow, about 4 cycles a minute. That makes the system a bit less loud than other ERDs. Because there is a piston between the fluids, there is very little mixing happening between the brine and the feedwater, usually less than 1.5% of the volume. It should be noted that a booster pump is required after the feedwater is pressurized by the DWEER ERD [35]. The working principle of a DWEER ERD can be understood better from Figure 14.

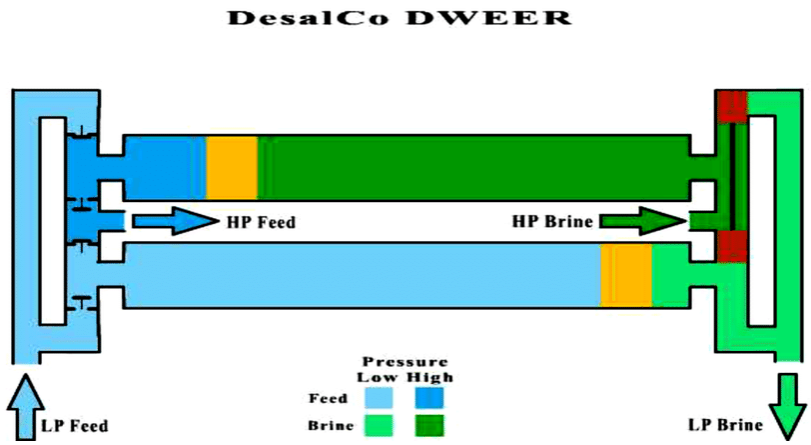

Figure 14. The working principle of DWEER ERD [36].

Another type of isobaric energy recovery device is called a PX (Pressure Exchange) ERD. This ERD have the same principle as the DWEER ERD. It relies on the pressure transfer from the brine to the feedwater. However, unlike the DWEER ERD, it uses one cylinder with a rotating ceramic piece in the middle with multiple holes for the fluids to go into. The cylinder is split into 4 smaller cylinders where each of the lower and higher brine and feedwater would be. The feedwater would enter one of the holes of the rotating part, and it would rotate to the other side where the brine will enter and transfer the pressure to the feedwater and pushes it to the other small cylinder. The lower pressure brine would rotate along with the ceramic piece and meet with the lower pressure feedwater in which in this situation, the feedwater would have higher pressure. Thus, pushing the brine to one of the smaller tubes to discard the low-pressure brine. Even though the brine makes contact with the feedwater, there is minimal mixing happening, about 6%. This is due to a water barrier that exists between the two fluids. And once the brine is about to reach the pressurized feedwater tube, it is obstructed by the rotating ceramic due to its unique design. Just like the DWEER ERD, a booster pump is needed after the ERD to pressurize the fluid to the pressure of the feedwater exiting the high-pressure pump. But unlike the DWEER ERD, since there is a rotating element in the system, PX ERD is expected to be louder than the DWEER ERD, at around 93 dB compared to that of 80 dB of the DWEER ERD.

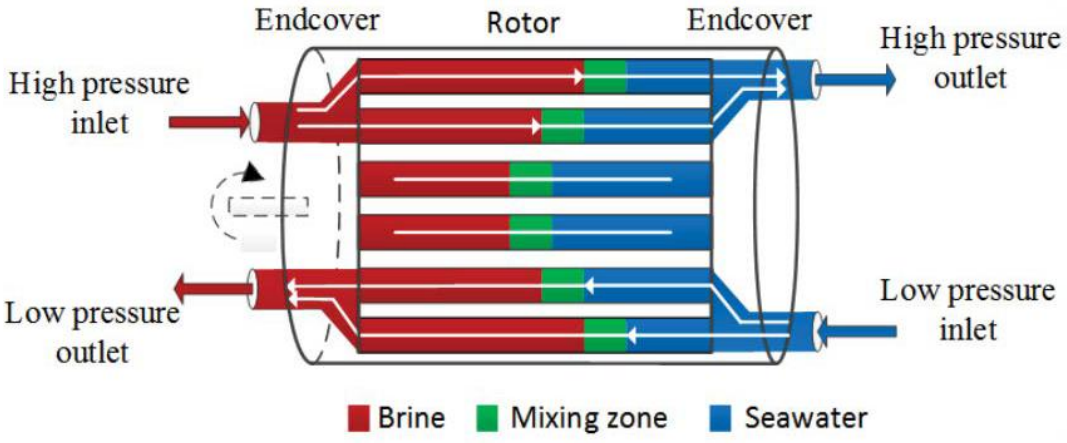

Figure 15. The working principle of the PX ERD [37].

While the Pelton turbine may have a high efficiency, it should be known that because it runs coupled with the motor and the pump, the efficiency would drop. The efficiency depends on the shape of the nozzle, fluid's flow speed, and fluid's pressure as can be seen in Figure 16. Since most of these parameters are constant for a regularly operated RO plant, it is recommended to pick the nozzle that would maximize the efficiency for the specific set of parameters that the RO plant usually runs at.

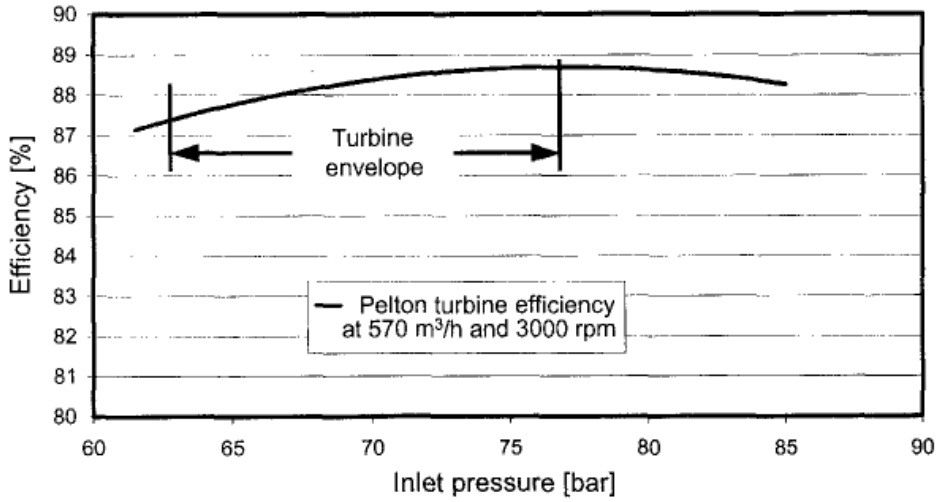

Figure 16. The efficiency of a Pelton turbine vs the inlet pressure with constant rotating speed and concentrate flow rate [38].

However, for isobaric energy recovery devices, usually the efficiency is not affected much by the flow rate as shown in Figure 17.

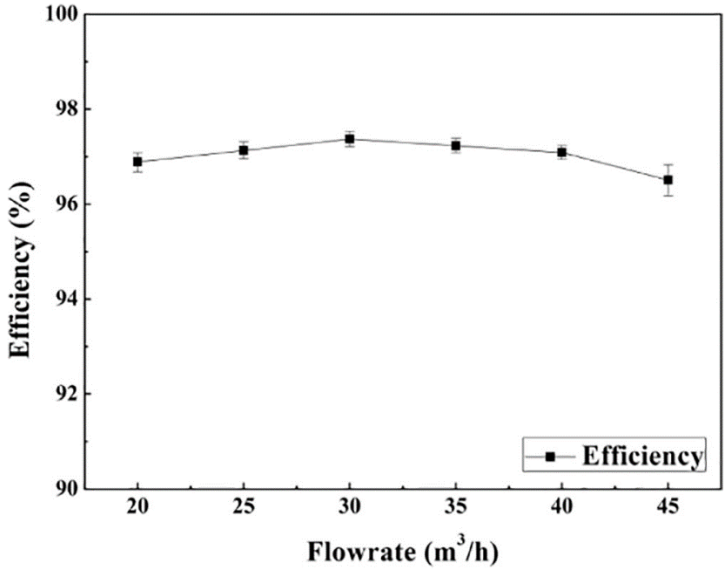

Figure 17. The efficiency vs flowrate of a DWEER ERD system [39].

Moreover, isobaric ERDs are more efficient compared to the Pelton turbine or Pelton turbocharger. Since the development of ERDs started with Pelton turbines, some plants use the Pelton turbine as an ERD successfully. However, with the advancement in ERD technology, more newer plants are opting to include an isobaric ERD instead. As the energy recovery efficiency of isobaric ERD is usually above 95%, while the energy recovery efficiency of Pelton turbines barely goes beyond 90%, and in just specific conditions [37].

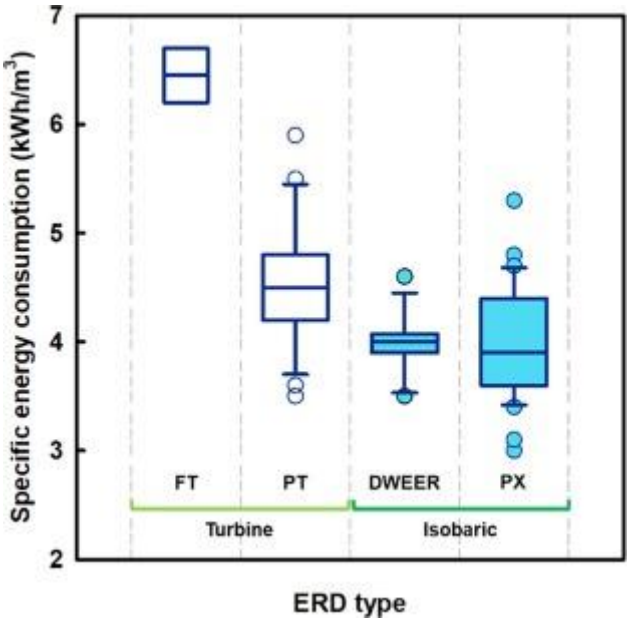

Figure 18. The SEC of desalinating water employing different ERDs. FT: Francis turbine. PT: Pelton turbine [32].

And ERD is usually a good investment in most cases, due to the high consumption of electricity. But for a region with very cheap electricity, it may not be a good investment due to the high capital cost [37].

2.5 Concentrate management methods

At the end of the desalination process, there will be a waste stream known as concentrate, or brine. The brine is a highly saline water, which can have up to double the amount of TDS compared to that of the feedwater, depending on the recovery ratio of the RO system. Moreover, as the concentrate factor increases with the increase in recovery ratio, it also depends on the type of desalination, if it is for seawater or brackish water. Generally, brackish water desalination has more recovery ratio compared to seawater desalination, the TDS of the source water is the reason for that [40]. This reject (the brine) is discarded as waste of the RO process, where some countries regard it as industrial waste like the US [41].

To discard the waste, projects rely on some concentrate management methods. These methods ensure the safe disposal of the concentrate, so it does not pollute or damage the environment around it. These methods can be divided into 6 major methods, surface water discharge, deep-well injection, sewer discharge, land disposal, evaporation ponds, and thermal evaporation.

2.5.1 Surface water discharge

Surface water discharge is the most popular concentrate management method with about 41 percent of all concentrate management methods done by this method in the US [41]. Mostly the surface water is the ocean, and mostly the desalination plants are large ones that produce large amounts of concentrate. To avoid damage to the environment and the marine life of the discarding site, a long pipe going to a certain length and depth into the ocean where the pipe has a diffuser at the end of the pipe to ensure the mixing of the concentrate with the seawater in a safe way such that the salinity of the area around the outfall pipe is not very high for the environment [41]. Moreover, if the intake and outfall pipes are both in the same body of water, which usually is, it should be made sure that the outfall area shall not interfere with the intake area of the intake pipe. This is usually done by modelling the plume of the concentrate discharge, and make sure that the intake pipe does not intersect the concentrate plume [40][41].

Rivers and lakes discharges are usually restricted to brackish water desalination [41]. But even then, it may not be optimal due to the depth of rivers and lakes being low compared to the ocean. Therefore, brackish water desalination outfall may be better discharged into the ocean instead. However, as in most cases, the brackish water source is groundwater where the aquifer is far away from the ocean, thus making discharging into the ocean an expensive option. A compromise between cost and environmental impact may have to be studied for these kinds of projects.

Usually, surface water discharge is the most affordable concentrate management method [40]. With the closer the desalination plant is to the shore, the cheaper it is to implement. Moreover, the volume of the concentrate also plays a role in the price of the discharging system, due to the need of pipes and pumps that can handle said volume.

Some desalination plants, usually the thermal desalination plants, are situated near power plants. Since power plants also have an intake and outfall infrastructure already implemented, this makes surface water discharge concentrate management method even more economical for that situation. Moreover, the concentrate can also be blended with the cooling water of that power plant [40].

2.5.2 Sewer discharge

This method is the second most common in the US, handling around 31 percent of the total concentrate management methods [41]. Very useful for inland desalination plants that are not close to the shore. In this method, the concentrate would be mixed with the sewage water or the wastewater. However, a permit is usually needed from the sewage agency where the concentrate will be discharged. Moreover, the concentrate needs pretreatments such as pH neutralization to be considered for the sewage discharge [41]. Unlike the surface water discharge method, this method is limited by the smaller amount of volume that can be discharged depending on the size of the sewage system. Otherwise, it may not be economical.

2.5.3 Deep well injection

This method of concentrate management may not be a sustainable one. Deep well injection depends on drilling a hole deep into the ground beyond and below the aquifers that are used for drinking water. It has many specific conditions, such as the transmissivity of the aquifer that the concentrate is discharged into, and the presence of a confining layer that would block the discharged concentrate from seeping into

aquifers that are used for drinking water [40][26]. This concentrate management method may not be economically feasible, unless the desalination plant is large enough [26]. Therefore, this method is usually reserved for inland desalination plants that process a large amount of volume.

2.5.4 Thermal evaporation

In this method, the concentrate is discharged onto a shallow pond, where with time, the solar energy would evaporate the concentrate water, reducing its volume. This way, the volume would be decreased, and a sludge of salt would be left, where it would be either left there at the pond or moved to another disposal site. Using this method would require a place with a dry and hot climate, where the evaporation rate would be high [26]. However, this method can be expensive due to the fact that it needs a large area of land, if the land is cheap, this method would be more economically feasible [26].

Moreover, the concentrate can be discharged into a solar energy pond [26]. Solar energy ponds depend on the salinity gradient of the water, where the highly saline water would be at the bottom, and the lower salinity water would be at the top. And due to the solar absorption, that happens at the usually dark colored surface at the bottom, the high salinity water heats up and does not rise due to the higher density, and the layers of salinity prevents the water from mixing, therefore there would be little to no convection heat transfer. Then, the heated water can produce electrical energy from a Rankine cycle.

2.6 Environmental Concerns

Since the reverse osmosis desalination process produces reject that is usually put back into the ocean, it may have a diverse effect on the ecology of the dumping location. For example, an endemic seagrass to the Mediterranean Sea, which is called Posidonia Oceanica, is affected greatly by the increase in the salinity of its

surrounding water. The Posidonia Oceanica has a mortality rate of 100% in water salinity of 50,000 TDS, while a considerable mortality rate in water salinity of 42,000 TDS [42]. Not to forget, that the reject produced by the reverse osmosis plant usually has a high concentration, which can be between 60,000 and 80,000 TDS. Therefore, it is recommended to avoid the spots in which the Posidonia Oceania grows around.

2.7 Drinking Water Guidelines

There are multiple drinking water guidelines that are followed by countries. Some countries follow the WHO guideline, some others follow the European drinking water guideline, while others would have their own drinking water guidelines. Most of these guidelines put a limit on the amount of dissolved solids present in the drinking water. Some for health-related concerns, while others for taste concerns. For example, boron is regulated for health-related concerns. While sodium and chlorine are regulated for taste concerns.

Since TRNC is in the Mediterranean, it is convenient to use the European drinking water guideline. The European drinking water guideline is shown in Table.

Table 3. The Eruopean drinking water guideline for different ions and pH. [43]

	Concentration (mg/l)
Chlorides	250
Sulfates	250
Sodium	200
Boron	1
pH	6.5-9.5

While the guidelines mentioned in Table 3 refer for each dissolved solid, there is another guideline that was suggested by WHO. This guideline is regarding the TDS of the drinking water. For a suitable tasting water, the TDS shall be below 500 mg/l. [44]

2.8 Photovoltaics

Photovoltaic (PV) cells are the most common type of solar energy harnessing instrument, in fact, it accounts for about 99% of solar cell technologies installed worldwide, totaling a capacity of 707495 MW of installed capacity as of 2020 [42]. PV is not just dominating the solar energy market, but also has the third biggest capacity of all renewables, as can be inferred from Figure 19, the PV portion of the whole renewable resources is about 24.45% [42]. In addition, comparing it to other renewable technologies it is booming at a very fast pace, as can be seen in Figure 20, with an increase of about 982% in capacity between 2011 and 2020, PV is placed at the top of fastest growing renewable energy sources [42].

Consequently, solar PV saw a steep decrease in LCOE (Levelized Cost of Energy) worldwide in the past decade, between 2010 and 2019, the global LCOE decreased by 82% from 0.378 USD/kWh to 0.068 USD/kWh [43]. This made utilizing PV panels actually an investment, where the PV panels would payback their cost in a few or several years, and then it is basically free electricity until the end of life of the PV panels (minus the O&M cost).

Other than the decline in price of PV, the scalability of PV is extremely practical. PV capacity can range from the small solar cell in common calculators to very large PV farm of 2000 MW capacity in Pavagada, India [47]. This is possible because large PV farms can consist of many PV cells connected to a single inverter that can handle a certain amount of power. Moreover, the PV cells are easily maintained, as they do not require a lot of maintenance.

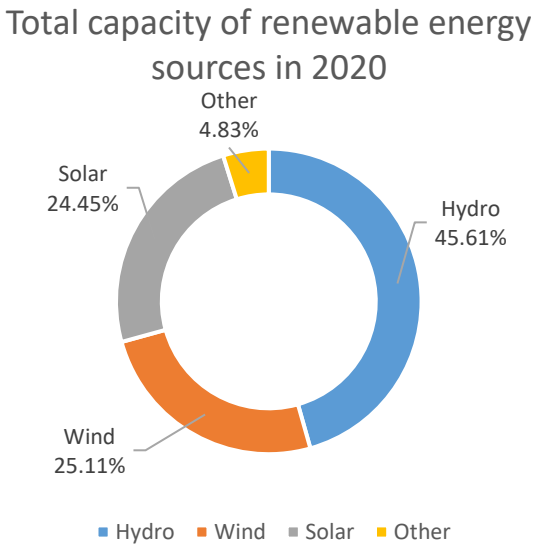

Figure 19. Total Capacity of renewable energy sources in 2020 [42].

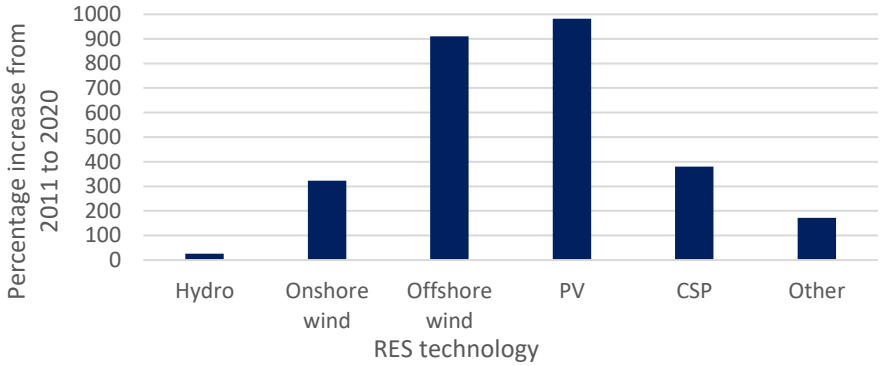

Figure 20. Percentage increase in the capacity of different RES technologies between the years 2011 and 2020 [42].

The way PV panels work depends on the photovoltaic effect. When a proton of sufficient energy hits a valence electron of a semi-conductor, the energy is absorbed by the electron and gets “freed” from the crystallized structure of the semi-conductor [45]. Thus, if there exists a potential difference, the freed electron will flow and create an electrical current. To create this required potential difference, two slices of a semi-conductor, mostly silicon, are doped with an impurity. If the silicon is doped

with a group 15 element, usually phosphorus, the slice would become n-type and have extra valence electrons, usually it is set on the top of the “sandwich”. While doping the silicon with a group 13 element, usually boron, creates a p-type slice, which have “holes” that carry positive charge, this slice is set to the bottom of the “sandwich” and it is the bigger slice of the two. With the two slices of the “sandwich” together, the electrons produced by the photovoltaic effect from the n-type slice can flow to the p-type slice and generate electricity. That makes a PV cell called a crystalline PV cell, which is the most common commercially PV cell available [46].

There are many factors that may affect the electricity production of a PV cell. It may be the presence of clouds, the longitude and latitude of the PV cell, the time of the year or the tilt angle of the PV cell. But it should also be noted that the efficiency of the PV cell is affected by the ambient temperature around the PV cell. The principal cause is the change in the open circuit voltage that decreases with the increase in temperature as seen in Figure 21. It should be noted that the short circuit current increases with temperature increase, thus increasing the power slightly. However, the decrease in the open circuit voltage overshadows the increase in the short circuit current [47].

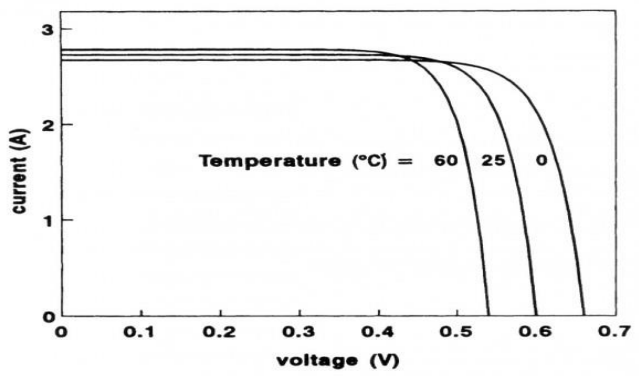

Figure 21. Open circuit voltage and short circuit current are affected by temperature [47].

As mentioned before, the most common PV panel technology is the “crystalline” PV panels that are made of silicon with a crystalline structure. But it should be known

that a silicon structure can also differ, other than monocrystalline molecular structure, there is also amorphous and polycrystalline. These molecular structures of silicon each have a PV panel technology built with them. Other than monocrystalline PV panels, there is polycrystalline PV panels, and thin-film amorphous silicon PV panels. Other than the silicon-based PV panels, there exists other panels with different material semiconductors or with organic based materials [48]. Usually, crystalline PV panels are considered first generation technology, while thin film is considered second generation technology [49].

There are differences between monocrystalline, polycrystalline, and thin film PV modules. One of these differences is that usually monocrystalline is more efficient in converting solar energy into electrical energy compared to polycrystalline and thin film PV modules. But for the cost of each module, it was found that monocrystalline is the most expensive per watt at 1.1$, followed by polycrystalline at 1.06$, and then thin film was the cheapest at 0.84$ [50]. However, some of the advantages of using the lowest efficiency thin film is that it is tolerant to high temperature and low light compared to crystalline modules. Moreover, it requires less materials to manufacture and it is physically flexible [49]. The high heat tolerance makes it suitable for countries situated in a hot climate, such as the Middle East region.

As for the lifespan of PV panels, there was a study done by Reindl et al. to find out the degradation rate in the power production of different PV module technologies. It was found that monocrystalline modules degrade the lowest at 0.8% per year, followed by polycrystalline modules degrading at a 1% per year, and finally thin film degrading at 2% per year [51]. However, most PV module manufacturers offer a guarantee that the PV panels would hold 80% of peak power production for 25 years [52]. Unfortunately, that only matches the degradation of monocrystal modules, which already has the lowest degradations. That means that manufacturers of polycrystalline and thin film modules may not be able to keep a guarantee of 80% in 25 years.

For a PV plant, there are other components other than the PV panels such as, cables and inverters. These components have their own efficiency, and they will cause a power loss from the electricity produced by the PV panels. For the cables, depending on the diameter of the cable or the layout of the plant, the power loss can change. Such as if the cable had a cross-sectional area of 1.5 mm2, 4 mm2, and 10mm2 it would have a power loss of 1.7%, 0.6%, and 0.2% [53]. While a layout can cause losses between 0.8% to 3% depending on the optimization of the layout, which can be said to be 1% [54]. Inverters convert the DC current produced by the PV modules, into AC current that is suitable for injecting into the grid. Therefore, for that conversion there would also be a power loss, which can account to about 3% [53].

Currently, the leader in the PV market is the monocrystalline PV panel, as it has reached 60% of the market share in the year 2018 [46].

2.9 Storage

Some studies have been conducted on the utilization of PV with RO desalination plant. Most of them must decide on how to utilize the solar energy as efficient as possible. One of the areas that are deeply investigated in this topic is what kind of storage is the best to be used [58].

Considering that PV panels only produce energy as long as there is sunlight, during nighttime, the panels will produce no energy, therefore the RO plant will not have energy to produce treated water during the nighttime. One of the ways that most PV projects consider is using a battery to store the electrical energy produced that are in excess of what the RO plant needs, and during the night the stored electrical energy will be used to run the RO plant. Another method of utilizing a storage is the usage of large water tanks to store treated water, where the RO plant will produce a much larger treated water than needed at the time, to compensate for the lack of production during the night. One final way that is getting more popular is the usage of the grid as a battery. The way it works is taking advantage of the net-metering mechanism

that more and more power companies are adopting. Net-metering is kind of a credit system, where if you produced extra electricity from your PV panels, you could feed the extra electricity to the grid, and then when needed, you will have a credit to use electricity from the grid when needed. This way it would be just like having batteries, but without going through the hassle of buying and installing physical batteries, instead having the grid as a "free" battery.

Going for a battery or even a water tank for storage may seem good at first, but the cost of having both of them seem to be more than that of having the grid as a battery. Therefore, the best idea is to feed the energy produced by the PV panels to the grid, and connect the RO plant to the grid, to take power directly from the grid. This method will make the project cheaper and more effective.

Moreover, running having a water tank storage of going battery-less is not optimal for an RO plant. RO systems are meant to run continuously, and a shutdown every time the sun sets is going to complicate things and make the system more expensive and less feasible. Using a tank storage is not impossible, but it may be costly, because when the RO system is shut down, it should stay pressurized and the water inside the water vessels should be of low TDS, mostly the permeate created from the RO is used [57].

2.10 PV Powered SWRO Projects

Saudi Arabia, the biggest producer of desalinated water, has planned and constructed the biggest PV driven SWRO plant in the world. Even though Saudi Arabia is one of the biggest oil producers in the world, powering their SWRO plant with PV panels seemed feasible for the oil rich country [58]. With a PV plant's capacity of 15 MW, the SWRO plant will be able to produce 60,000 m^3/day [59]. The SWRO plant also has the infrastructure to increase the capacity to 90,000 m^3/day [60]. The pretreatment process consists of a DAF process followed by a UF unit. While the 15 MW plant will have one axis trackers to optimize the solar power harvesting [61].

With a specified energy consumption of 3.7 kWh/ m^3, the construction price of the PV-SWRO plant in Al Khafji was estimated to be 152 million euros [62].

One of these studies shows a research institute of a similar size as METU NCC, done in Masdar Research Institute located at Abu Dhabi, UAE [63]. Their feedwater is similar to that of METU NCC. Where their saltwater comes from the Persian Gulf (also known as the Arabian Gulf), having salinity of around 45,000 TDS in that region [64]. However, the study used water having a salinity of around 48,761 TDS. Therefore, it is more than Cyprus' coastal seawater salinity of around 39,100 TDS. And their research has similar goals to this one. The study considered using different methods of energy or water storing, but it was determined that using the grid as a battery would be the best option, by feeding all the power produced by the PV panels to the grid and using the energy later on when needed. This method of saving the energy when it is in excess seems to be the cheapest option for that institute. The RO plant would produce 200 m^3/d with a recovery of 40%, having a single stage with 12 pressure vessels, each containing 8 membrane elements. There was no mention of an energy recovery device. But judging from the SEC of 6.99kWh/ m^3, an energy recovery device was not used. While the PV plant would have a capacity of 720 kW that would also produce extra electricity that would not be used to run the RO plant and therefore sold to the grid. Overall, the feasibility study showed that the cost of the water would be 0.6$/ m^3 with and equity pay back of 23.3 years. Moreover, since PV panels are used, there would be a reduction of 1,035 tons of CO_2 annually. Some of the ideas that were not considered in the study was the location of the plant and the post-treatment options. As the study was done in 2015, it would be interesting to see how the same plant would perform in the year 2021.

Another study was done experimentally in the Greek Thirasia island in the Mediterranean Sea [65]. The study considered two small capacity PV-RO and SR-RO (Solar Rankine-Reverse Osmosis) plant, where the PV would have a capacity of just 846 W. The PV-RO system would run during the daytime, and when there is no sun, the system would not be running. This is due to the system having no battery or storage. It was shown that the price of a meter cube of water changes with the month.

Where in the summer months it would be cheaper than winter months. This is due to the fact that there is more sunlight during the summer months. The SEC of the water with PV-RO was found to be 4kWh/ m^3 over the year due to the presence of an energy recovery device. However, since the study was done in 2006, the prices of both the RO membranes and the PV panels prices were much higher than the current prices. This ended up making the cost of water around 4.47€/ m^3. It should be noted that there was no mention of using any pretreatment processes in this experimental study. Having a pretreatment process before the RO process would increase the energy consumption. Also, the fact that the salinity around the island (having a conductivity of 35 mS/cm) is lower than that of the coastal regions of Cyprus, would make the SEC lower for their RO system.

Another extensive study was done to desalinate brackish water to irrigate crops in the Jordan Valley [66]. The study was done on estimating the cost of water for desalinating brackish water using different membranes and their performance in salt rejection. The PV plant consisted of capacity ranging from 15 to 120 kW. The study compared the price of water with different energy sources compared to PV. The study also compared the price of water for different parameters such as: the type of membrane used, effect of static head, feedwater salinity, inverter configuration, energy recovery inclusion, and single and two stage RO plant configuration. The effect of each parameter was considered and placed in a sensitivity analysis chart that shows how much the water price is affected by these parameters.

A study was done on the feasibility of using a PV-RO system to produce water was done by MIT [66]. The feasibility study considered its model in other locations of the world. Using different parameters such as total insolation in a day of each location, salinity, and daylight hours. Using these parameters, the feasibility of having a PV-RO system instead of a Diesel engine run RO system was determined for locations around the world. It was shown that the region of Northern Central Africa, South Africa, the Middle East, and Australia to be feasible to have a PV-RO system instead of the RO system being run by a Diesel engine. This feasibility study was done in 2010, where the price of PV was 2.04$/W while in 2019 the price was

0.38$/W [67]. Using the new price, it is expected for many more regions to have PV-RO to be feasible.

As for TRNC, there are a few desalination plants in the country, otherwise the use of desalination is limited in TRNC. One desalination plant for hotels in the Karpaz region is estimated to produce 2000 m^3/day with a cost of 0.95 USD/m^3 [70]. While two desalination plants at the coastline would cost 0.7 and 0.84 USD/m^3 for capacities of 1000 and 2000 m^3/day, respectively. While, in the southern part of the island, desalination plants have been used in a great extent to produce fresh water. Where the total freshwater produced by desalination plants accounts for 65 million m^3/year. Where the average cost of the desalinated water is around 1.08 Euros/m^3, while the SEC is estimated to be 4 kWh/m^3. There is a lack of studies available in the literature that discusses the use of solar power or renewable energies coupled with reverse osmosis plants. However, one study showed that the total energy requirement of RO produced water, that meets the municipal water demand of TRNC, can be provided with 0.25 km^2 and 0.70 km^2 of PV panels area for brackish and salt water, respectively [71].

CHAPTER 3

STUDY AREA AND DATA

3.1 Solar Resources in TRNC and METU NCC

Northern Cyprus being situated in the Eastern Mediterranean, makes it rich in solar resources. For an average year, Northern Cyprus receives between 1900 kWh/m^2 to 2100 kWh/ m^2 for the whole year, thus making solar energy a very useful resource to be taken advantage of in this region [68]. As for the campus, the data collected for 10 years in the campus revealed that the campus receives around 1950 kWh/m^2 global horizontal irradiance (GHI) a year [68]. Comparing the GHI of Cyprus with that of the leading European country in PV capacity, Germany. Germany has a GHI of 1066 kWh/m2 [69]. In other words, if the PV capacity of Germany was installed in Northern Cyprus, it would produce up to 80% more electricity without considering the effect of temperature and wind speeds of Northern Cyprus.

Between the years 2003 and 2017, the typical metrological year (TMY) data was measured. TMY data has many weather parameters that are the average of all these years it was measured in. It includes the data for the global horizontal irradiance (GHI), direct normal irradiance (DNI), and diffuse horizontal irradiance (DHI). Out of these three parameters, DNI can be argued to be the most useful to work with. For the case of concentrating solar power (CSP) panels, DNI is the only variable that affect the performance of the CSP. But for the case of PV panels, DNI and DHI both affect the performance of the PV panel. DNI depends on the location of the PV panel and whether there is a shadow, or more importantly, a cloud blocking the sun for that PV panel. While DHI depends highly on the diffuse effect of the clouds and molecules in the atmosphere. Using the TMY data, the average daily DNI in each month was obtained and plotted on Figure 22.

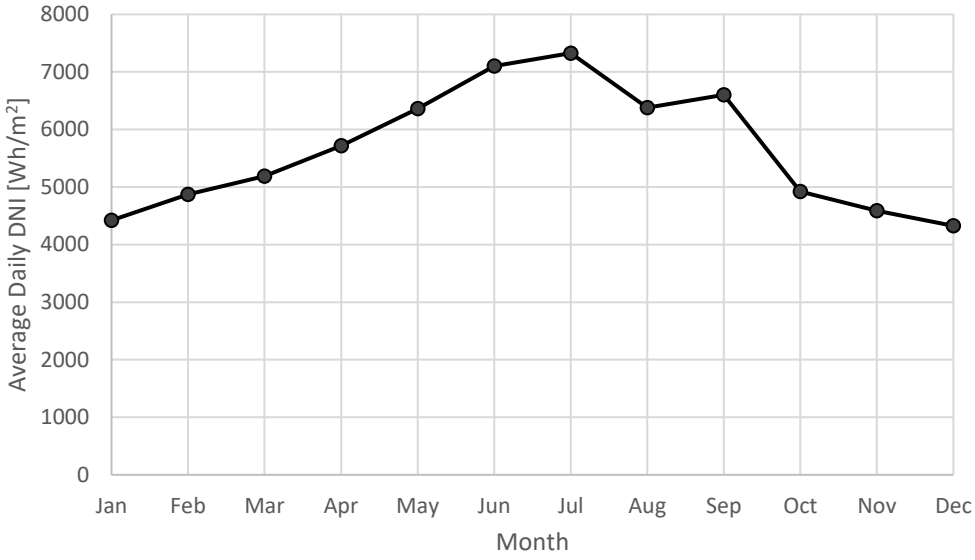

Figure 22. The monthly average daily DNI in METU NCC between the years 2003-2017.

3.2 Air and Sea Temperatures in METU NCC

Air temperature is an important factor for solar PV panels, because it affects the efficiency of the PV panels, where the higher the air temperature is, the lower the efficiency of the PV panel is. Yearly average air temperature in Northern Cyprus ranges from 20-24 °C [68]. While the campus has a yearly average temperature of 15.9 °C with a median of 17.4 °C. The reason the yearly average is lower than that of source [68] is that the campus is built on top of a hill and the space around the campus is not built on, i.e., open fields. This makes the campus a great place to install PV panels to harness solar energy.

Considering the RO process, it is known that sea water temperature affects the RO process, it is important to know the seawater temperature. The average sea water temperature varies during the year in Guzelyurt. The annual average around the coast is about 22.1 °C. While the minimum and maximum temperatures are 15 and 30 °C, which occurs in March and July respectively [70].

3.3 Water Demand of METU NCC

Over the period of 7 years from 2014 to 2020, the amount of water used by the university's buildings did not seem to vary much between the years, usually ranging between 100-113 tons of water per year. The only exception is the year 2020 where the COVID-19 pandemic was ongoing, and the education shifted to online education. In Table 4 the amount of water used by the buildings can be seen.

Table 4. The total and maximum consumption of water in the university's buildings between the years 2014-2020.

Year	2014	2015	2016	2017	2018	2019	2020
Total consumption [Tons]	107019	106012	101897	110456	101765	113281	77768
Month of maximum consumption	Mar	Dec	Dec	May	Dec	Jun	Apr
Maximum consumption [Tons]	14463	13070	13158	14496	12750	15224	12740

And the total consumption of each month of these years can be seen in Figure 23. The data in grey are the ones from the year 2020 where the pandemic reached the island. That year the education was conducted remotely. Therefore, not many students resided in the campus.

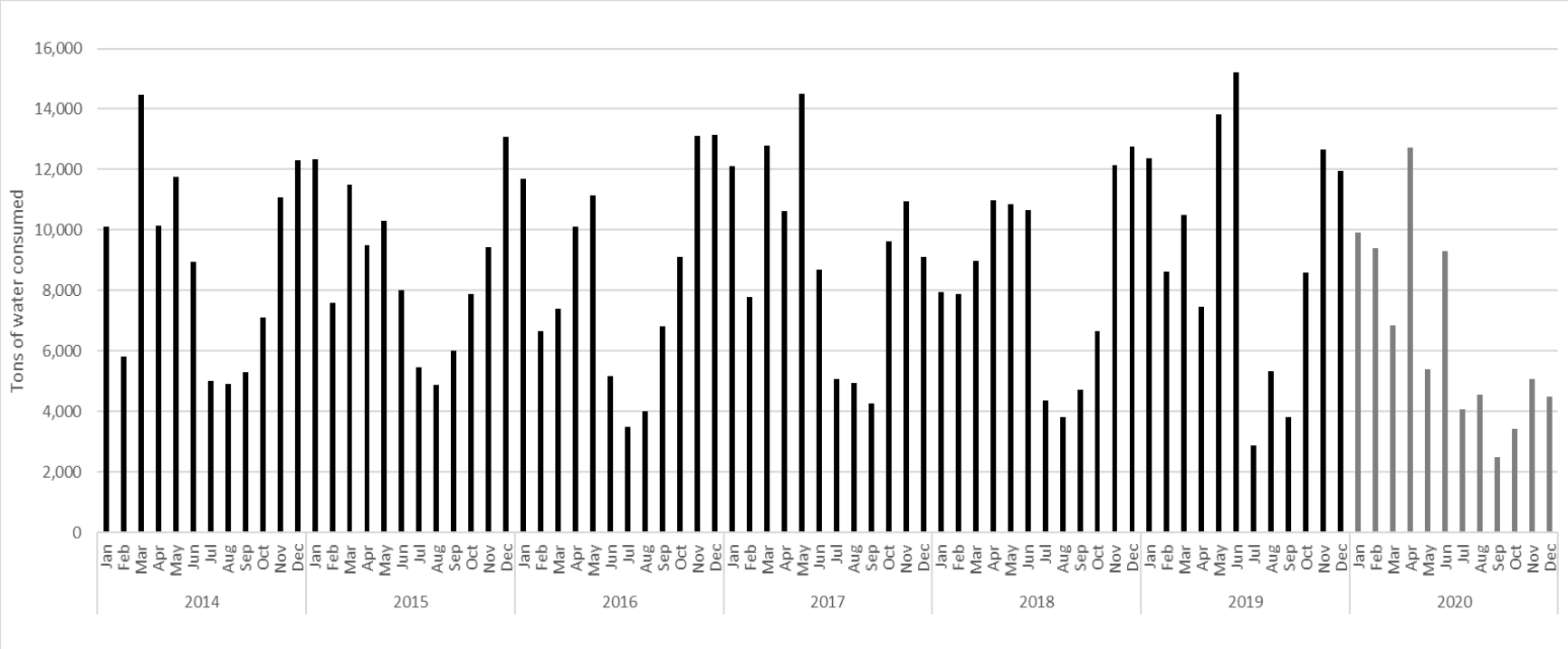

Figure 23: The tons of water consumed in the university's buildings over the 7 years period from 2014-2020

As can be seen from Table 4 and Figure 23 there is no obvious pattern in the months with maximum consumption, except that December seems to be the month with most frequent maximum consumption. This should be taken into considerations in the design of the capacity of the desalination plant. Because the maximum consumption and the month of the maximum consumption seem to be unpredictable.

Looking at Table 4 and Figure 23, the maximum annual consumption was 113,281 tons of water, while the maximum monthly consumption was 15,224 tons of water and both consumptions were in the year 2019. It appears that the water consumption of the month of June 2019, is around 161% of the average monthly consumption of the year 2019. Therefore, not all months would have the average monthly consumption of their year. In Table 5, it is shown how much the consumption of the maximum month differs from the average monthly consumption for each year.

Table 5. The ratio of maximum monthly consumption.

Year	2014	2015	2016	2017	2018	2019	2020
Total	107019	106012	101897	110456	101765	113281	77768
Monthly Average	8918	8834	8491	9205	8480	9440	6481
Max value	14463	13070	13158	14,496	12750	15224	12740
Max month	Mar	Dec	Dec	May	Dec	Jun	Apr
ratio of maximum monthly consumption to a monthly average [%]	162.17	147.95	154.96	157.49	150.35	161.27	196.59 *

*The year 2020 is an outlier, because the first semester in the calendar year was done face to face, while the second semester was done remotely.

Apart from the year 2020 which is an outlier, the maximum monthly consumption ranges from around 148% to 162%. This range is below the recommended addition of 180% of the maximum annual water consumption according to [71]. Nevertheless, there shall be hours which exceed the hourly average of an annual consumption by

more than 180%, up to 260% [72]. But it does not make sense economically to prepare for that peak consumption. Some ways to be able to meet the demand includes getting the water from the government, or a better solution is to use a storage tank to store a one- or two-days' worth of permeate. The latter seem to be a more optimum solution.

Using the 180% maximum annual water consumption recommendation, the capacity of the plant should be around 204,000 m^3 per year. Which is around 558.9 m^3 per day, or about 23.3 m^3 per hour.

Over the past 7 years, no significant increase in water usage has been observed. Therefore, the plant should be able to provide for the buildings of the campus over the lifetime of the plant. Moreover, if more water is needed, the plant will be retrofittable, which will make it easy to expand the capacity of the RO plant.

METHODOLOGY

With the decrease in PV panel prices, it makes the usage of PV panels with desalination technologies has become very attractive. And the best technology to use it with is RO desalination. This is due to the fact that PV produces electrical energy, and RO desalination needs electrical energy only to run the pumps. Moreover, RO is the one conventional technology with the least SEC. This makes coupling PV and RO a very strong method of producing fresh water using a renewable energy source. And just like PV cells, RO desalination plants are also scalable, which can range from a few to hundreds of thousands of cubic meters of fresh water produced a day. And since METU NCC campus is relatively small in size compared to other communities, only a relatively small desalination plant is needed, which makes PV and RO the best technologies to use for desalinating seawater to meet the demand.

4.1 Reverse Osmosis Methodology

4.1.1 Modeling equations for RO

- **Recovery**

One of the most important attributes in an RO desalination system is its recovery rate of the permeate. In other words, how much permeate is produced from a certain flow of feed water. Usually, BWRO recovery is around 70-97% while SWRO is around 35-45% [73]. It is shown in percentage. The equation of the permeate recovery is calculated using Equation 1 [10].

$$\%R = \frac{Q_p}{Q_f} = \frac{Q_p}{Q_p + Q_c} \qquad \text{Equation 1}$$

Where %R is the percent recovery rate of the permeate, Q_p the flow rate of the permeate, Q_f the flow rate of the feed, and Q_c the flow rate of the concentrate.

- **Salt Rejection**

Salt rejection is a characteristic of the membrane itself. However, it can be affected by external factors such as the temperature of the feedwater and the condition of the membrane whether it has fouling or not. Just like the name suggests, salt rejection is the amount of salt that is "rejected" or does not pass the membrane onto the permeate. {talk about the usual salt rejection of membranes for brackish and saltwater}. It can be calculated by looking at the difference between the concentration of salt in the permeate and that of the feedwater as shown in Equation 2. It is usually given by the producer of the membranes and is shown in percentage. [10]

$$\%\ Rejection = \frac{C_f - C_p}{C_f} \qquad \text{Equation 2}$$

Where C_f is the feed's salt concentration and C_p is the permeate's salt concentration.

Salt passage is a parameter that is related to salt rejection, and it is the opposite of salt rejection. It is the amount of salt that passes to the permeate Equation 3 [10].

$$\%\ Salt\ passage = 100 - \%rejection \qquad \text{Equation 3}$$

- **Osmotic Pressure**

As mentioned before the osmosis process would have an osmotic pressure associated to it depending on the concentration of salt in the solute. It is important to know the osmotic pressure of the feedwater in order to exceed it. Once exceeded the water will flow on the opposite direction of the natural osmosis process, albeit the reverse osmosis process. The osmotic pressure can be calculated using Equation 4 [78].

$$\pi = R(T + 273.15)\sum(m_i) \qquad \text{Equation 4}$$

Where π is the osmotic pressure, R is the universal gas constant, T is the temperature in Celsius, and $\sum(m_i)$ is the summation of molar concentrations of all the salts or solubles.

A simplification of Equation 4 can be used instead, Equation 5 uses the total dissolved solids of the solution instead, making it easier to get the osmotic pressure. However, it is an approximation [75].

$$\pi = 0.77\left(\frac{TDS}{1000}\right)[bars] \qquad \text{Equation 5}$$

Where TDS is the total dissolved solids of the solution. Keep in mind that using Equation 5 will give the osmotic pressure in bars.

- **Average Feed Salinity and Average Feed Osmotic Pressure.**

Since the design of RO systems usually uses spiral membrane elements (show diagram of the salt gradient in spiral elements), there would be a salt concentration gradient along the element's length, and also along the pressure vessel's length as shown in Figure 24.

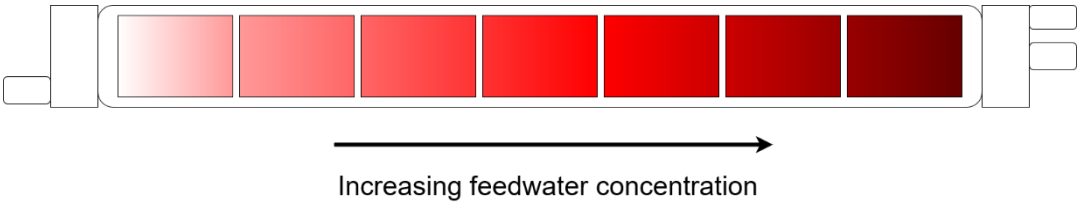

Figure 24. The feedwater concentration gradient along an RO pressure vessel.

This causes the salt concentration to be different depending on the location where the water is passing through the membrane along the length of the element. Because of that difference, the average feed salinity will be used, it will estimate the salt concentration in the feedwater in the element as a whole. To do that the average feed salinity can be calculated using Equation 6 [78].

$$AFS = 0.5(C_f + C_c) = 0.5C_f(1 + \frac{1}{1-R}) \qquad \text{Equation 6}$$

Where AFS is the average feed salinity.

Using AFS the average feed osmotic pressure can be obtained using Equation 5. That average feed osmotic pressure is the osmotic pressure that is usually used in the calculations of other equations.

- **Net Driving Pressure**

As mentioned before, once the osmotic pressure is exceeded, the pressure will force the water to go through the reverse osmosis process. However, osmotic pressure is not the only pressure that should be exceeded. Other pressures such as the pressure drops between each element, permeate back-pressure, and the permeate osmotic pressure should be accounted for. The net driving pressure (NDP) would then be the pressure at which the feedwater is driven with, passing through the membrane element. It would account for the osmotic pressure of the feedwater as well as the other pressures mentioned. The NDP can be calculated using Equation 7 [78].

$$NDP = P_f - \bar{\pi} - P_p - 0.5P_d + \pi_p \qquad \text{Equation 7}$$

Where P_f is the feedwater pressure, $\bar{\pi}$ is the average feed osmotic pressure, P_p is the permeate back-pressure, P_d is the pressure drop between membrane elements, and π_p is the permeate osmotic pressure.

It should be noted that usually the osmotic pressure of the permeate is negligible as it would be very small. Additionally, if the permeate is introduced to an open storage tank, the permeate back-pressure would be zero.

- **Concentration Polarization**

After the salt is rejected by the membrane, there would be a boundary layer that forms on top of the membrane surface. This boundary layer will have increased salt concentration as compared to the feedwater that is outside the boundary layer. Figure 25 should clarify the concentration polarization phenomenon.

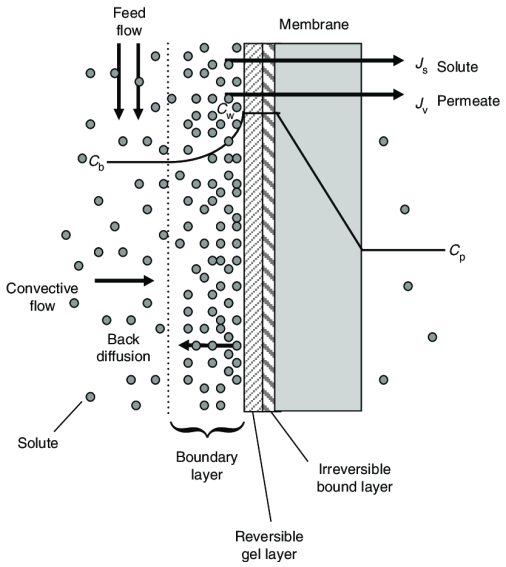

Figure 25. Concentration polarization on a membrane with fouling [31].

The concentration polarization affects the performance of the RO membrane. negatively. Such as [74][25]:

- It decreases the permeate flow Q_p because it causes a hydraulic resistance.
- It increases the flow of salt into the permeate.
- It increases the osmotic pressure at the membrane's surface and with that decreases the NDP.
- It can cause scaling and fouling due to the salt exceeding the solubility limit, where the salt would precipitate at the membrane's surface.

To quantify the effect of concentration polarization, concentration polarization factor (CPF) is used. It is a ratio of the salt concentration at the membrane surface and the bulk concentrations. It is calculated using Equation 8.

$$CPF = \frac{C_s}{C_b} \qquad \text{Equation 8}$$

Where C_s is the concentration at the membrane's surface, and C_b is the bulk concentration.

However, it is difficult to obtain the concentration at the membrane's surface. So instead, Equation 9 can be used [78].

$$CPF = K_p exp\left(\frac{Q_p}{Q_f}\right) = K_p exp\left(\frac{2R_i}{2 - R_i}\right) \qquad \text{Equation 9}$$

Where K_p is a constant that is affected by the membrane's geometry and dimensions. While R_i is the membrane element's recovery.

- **Temperature Correction Factor**

Since temperature plays a role in the performance of the system. It is important to know the effect of the temperature on the membranes. Such effect can be called the TCF (Temperature Correction Factor). The reference temperature is set at 25 °C where the TCF would be 1. Otherwise for other temperatures, the TCF can be calculated using Equation 10. [76]

$$TCF = \begin{cases} EXP\left[2640\left(\frac{1}{298} - \frac{1}{273 + T}\right)\right] \; For\; T \geq 25\,°C \\ EXP\left[3020\left(\frac{1}{298} - \frac{1}{273 + T}\right)\right] \; For\; T < 25\,°C \end{cases} \qquad \text{Equation 10}$$

- **Average Permeate Flux**

Average permeate flux is an important parameter for designing the RO plant. Usually, when the engineer responsible for designing the RO system, they set an average permeate flux for the system that it would follow. It is also called the "design flux". The average permeate flux expresses the amount of permeate produced per

meter square of a membrane element's surface area. It can be calculated using Equation 11 [78].

$$APF = \frac{Q_p}{N_E \cdot S_E} \qquad \text{Equation 11}$$

Where APF is the average permeate flux, N_E is the number of elements, and S_E is the surface area of the element.

- **Water Passage**

The water passage may be the most important parameter of an RO system along with the permeate's salt concentration. Simply put, the water passage is the amount of permeate that is produced by passing the feedwater through the membrane of the element. It can be calculated using Equation 12 [78].

$$Q_p = A \cdot S \cdot NDP \cdot CPF \qquad \text{Equation 12}$$

Where A is the water transport coefficient of the membrane. It can also be called the water permeability of the membrane.

- **Permeate Salinity**

To calculate the permeate salinity of a single element, Equation 13 is used.

$$C_p = \frac{AFS \cdot B \cdot S}{Q_p} \cdot CPF \qquad \text{Equation 13}$$

- **Concentrate Salinity**

To calculate the concentrate salinity of a single element, the conservation of mass theory was employed as shown in Equation 14.

$$C_c = \frac{AFS \cdot Q_f - C_p \cdot Q_c}{Q_c} \qquad \text{Equation 14}$$

- **Energy Recovery**

For energy recovery, the energy of the fluid is required for both the feed and the concentrate. That way, there would be an energy transfer from the concentrate to the feed's fluid energy as follows in Equation 15 [81].

$$\eta_{ERD} = \frac{Q_{fo} \cdot P_{fo} + Q_{co} \cdot P_{co}}{Q_{fi} \cdot P_{fi} + Q_{ci} \cdot P_{ci}} \qquad \text{Equation 15}$$

Where η_{ERD} is the ERD's average efficiency, P is the pressure of the fluid, and Q is fluid's flow rate. While the subscript fo is the feedwater at outlet, fi is feedwater at inlet, co is the concentrate at outlet, and ci is the concentrate at inlet of the ERD.

With having the knowledge of the efficiency of the ERD, inlet feed properties, inlet concentrate properties, outlet concentrate properties, and outlet feedwater flow rate. The feedwater pressure at the inlet can be obtained.

4.1.2 RO Plant Design

- **Pretreatment**

The pretreatment options that are available are comparable. But for this RO plant, the pretreatment option would be done using conventional pretreatment. Mostly for because it is a cheaper option. Moreover, there are algae that grow up from time to time during the year at the intake beach, Akdeniz beach. Therefore, using a UF pretreatment would cause a lot of biofouling, hence the usage of conventional pretreatment consisting of DAF and MMF. The process of pretreatment can be seen in Figure 26. And chlorine will be added before the pretreatment process.

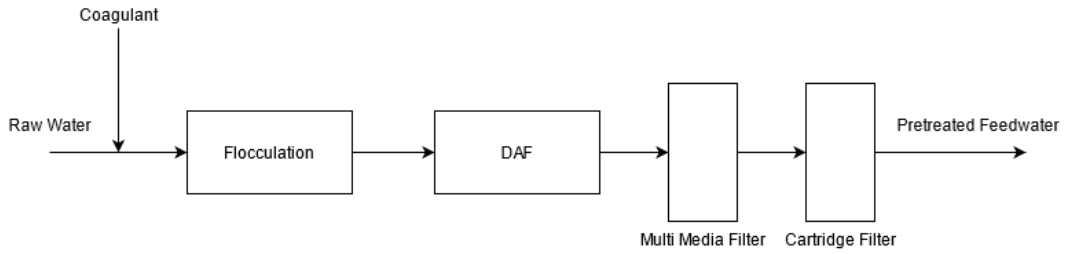

Figure 26. The pretreatment process.

- **RO Layout**

For RO plant design, a program developed by DuPont called WAVE was used. Using the program, several projections were carried out by optimizing process parameters. Two configurations were brought up to be the best, and they are presented here.

As for the RO plant's layout, the needed permeate would need a boron concentration of lower than 1 mg/L according to the European Commission. Therefore, a two-pass layout is needed, in which NaOH is added before the second pass to improve boron rejection. As for the membrane types, the first pass would have SWRO membranes, while the second pass will have BWRO membranes. The membranes to be used are SW30HRLE-440i™ and SEAMAXX-440i™ for the SWRO membranes, while XLE-440i™ is used for the BWRO membranes. The membranes are FilmTec™ membranes produced by DuPont.

Another configuration that shall be considered is the usage of a single pass two stage RO system. Using this configuration would result in a water quality that is worse than that of the double pass configuration. However, after optimizing it, the quality can be acceptable at under 500 TDS which matches the recommendation by WHO [77].

The number of stages in the RO plant affects the performance of the RO plant. One stage layout has the advantage of having less capital cost, but a two-stage layout has more recovery and is more energy efficient considering the SEC. For the two-pass layout, it will only be applied to the first pass.

Moreover, since an ERD is also essential in order to reduce the energy required to run the plant. It will be considered in the configurations. A comparison of both the configurations with and without ERD will be considered to see how effective it works.

- **Double Pass Configuration**

For the first configuration, the plant layout with an ERD can be seen in Figure 27. While without ERD it can be seen in Figure 28.

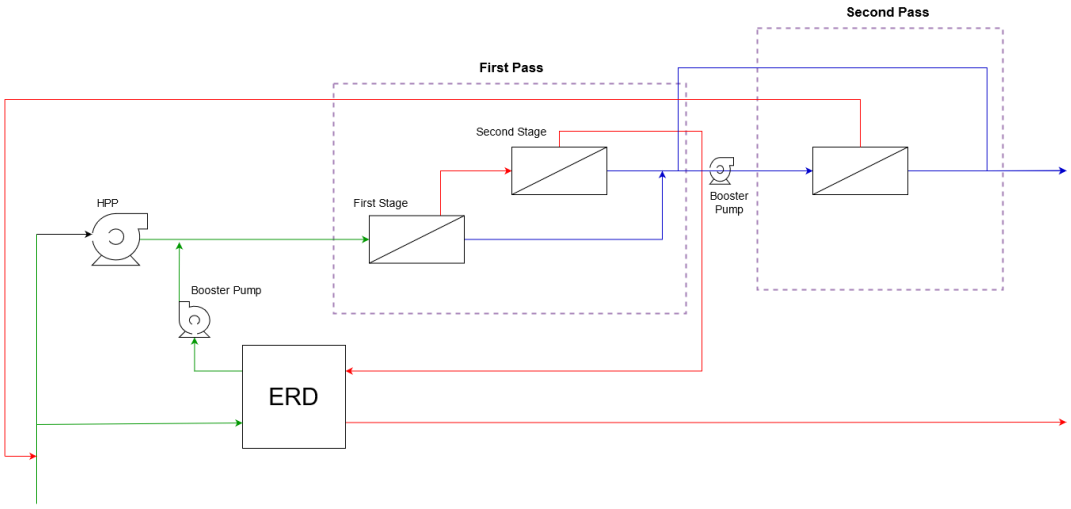

Figure 27. Double pass configuration, two stages first pass, one stage second pass with an ERD, where green is feedwater, blue is permeate, red is concentrate.

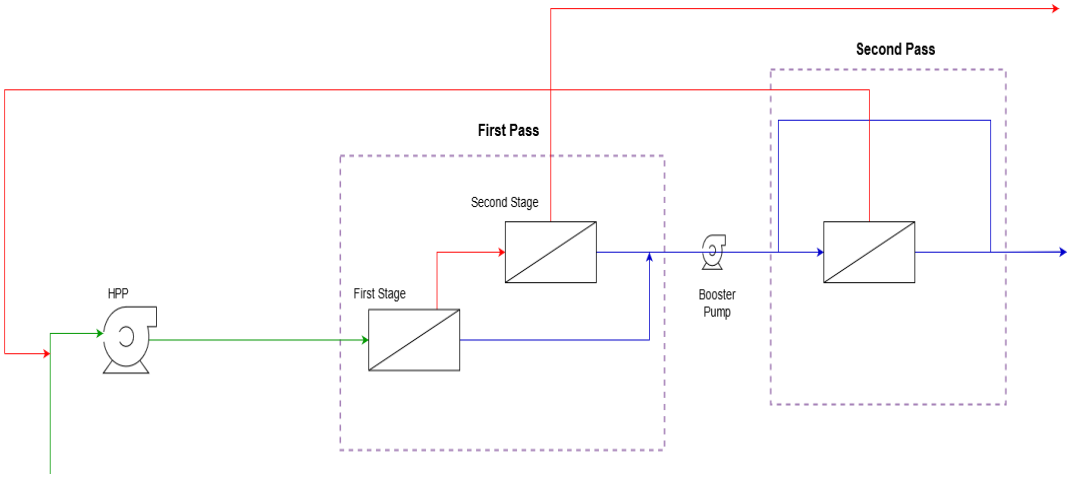

Figure 28. Double pass configuration, two stages first pass, one stage second pass without an ERD, where green is feedwater, blue is permeate, red is concentrate.

For this configuration, an internally staged design (ISD) would be implemented for the first stage of the first pass. It would use SW30HRLE-440i for the first three membranes in the pressure vessel, while the other four would be SEAMAXX-440i membranes. It can be better understood by looking at Figure 29.

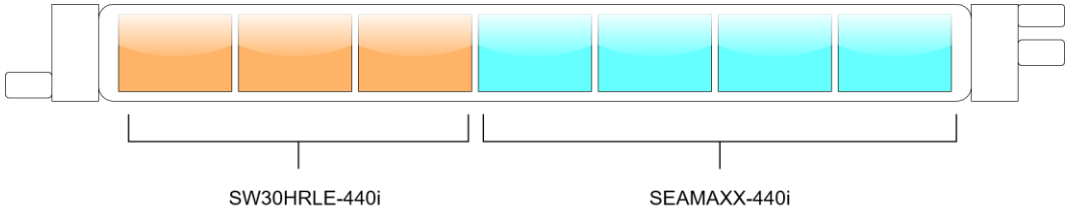

Figure 29. The internally staged design of the first stage vessels of the first pass.

As for the second stage in the first pass, the membranes used would be SEAMAXX-440i for all membranes in the pressure vessel.

Before the feedwater enters the first pass, HCl is added to prevent the scaling risk.

As for the second pass, XLE-440i BWRO membranes would be used. Before the water enters the second pass, NaOH is added to increase the pH which will improve the boron rejection. The increase in pH will cause some scaling risk, therefore antiscalant is also added. Moreover, a percentage of the permeate from the first pass would bypass the second pass to the product of the RO plant.

- **Second Configuration**

The second configuration would only have one pass and two stages. Both of the stages would use SW30HRLE-440i membranes in all the pressure vessels. The configuration's layout with an ERD can be seen in Figure 30. While without an ERD it can be seen in Figure 31. Before the feedwater enters the RO membranes, NaOH is added to improve boron rejection, while antiscalant is added to prevent scaling.

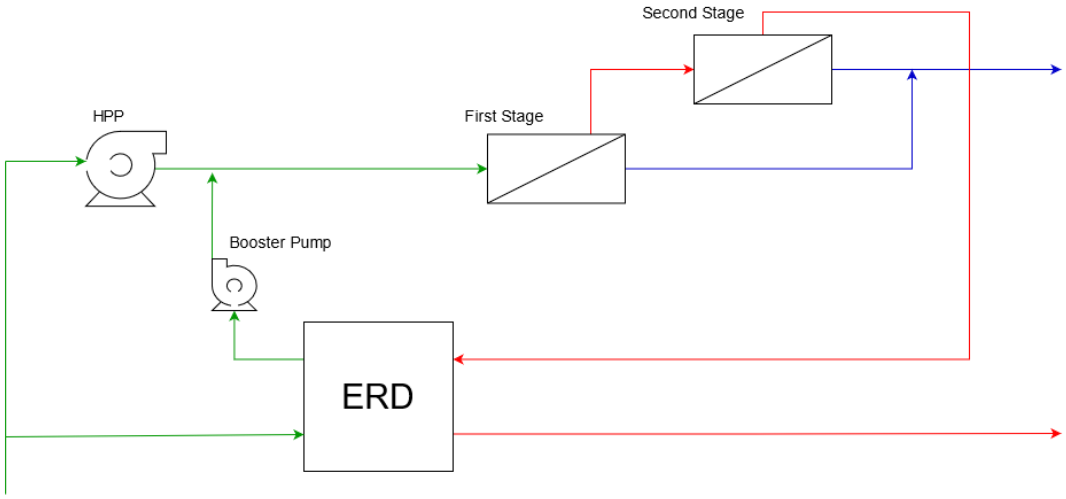

Figure 30. Single pass configuration, two stages single pass with an ERD, where green is feedwater, blue is permeate, red is concentrate.

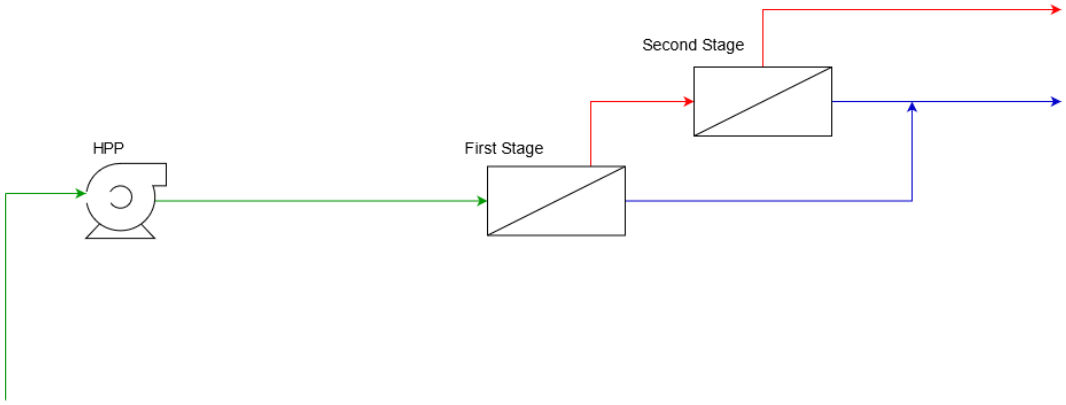

Figure 31. Single pass configuration, two stages single pass without an ERD, where green is feedwater, blue is permeate, red is concentrate.

- **Posttreatment**

After the RO process, the pH will need to be adjusted to drinkable levels. To do that, hydrated lime and CO_2 will be used to adjust the pH. Moreover, the permeate will need to be disinfected with chlorine.

4.2 PV Methodology

4.2.1 Modeling Equations for PV

The position of the Sun is of utmost importance for those who want to make the most effective use of their solar panels. As the amount of solar energy that strikes an arbitrary area on Earth depends highly on the position of the sun and the position of that said area, whether it is inclined, horizontal, or vertical. Moreover, the inclination or the direction of inclination is going to affect the average solar energy absorbed greatly.

Most of these geometries are going to be angles related to the sun's position. Mostly in relation to the Earth's North and South directions.

Therefore, there should be a clear understanding over where the Sun would be in any given time or the geometry of the solar panel used, in order to produce the highest amount of energy efficiently by positioning the PV panel to the best position.

- **Solar Time**

Solar time indicates the location of the sun on the sky. If it is noon at solar time that means the sun is at its highest position in the sky. Solar time is important in the calculation of the geometric position of the sun related to the specified location. Solar time is denoted as t_s and the way to calculate it is using Equation 16 [82].

$$t_s = t_{std} + \frac{4(L_{std} - L_{loc}) + E}{60} \qquad \text{Equation 16}$$

Where t_{std} is the local time, which is converted to decimal, 24h display. It should be noted that the daylight-saving time should not be considered, and only the non-daylight-saving time should be considered. As for the L_{std} and L_{loc} they are the standard meridian for the local time zone and the longitude of the location

respectively, both in degrees. E denotes the equation of time, in minutes. E can be calculated using Equation 17 [82].

$$E = 229.2[7.5 \times 10^{-5} + 0.001868\cos(B) - 0.032077\sin(B) - 0.014615\cos(2B) - 0.04089\sin(2B)] \quad \text{Equation 17}$$

Where B is calculated in Equation 18 [82].

$$B = (n-1) \cdot \frac{360°}{365} \quad \text{Equation 18}$$

Where n is day of the year, ranging from 1 to 365.

- **Zenith Angle, Solar Altitude Angle and Solar Azimuth Angle**

The direction of beam radiation is crucial for the calculation of the energy absorbed by the solar panel. Most importantly, the calculating of all these sun related angles, is to get the angle of incidence.

The first angle to be started with is the zenith angle. Zenith angle is the angle between normal of the horizon and the beam radiation of the sun. It should be noted that when the zenith angle is above 90° it means that the sun is below the horizon.

The solar altitude angle is just the compliment of the Zenith angle. It should be noted that if the solar altitude angle is negative, that means the sun is below the horizon.

Another important angle is the solar azimuth angle. The solar azimuth angle is the angle enclosed by the South and the sun's beam projection on the horizontal plane. Both the zenith angle, solar altitude angle and the azimuth angle are denoted by Greek alphabets which are θ_z, α_s and γ_s respectively. A comprehensible way of showing the zenith angle and the solar azimuth angle can be seen in Figure 32.

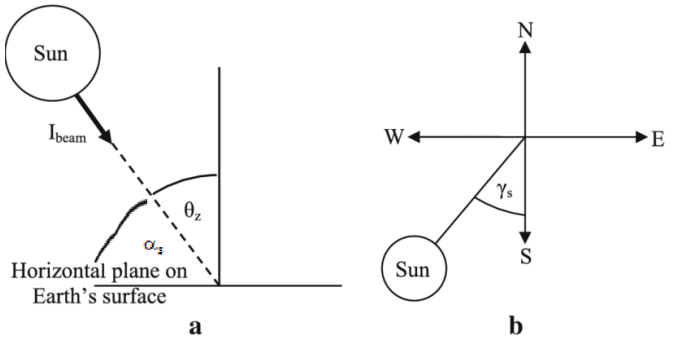

Figure 32. a) The zenith angle and solar altitude angle. b) The solar azimuth angle [78].

- **Latitude**

Latitude lines are imaginary horizontal circles that define the location with respect to the equator. The equator has an angle of 0°, while approaching the north goes into the positive where the North pole is considered as 90°. On the other hand, towards the South it is negative, therefore the South pole is -90°. It is denoted by the Greek letter φ.

- **Declination Angle**

The declination angle is defined as the angle between the sun and the equator at solar noon. The reason there is a declination angle is because of the obliquity of the Earth. Thus, the declination angle cannot exceed the tilt value in both directions. Therefore, the declination angle is confined between -23.45° and 23.45°. The declination angle reaches the extremities in the summer and winter solstices (23.45° in the summer solstice and -23.45° in the winter solstice), while it is 0° at the two equinoxes. The declination angle is denoted by the Greek letter δ. To calculate the declination angle, Equation 19 is used [82].

$$\delta = 23.45 \sin\left[360° \cdot \left(\frac{284 + n}{365}\right)\right] \qquad \text{Equation 19}$$

Figure 33 illustrates the declination angle to ease the comprehension of what the declination angle is.

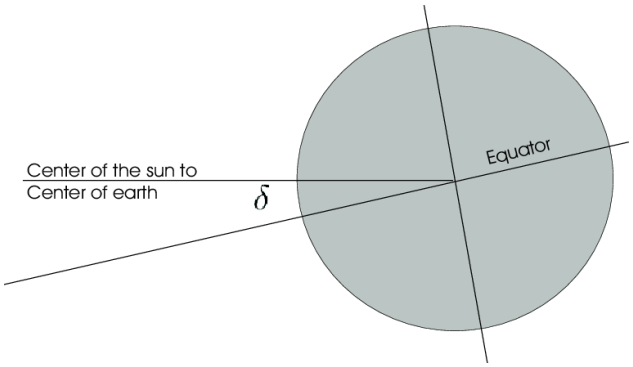

Figure 33. The declination angle [79].

- **Hour Angle**

The hour angle is the angle between the meridian (longitude) parallel to the sun and the meridian of the concerned location as shown in Figure 34. In other words, it can be defined as the solar time in terms of angles. The hour angle increases by 15° an hour, where at the morning it is a negative angle, while in the afternoon it is a positive angle. At solar noon, the hour angle is 0°. The hour angle is denoted by the Greek letter ω and can be calculated using Equation 20 [82].

$$\omega = (t_s - 12) \times 15° \qquad \text{Equation 20}$$

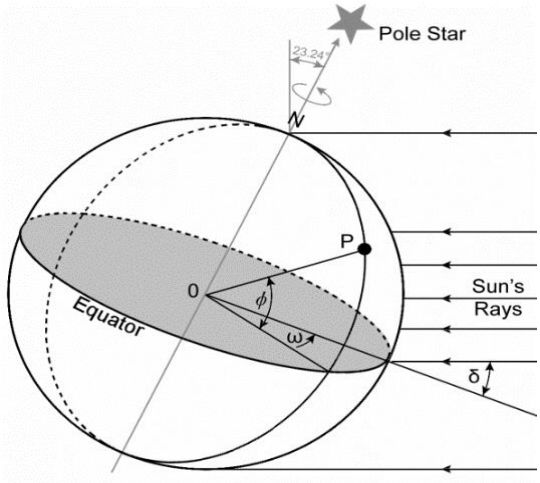

Figure 34. The hour angle on Earth with respect to the sun's rays. [80]

- **Tilt Angle and Surface Azimuth Angle**

Tilt angle and surface azimuth angle are the two angles that apply to an arbitrary surface on Earth. It does not have anything to do with the sun. However, these two angles affect the magnitude of the sun's radiation hitting said arbitrary surface. The tilt angle is the angle between the surface and the horizontal ground, while the surface azimuth angle is the angle between the projection of the surface's normal on the horizontal ground and the South. It should be noted that the tilt angle cannot exceed 180° and is always positive. Moreover, the surface azimuth angle is defined between -180° and 180° where it would be negative to the East of the South, while being positive to the West of the South. Both the tilt angle and surface azimuth angle are illustrated in Figure 35 as β and γ respectively.

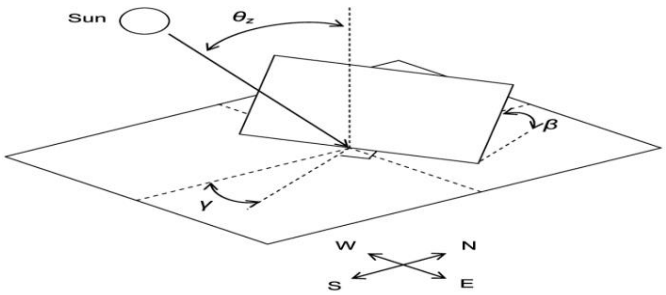

Figure 35. The tilt angle and the surface azimuth angle of a flat surface along with the zenith angle. [81]

- **Angle of Incidence**

The angle of incidence, which is denoted by the Greek letter θ, is defined as the angle between the solar rays on a surface and the surface's normal as seen in Figure 36. This angle is very essential in the design of solar panels as it is the value when minimized the total energy incident on the surface would be maximized. The angle of incidence can be calculated using Equation 21 [82].

$$\theta = \cos^{-1}(cos\theta_z \cdot cos\beta + sin\theta_z \cdot sin\beta \cdot \cos(\gamma_s - \gamma) \quad \text{Equation 21}$$

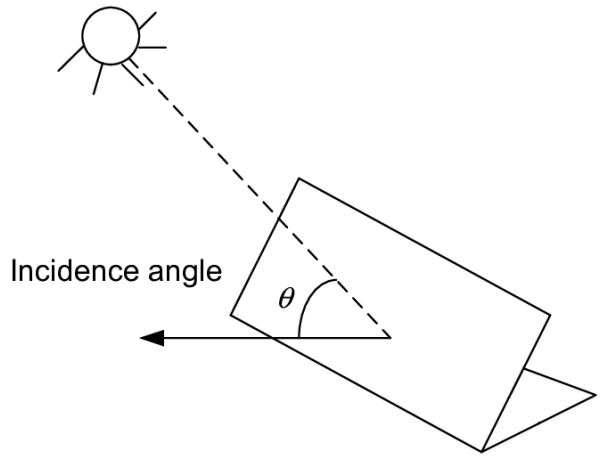

Figure 36. The incidence angle (angle of incidence) between a flat surface and the sun. [82]

- **Solar Resources**

The source of the energy that the PV cells harvest is the solar radiation as mentioned before. The amount that the solar radiation hit on a surface on Earth differs from the amount that hits a similar sized area before entering the atmosphere. It also depends on the time of the year. Therefore, to calculate the extraterrestrial radiation on a certain day of the year, Equation 22 is to be used [82].

$$G_{on} = G_{sc}\left[1 + 0.033\cos\left(\frac{360°n}{365}\right)\right] \qquad \text{Equation 22}$$

Where G_{on} is the normal extraterrestrial irradiance, G_{sc} is the solar constant which equals 1367 W/m^2 and n is the day number of the year.

However, there are some attenuations that happen to the solar radiation due to some scattering of the rays when the rays hit some air molecules and such. This type of scattering is called Rayleigh scattering. Moreover, some of the radiation is absorbed by some molecules in the atmosphere like ozone, carbon dioxide or water vapor.

- **Terrestrial Solar Radiation Component**

Due to the scattering mentioned in the paragraph above, there are some rays that are not directly parallel to the sun's normal. These rays are either diffused rays or reflected rays. Diffuse rays are reflected by the molecules in the atmosphere, while the reflected rays are reflected by objects found on the surface of the earth such as buildings and mountains. Therefore, the solar radiation hitting the surface of the Earth has 3 components which are, beam radiation which is directly coming from the sun, diffuse radiation and reflected radiation.

The way the diffused radiations are considered in this project is by applying an isotropic diffuse sky model, which assumes that radiation is with the same magnitude coming from all angles surrounding a tilted surface.

To find the beam radiation hitting a tilted surface, the normal radiation (DNI) is multiplied by the cosine of the angle of incidence as shown in Equation 23 [82].

$$G_{bT} = G_{b,n}\cos(\theta) \qquad \text{Equation 23}$$

Where θ is the angle of incidence, the subscript T stands for tilted, the subscript b stands for beam and the subscript n stands for normal.

As for the diffused radiation, using the isotropic diffuse sky model mentioned before, one can calculate the diffuse irradiance using Equation 24 [82].

$$G_{dT} = G_d\left(\frac{1+\cos(\beta)}{2}\right) \qquad \text{Equation 24}$$

Where β is the tilt angle, the subscript dT stands for diffused on a tilted surface, and the subscript d means diffused on a horizontal surface.

The reflected irradiance will not be considered in this paper.

The hourly beam and diffuse insolation follow a similar equation to Equation 11 and 12 as can be seen from Equation 25 and Equation 26 [82].

$$I_{bT} = I_{b,n}\cos(\theta) \qquad \text{Equation 25}$$

$$I_{dT} = I_d\left(\frac{1+\cos(\beta)}{2}\right) \qquad \text{Equation 26}$$

Where I stands for the hourly insolation.

Using both the direct and the diffuse irradiance or insolation, the total irradiation or insolation can be calculated.

- **Performance Evaluation of PV cells.**

As mentioned before, the temperature of the PV cell will affect its efficiency. There is a way to estimate both the PV cell temperature and the efficiency of the PV cell. There is something called a nominal operating cell temperature (NOCT) which comes with the PV cells' manual. It is a temperature with certain reference conditions (like ambient temperature, wind speed, air mass and total irradiance) the cell is running on when the reference efficiency is measured. Using these conditions along with the reference efficiency, one can estimate the cell temperature and the cell efficiency. To calculate the temperature of the cell, Equation 27 is used [88].

$$T_{cell} = T_{amb} + \left(NOCT - T_{ref}\right)\frac{G}{G_{ref}} \qquad \text{Equation 27}$$

Where T_{cell} stands for cell temperature, T_{amb} stands for ambient temperature, NOCT is the nominal operating cell temperature, T_{ref} is the reference temperature and G_{ref} is the reference irradiance.

As for the cell efficiency, it can be calculated using Equation 28 [89].

$$\eta_{pv} = \eta_{pv,ref}\left[1 - \left|\beta_{ref}\right|\left(T_{cell} - T_{ref}\right)\right] \qquad \text{Equation 28}$$

The symbol η stands for efficiency, β is the temperature coefficient, the subscript ref is for reference and pv is for photovoltaic.

Therefore, to find the hourly energy production that the PV panel would produce, the hourly total insolation on the PV panel would be multiplied by the panel's efficiency and area. The total plant's energy production can be calculated by multiplying the hourly energy production of a PV panel, by the number of panels in the plant. All of this can be calculated using Equation 29 [82].

$$E_{gen} = A_{PV} \cdot \eta_{pv} \cdot (I_{dT} + I_{bT}) \cdot N_{PV} \qquad \text{Equation 29}$$

Where A_{PV} is the area of the PV panel, and N_{PV} is the number of PV panels used in the plant.

Performance ratio is a way to know how well the PV cells are working compared to the referenced conditions. It is also the ratio between the electricity generated in the AC current (after all the losses due to cabling and other causes) to that of the energy produced in the DC stage. Performance ratio can be calculated using Equation 30 .

$$PR = \frac{\int Power_{AC}(t)dt}{\int G(t) \cdot A \cdot \eta_{pv,ref}\, dt} \qquad \text{Equation 30}$$

The A in the denominator is the total surface area of all the PV cells in the plant. Power is the power generated by the plant.

The capacity factor is another performance evaluation value that is used. It is the ratio between the total energy generated by the plant and that of the plant if it was working the whole time on full capacity (8760 hours a year). It can be calculated using Equation 31 [90].

$$CF = \frac{yearly\ generated\ energy}{installed\ capacity\ \cdot\ (8760)} \qquad \text{Equation 31}$$

Here CF is the yearly capacity factor.

- **Inverters**

Inverters are important instruments in a PV plant. An inverter converts the direct current (DC) into alternating current (AC). AC is the type of current mostly used in grid connections because of the less losses that occur within an AC compared to DC. An inverter has a maximum power that it run on, and a maximum voltage that a string can run on. Therefore, using the voltages produced by the PV panels, the amount of PV panels that would be connected to a single string can be calculated as can be seen in Equation 32 [91].

$$max\ \#\ of\ modules\ per\ string = \frac{V_{max.inv}}{V_{oc,max}} \qquad \text{Equation 32}$$

Where $V_{max.inv}$ is the maximum voltage per string of an inverter and $V_{oc,max}$ is the maximum open circuit voltage of the PV module.

To calculate the maximum open circuit voltage of a PV module, Equation 33 is used [91].

$$V_{oc,max} = \frac{T_{min} - T_{stc}}{K_{V_{OC}}} + V_{OC} \qquad \text{Equation 33}$$

Where V_{OC} is the nominal open circuit voltage, T_{min} is the minimum ambient temperature expected, T_{stc} is the standard ambient temperature used to obtain the nominal open circuit voltage, and $K_{V_{OC}}$ is a constant at which the open circuit voltage changes with temperature.

Obtaining the minimum amount of PV panels is also required in order not to put too few PV modules in a string. To calculate the minimum number of modules per string, Equation 34 is used [91].

$$min\ \#\ of\ modules\ per\ string = \frac{V_{min.inv}}{V_{oc,min}} \qquad \text{Equation 34}$$

Where $V_{min.inv}$ is the minimum voltage per string of an inverter and $V_{oc,min}$ is the minimum open circuit voltage of the PV module.

To calculate the minimum open circuit voltage of a PV module, Equation 35 is used [91].

$$V_{oc,min} = \frac{T_{max} + \Delta T_{cell,max} - T_{stc}}{K_{mp}} + V_{mp} \qquad \text{Equation 35}$$

Where T_{max} is the maximum ambient temperature expected, $\Delta T_{cell,max}$ is an assumed difference in temperature between the cell temperature and ambient temperature, V_{mp} is the voltage at maximum power of the PV module, and K_{mp} is a constant at which the maximum power voltage changes with temperature.

To choose the number of PV modules per string, it shall be between the minimum and maximum number of PV modules per string.

Afterwards, it is important to decide how many strings there shall be per inverter, to do that Equation 36 is used [91].

$$\#\ of\ strings\ per\ inverter = \frac{P_{max,inverter}}{P_{string}} \qquad \text{Equation 36}$$

Where $P_{max,inverter}$ is the maximum power for the inverter, and P_{string} is the power of each string.

To calculate the power of a string, Equation 37 is used [91].

$$P_{string} = \#\ of\ modules\ per\ string\ \times P_{module} \qquad \text{Equation 37}$$

Where P_{module} is the power of the PV module.

4.2.2 PV Plant Design

For the PV plant, the design is the common design of a PV plant that can be found in other plants in the world. Which is having an array of PV panels covering an area as packed as possible, with taking the panels' shadow in consideration. It would be fixed and pointed towards the south. The PV panels would also have a tilt angle that is optimized depending on the latitude of the location of the PV panels. This tilt angle would be at around 27° for optimum energy production throughout the year in METU NCC's location. A one-axis or two-axis trackers can be considered. However, due to the high capital cost and the maintenance cost of the trackers, it is recommended to have fixed solar panels instead. The PV panel to be used is shown in Table 6.

Table 6: The properties of the PV panel to be used.

Property	Value
Name of panel	CWT395-72PM
Peak power [W]	395
Efficiency [%]	19.78
V_{oc} [V]	49.54
k_{Voc} [%]	-0.27
V_{mp} [V]	41.07

The PV plant size will depend on the energy consumption of the RO plant. In which the overall SEC would be multiplied by the total water produced and the PV plant will be sized accordingly.

It should be kept in mind that the PV-RO plant will use the grid as a battery. Feeding it the extra electricity that is produced during noon hours or sunny days, and take the extra electricity back in the evening or when needed.

In order to convert the current from DC to AC, which is suitable for the grid, an inverter is needed. There are two inverters that are considered in this project and their specifications are shown in Table 7.

Table 7. The specifications of the inverters to be used in the project.

Inverter	GW25K-DT	GW50K-MT
Maximum power [W]	32500	65000
Maximum voltage [V]	950	1000
Minimum voltage [V]	250	200
Nominal voltage [V]	620	620
Maximum current [A]	20	20
Euro efficiency* [%]	98.3	98.3

*Euro efficiency is the efficiency of the inverter in a middle-Europe climate.

Keep in mind, due to the losses of inverters, climate and cable losses, the overall efficiency, excluding the efficiency of the PV modules, was assumed to be 86%

4.3 Water Transportation Equations

Since the water will have to be pumped to the campus from the shore, designing the piping system is an important measure for selecting the amount of material and the type of materials to be used in the piping system. More importantly, the amount of energy required to pump the water will be obtained using these equations. Thus, obtaining the energy requirement and the type of pump to be used in the system.

The most crucial equation to be used is the Bernoulli's equation with friction losses as written in Equation 38. One thing to keep in mind is that Equation 38 is the head form of the Bernoulli's equation [92].

$$\frac{P_1}{\rho g} + \frac{v_1^2}{2g} + z_1 = \frac{P_2}{\rho g} + \frac{v_2^2}{2g} + z_2 + h_L \qquad \text{Equation 38}$$

Where P is the pressure at that point, ρ is the density of the fluid, g is the gravity acceleration constant, v is the velocity of the fluid, z is the elevation for that location, and h_L is the total head loss. 1 and 2 subscripts refer to the locations of the fluid. The location can be the inlet and outlet of a pipe.

Another way of finding the total power required to pump the water is by using Equation 39 [93].

$$H_{req} = z_{outlet} + \Delta z + h_{l,per\ 100m} \cdot \frac{s}{100} \qquad \text{Equation 39}$$

Where H_{req} is the power required to pump the fluid in head, z_{outlet} is the required head at the outlet of the pipe, Δz is the difference in elevation in m, $h_{l,per\ 100m}$ is the head loss per 100m of distance for the pipe used, and s is the distance travelled by the water in m.

To find the head loss per 100m of the pipe, the empirical Equation 40 is used [83].

$$h_{l,per\ 100m} = \left(\frac{608704451}{d^{4.8655}}\right)\left(\frac{Q}{C_{HW}}\right)^{1.85} \qquad \text{Equation 40}$$

Where, d is the inner diameter of the pipe in mm, Q is the flow rate in l/min, and C is the Hazen-Williams roughness coefficient.

To find the energy required to pump the water per day in kWh, Equation 41 is used [95].

$$E_{req} = \frac{Q\rho H_{req} g}{(3600\left[\frac{s}{h}\right] \cdot 1000\left[\frac{w}{kW}\right])} \cdot 24\left[\frac{h}{day}\right] \cdot \eta_{pump} \qquad \text{Equation 41}$$

Where ρ is the density of water to be pumped, Q is the flow rate in m^3/h, g is the gravity acceleration constant, and η_{pump} is the pump's efficiency.

The density of water changes with TDS, an approximation of the density of water can be done using the empirical Equation 42 [84].

$$\rho = 1 + TDS \cdot (\rho_{DI} \cdot 6.95 \times 10^{-7}) \quad \text{Equation 42}$$

Where ρ_{DI} is the density of di-ionized water, usually 997 kg/ m^3 at 25 °C.

4.4 Water Pumping System

For the water pumping system, two systems will be considered. One for the intake and another for the transportation of water to the campus.

The water intake shall be done at 500 meters distance from the beach, but due to the natural sub-sea surface pressure, the water would be pushed to the same sea level elevation. Therefore, the effective pumping would be done over just 45 meters as shown in Figure 37.

Figure 37. The distance between the beach and the proposed RO plant's location [85].

While the transportation to the campus would be done over 6.23 km to reach the water treatment plant of METU NCC as seen in Figure 38. But for calculations, 6.2 km was considered.

Figure 38. The distance between the proposed RO plant's location and the water treatment plant of METU NCC [85].

As for the elevation between the proposed RO plant's location and the elevation of the water treatment plant of METU NCC, it was estimated to be around 70 metres using a topographic map as shown in Figure 39. The RO plant's elevation is assumed to be at sea level.

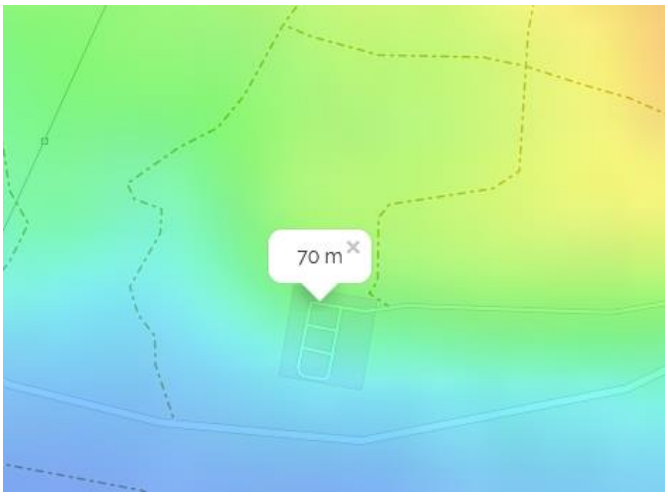

Figure 39. The elevation of METU NCC's waste water plant [86].

4.5 Economic Analysis Equations

For the economic analysis of the project, one of the most important parameters is the levelized cost of energy (LCOE) and levelized cost of water (LCOW). These two parameters are similar to each other, but LCOW depends on LCOE. The LCOE is a calculation of the overall lifetime of the PV plant costs divided by the amount of

energy produced during its lifetime. While LCOW is the lifetime of the RO plant costs divided by the amount of water produced during its lifetime with taking LCOE into account. Keep in mind that the effect of the discount rate is taken into account for both LCOE and LCOW. The equations for LCOE and LCOW are shown in Equation 43 and Equation 44 respectively [99][100].

$$LCOE = \frac{C_{PV} + \sum_{t=1}^{n}\left(\frac{AMC_t + F_t}{(1+r)^t}\right)}{\sum_{t=1}^{n}\left(\frac{E_{gen,t}}{(1+r)^t}\right)} = \frac{C_{PV} \cdot CRF + (AMC_t + F_t)}{E_{gen}} \quad \text{Equation 43}$$

$$LCOW = \frac{C_{RO+PV} + \sum_{t=1}^{n}\left(\frac{AMC_t + ACC_t + ALC_t}{(1+r)^t}\right)}{\sum_{t=1}^{n}\left(\frac{Q_{pa,t}}{(1+r)^t}\right)} = \frac{C_{RO+PV} \cdot CRF + (AMC + ACC + ALC)}{Q_{pa}} \quad \text{Equation 44}$$

Where C is the capital investment, AMC is the annual maintenance cost, F is the fuel cost, r is the discount rate, E_{gen} is the annual energy production, ACC is annual chemicals cost, ALC is the annual labor cost, Q_{pa} is the annual water production, n is the project lifetime, and CRF is the capital recovery factor.

The capital recovery factor can be calculated using Equation 45 [101].

$$CRF = \frac{r(1+r)^n}{(1+r)^n - 1} \quad \text{Equation 45}$$

Keep in mind that C and AMC would be different for the RO plant and PV plant. Also, AMC should include the membranes and inverters that are changed every few years.

Also, since PV modules produce energy from solar energy, which is free, the fuel costs would be zero for a PV plant.

4.6 PV-RO System Components and Costs

In this section, the cost of all the equipment, chemicals, membranes, and other components are decided.

- **PV Plant Costs**

For the PV plant, the costs of the PV panels, inverters and mounts and cables was considered and is shown in Table 8.

Table 8. The prices of the PV plant components

Component	TL	USD
CWT396-72PM PV panel [100]	1764.36	207.72
GW25K-DT inverter [101]	21941.60	4279.15
GW50K-MT inverter [102]	36330.00	2584.40
Mounts and cables per 2 panels [103]	120.00	14.13

While the maintenance of the PV panels is assumed to be 12 USD per kW of capacity.

- **Water Transport Costs**

For the water transport systems such as the intake and campus water delivery, the components are shown in Table 9.

Table 9. The prices of the water transport system components

Component	TL	USD
HDPE 140 per m [104]	45.74	5.39
HDPE 125 per m [104]	36.02	4.24
HDPE 110 per m [104]	28.35	3.34
PACER SE2HL pump [105]		830

The HDPE pipes are assumed to have a Hazen-Williams coefficient of 150.

- **RO Plant Costs**

Since the RO plant has many different components, the costs of the components will be split into different sections. For the first section, the price of the membranes, pressure vessels, pumps and ERD are shown in Table 10.

Table 10. The prices of the RO plant equipment.

Component	USD
SW30HRLE-440i [106]	649.00
Seamaxx-440i [106]	677.00
XLE-440i [106]	600.00
SW pressure vessel [107]	2000.00
BW pressure vessel [108]	1000.00
HPP [109]	57000.00
HPP motor [110]	12000.00
Booster pump [110]	17000.00
Booster pump motor [110]	4000.00
ERD [111]	51000.00

Note that all the pumps, including the ones from the water transport system, are assumed to have an efficiency of 73.6%, which is at the lower end of efficiencies.

For other costs such as construction, installation, piping etc., it is hard to know the exact price of these components. Therefore, they were picked as percentages of the total cost, where the previous costs in Table 11 along with an assumed pretreatment price of 400000 USD, will help deciding the total price [112] [113].

Table 11. The percentage cost of the other components of the RO plant.

Component	% of total CAPEX
Piping	14.36
Equipment and materials	25.76
Construction	18.16
Installation	8.02
Design	6.33
Legal	1.06
Pretreatment	16.89
Posttreatment	0.17

Since some of the equipment such as the membranes and cartridge filters have limited life. There would be a replacement needed to be done annually. The costs of annual replacements and maintenance are shown in Table 12.

Table 12. The annual replacement and maintenance costs.

Component	Replacement ratio
Granular media replacement [26]	0.6· (daily permeate production)
Cartridge filters [26]	3.6· (daily permeate production)
Membrane replacement [114]	14% of the cost of a membrane
Maintenance*	1% of the total RO cost

*Maintenance is assumed to be 1% of the total RO cost

As for the price of chemicals used annually in conditioning the water, the costs are shown in Table 13.

Table 13. The annual chemical costs.

Component	USD
NaOH (per kg) [115]	0.27
HCl (per kg) [116]	0.40
Other chemicals (per m^3 of permeate) [117]	0.02
RO cleaning chemicals (per m^3 of daily permeate) [26]	3.40

- **Assumptions**

In this section, some assumptions regarding the situation that the PV-RO plant would operate with. These assumptions are shown in Table 14.

Table 14. Assumptions made for the PV-RO system operation.

Assumption	Value
Project life	30 years
Discount rate	8%
Water market price	0.75$*
Pumps' efficiencies	73.6%

*As of August 2021, the market price was about 0.75$.

CHAPTER 4

RESULTS & DISCUSSION

5.1 RO Performance

There are two RO configurations that are considered in the design of the PV-RO plant. One of them is a single pass two stage configuration, while the other is double pass with a two stage first pass. Both configurations were considered with and without an ERD. The general specifications of both configurations are shown in Table 15.

Table 15. General specifications of the single pass and double pass configurations.

Configuration	Double pass	Single pass
Feed flow rate [m^3/day]	1185	1400
Recovery [%]	47.3	40
Permeate flow rate [m^3/day]	560	560
Permeate TDS [at 22.1 °C]	144.2	306.2
Flow of concentrate [m^3/day]	623.2	838.2
Concentrate TDS [mg/l]	77164	67745

- **Double Pass Configuration**

The double pass configuration was optimized for the least amount of energy consumption, but also considering other variables such as water quality. The details of the configuration can be seen in Table 16.

Table 16. The details of the double pass configuration at 22.1 °C.

Pass	First pass	Second pass
Number of pressure vessels	7+4	1
Elements per pressure vessel	7	6
Number of elements	77	6
Feed flow [m^3/d]	1247	187.8
Feed TDS [mg/L]	38890	1843
Feed pressure [bar]	54.1	6.7
Concentrate recycled to feed [%]	0	100
Permeate directly going to produce [%]	70	100
Permeate produced [m^3/d]	625.7	122.1
Net permeate produced [m^3/d]	560	
Permeate TDS [mg/L]	663.5	85.78
Net permeate TDS [mg/L]	144.2	
Recovery [%]	50.2	65
Net recovery [%]	47.3	
Specific Energy (w/o ERD) [kWh/ m^3]	4.07	0.38
Specific Energy (w/ ERD) [kWh/ m^3]	2.21	0.38
Net Specific Energy (w/o ERD) [kWh/ m^3]	4.63	
Net Specific Energy (w/ ERD) [kWh/ m^3]	2.55	
SEC reduction from employing an ERD [%]	45%	

The double pass configuration is a better boron rejector compared to the single pass configuration. This is the reason a double pass configuration is considered. A detailed layout of the configuration is shown below in Figure 40. The detailed layout shows numbered flows, which will be further detailed in Table 17.

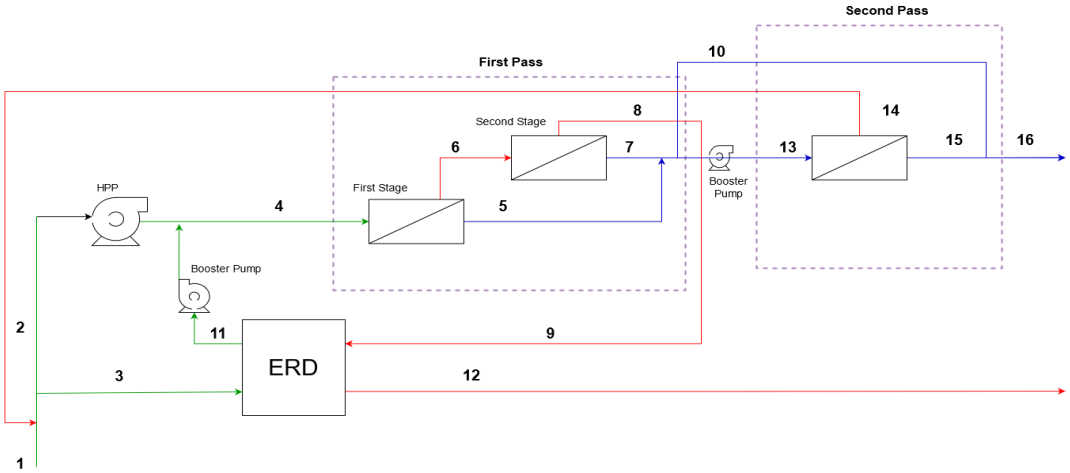

Figure 40. First configuration, two stages first pass, one stage second pass with an ERD, where green is feedwater, blue is permeate, red is concentrate. Flows are numbered from 1 to 16.

Table 17. Flow properties of the double pass configuration with an ERD at 22.1 °C.

Flow no.	Flow [m^3/d]	Pressure [bar]	TDS [mg/l]
1	1247	3	40667
2	634.4	3	40667
3	612.6	3	38890
4	1247	54.1	40018.15
5	586.1	0	387.94
6	662	52.8	72847
7	39.6	0	4700
8	623.2	51.3	77164
9	623.2	51.3	77164
10	437.9	0	158.8
11	612.6	50.08	41186
12	623.2	1	74906.6
13	187.8	6.6	1843
14	65.7	5.6	5108
15	122.1	0	83.66
16	560	0	144.2

While the layout without ERD is shown in Figure 41. And the flow properties are shown in Table 18.

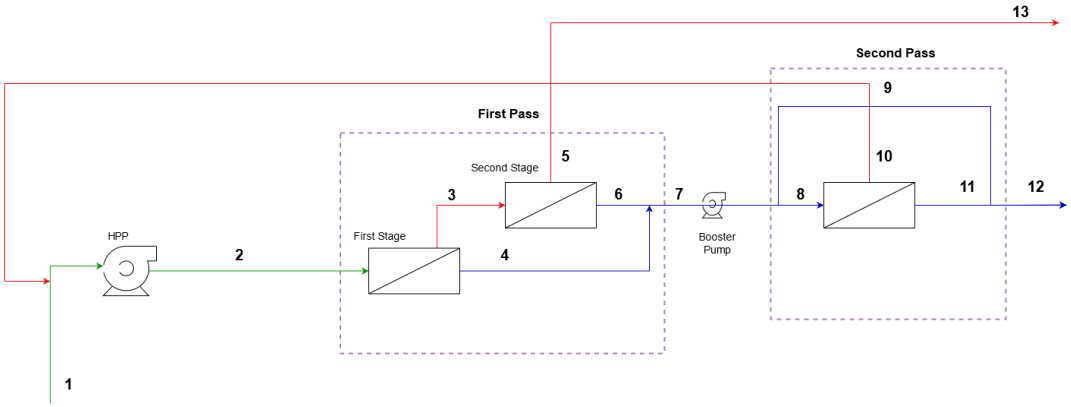

Figure 41. First configuration, two stages first pass, one stage second pass without an ERD, where green is feedwater, blue is permeate, red is concentrate. Flows are numbered from 1 to 13.

Table 18. Flow properties of the double pass configuration without an ERD at 22.1 °C.

Flow no.	Flow [m^3/d]	Pressure [bar]	TDS [mg/l]
1	1185	3	40667
2	1247	54.1	38918
3	662.5	52.7	72910
4	586.1	0	387.94
5	623.2	51.3	77164
6	39.6	0	4700
7	625.7	0	663.5
8	187.7	6.7	1935
9	438	0	160.1
10	65.7	5.7	5370
11	122	0	85.78
12	560	0	144.2
13	623	51.3	77229

It needs to be kept in mind that these values differ when the temperature of the water changes. For Table 17 and Table 18, the temperature was done at design temperature of 22.1 °C, which is the average water temperature of Akdeniz. The effect of temperature can be seen in Table 19. Where 15 °C is the lowest sea temperature, 22.1 °C is the average sea temperature, and 30 °C is the maximum sea temperature in Akdeniz.

Table 19. The effect of temperature on the performance of the RO plant in the case of the double pass configuration.

Temperature	15 °C	22.1 °C	30 °C
Permeate TDS [mg/l]	104.5	144.2	218.2
SEC (w/o ERD) [kWh/ m^3]	4.63	4.63	4.64
Chemical dosage [mg/l]	HCl: 45.2	HCl: 42.1	HCl: 39.0
	NaOH: 79.4	NaOH: 94.5	NaOH: 127.7

The temperature also has an effect on the salt rejection of certain salts in the seawater. The permeate concentrations of certain salts in the seawater are shown in Table 20 along with the effect of temperature on the concentrations.

Table 20. The ionic composition of the permeate at sea temperature of 15 °C, 22.1 °C and 30 °C and the pH, for the double pass configuration.

Ion	15 °C [mg/l]	22.1 °C [mg/l]	30 °C [mg/l]
K^+	1.59	2.21	3.37
Na^+	36.54	50.57	76.93
Mg^+	0.89	1.19	1.74
Ca^{+2}	0.27	0.36	0.53
Sr^{+2}	0.01	0.01	0.01
HCO_3^-	1.42	1.58	2.07
Cl^-	59.33	82.07	124.6
Br^{-1}	0.74	1.02	1.57
SO_4^{-2}	0.87	1.15	1.65

Table 20 continued.

SiO_2	0.01	0.01	0.01
Boron	0.5	0.7	1
CO_2	0.74	1.02	1.57
TDS	104.5	144.2	218.2
pH	5.1	5.3	5.7

As can be seen, the design accounts for all the temperatures that the seawater can be in. The TDS is always below the WHO recommendation of 500 mg/l, while the boron is always at 1 mg/l or less, as required by the European Commission. It can also be seen that the pH of the permeate is acidic, and therefore a posttreatment is required for the permeate before being potable.

- **Single Pass Configuration**

Just as the double pass configuration, the single pass configuration was optimized for energy consumption and water quality. The details of the single pass configuration are shown in Table 21.

Table 21. The details of the single pass configuration at 22.1 °C.

Pass	First pass
Number of pressure vessels	7+4
Elements per pressure vessel	7
Number of elements	77
Feed flow [m^3/d]	1397
Feed TDS [mg/L]	40782
Feed pressure [bar]	51.3
Concentrate recycled to feed [%]	0
Permeate directly going to produce [%]	100
Net permeate produced [m^3/d]	560
Net permeate TDS [mg/L]	306.2

Table 21 continued.

Net recovery [%]	40
Specific Energy (w/o ERD) [kWh/ m^3]	4.84
Specific Energy (w/ ERD) [kWh/ m^3]	2.25
SEC reduction from employing an ERD [%]	53.5%

Comparing Table 21 with Table 16, the SEC without ERD of the single pass configuration is more than that of the double pass. However, after employing an ERD, it had a better effect on the single pass configuration, reducing the SEC by 53.5% compared to 45% of the double pass SEC. This is due to the design of the double pass configuration. Where the concentrate from the second pass does not pass through an ERD to have its fluid's power recovered. While the single pass configuration just had one pass, where all the concentrate passes through an ERD and a portion of the fluid's power is recovered.

While the detailed layout of the single pass configuration with an ERD which has numbered flows can be seen in Figure 42. The flows properties are shown in Table 22.

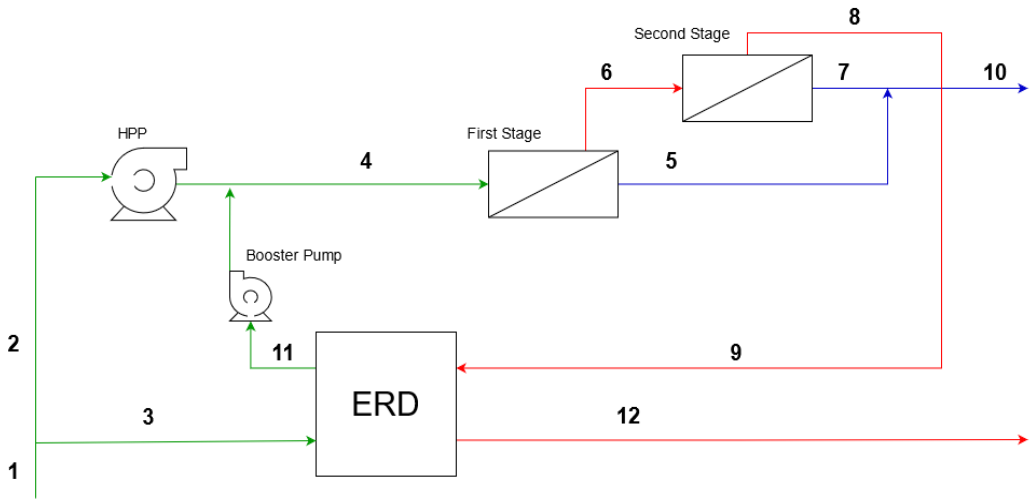

Figure 42. Second configuration, two stages single pass with an ERD, where green is feedwater, blue is permeate, red is concentrate. Flows are numbered from 1 to 12.

Table 22. Flow properties of the single pass configuration with an ERD at 22.1 °C.

Flow no.	Flow [m^3/d]	Pressure [bar]	TDS [mg/l]
1	1400	3	40667
2	1247	51.3	573.05
3	823.95	3	40782
4	1397	51.3	41736
5	509.3	0	205.3
6	888.7	49.6	63,971
7	50.7	0	1320
8	838.2	47.6	67745
9	838.2	47.6	67745
10	560	0	306.2
11	122	0	85.78
12	838.2	1	66154.72

The layout of the single pass configuration without an ERD is shown in Figure 43. While the flow properties are shown in Table 23.

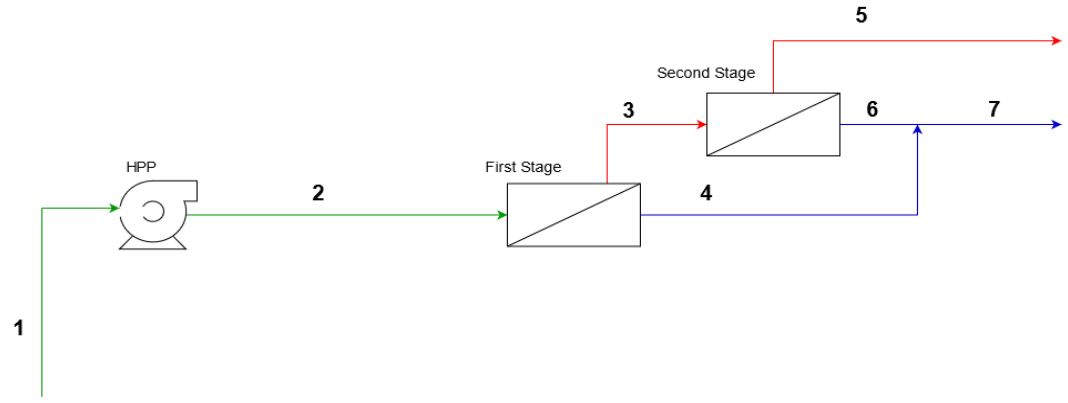

Figure 43. Second configuration, two stages single pass without an ERD, where green is feedwater, blue is permeate, red is concentrate. Flows are numbered from 1 to 7.

Table 23. Flow properties of the single pass configuration without an ERD at 22.1 °C.

Flow no.	Flow [m^3/d]	Pressure [bar]	TDS [mg/l]
1	1400	3	40667
2	1397	51.3	40782
3	888.7	49.6	63971
4	509.3	0	205.3
5	838.2	47.6	67745
6	50.7	0	1320
7	560	0	306.2

Just like the first configuration, temperature effect has been taken into account and is shown in Table 24.

Table 24. The effect of temperature on the performance of the RO plant in the case of the single pass configuration.

Temperature	15 °C	22.1 °C	30 °C
Permeate TDS [mg/l]	204.2	306.2	465.9
SEC (w/o ERD) [kWh/ m^3]	4.88	4.84	4.83
Chemical dosage [mg/l]	NaOH: 28.5	NaOH: 36.7	NaOH: 45.8

Just like in the double pass configuration, the temperature will affect the salt rejection of certain salts. The effect can be seen in Table 25.

Table 25. The ionic composition of the permeate at sea temperature of 15 °C, 22.1 °C and 30 °C and the pH, for the single pass configuration.

Ion	15 °C [mg/l]	22.1 °C [mg/l]	30 °C [mg/l]
K^+	3.19	4.79	7.29
Na^+	72.76	109.3	166.8
Mg^+	1.78	2.69	4.12
Ca^{+2}	0.55	0.83	1.27
Sr^{+2}	0.01	0.02	0.03
HCO_3^-	0.93	1.19	1.55
Cl^-	118.8	178.6	272.5
Br^{-1}	1.23	1.85	2.81
SO_4^{-2}	1.75	2.64	4.07
SiO_2	0.01	0.02	0.02
Boron	0.55	0.73	0.94
CO_2	1.25	1.86	2.82
TDS	204.2	306.2	465.9
pH	7.8	8	8.1

As can be seen, the Boron is always below 1 mg/l within the lowest and highest seawater temperature in Akdeniz. Also, unlike the double pass configuration, the pH of the permeate is within the acceptable drinking water range. However, posttreatment is still needed. As for the TDS, it is higher than the double pass configuration's TDS, which is expected due to the lack of further salt rejection that the second pass would provide. Nevertheless, the TDS is still below 500 mg/l within all seawater temperatures that will occur within the year.

While the chloride concentration at 30 °C was predicted to be 272.5 mg/l, which is above the 250 mg/l recommended by the European drinking guideline. However, since the guideline specify that it is for taste considerations, it can be accepted, as it is just an increase of 22.5 mg/l. If there were concerns about the taste, the recovery of the RO plant can be reduced to increase the rejection.

5.2 Pretreatment and Water Transportation Performance

The pretreatment process consists of DAF and a dual media filter has a specific energy consumption of 0.16 kWh/ m^3, the volume is considered as the pretreated water going to the RO plant [118].

As for the intake and water transportation to the campus, the energy required per day was obtained with taking into account losses due to friction. The diameter of the pipe was decided to reduce friction that occurs within the walls of the pipe, but also making sure that the water is not moving slowly to avoid solids from scaling the pipes. The details of water transportation are shown in Table 26.

Table 26. The details of the intake and campus delivery water transportation for both configurations.

Configuration	Double pass		Single pass	
Process	Intake	Campus delivery	Intake	Campus delivery
Pipe outer diameter [mm]	125	110	140	110
Length [m]	45	6200	45	6200
Elevation [m]	2	70	2	70
Flow rate [m^3/h]	51.96	23.33	58.2	23.33
Water velocity [m/s]	1.38	0.8	1.23	0.8
Head loss per 100 m [m]	1.44	0.61	1.03	0.61
Water density [kg/ m^3]	1025.2	997.1	1025.2	997.2
Required outlet head [m]	1	1	1	1
Required pumping head [m]	3.65	108.82	3.46	108.8
Required power [kW]	0.53	6.9	0.56	6.9
Required daily energy [kWh]	12.7	165.57	13.51	165.54

As can be seen from Table 27, the required energy to pump the permeate to the campus is much higher than that of the intake water transport. This is due to the high elevation and long distance that the water needs to be transported along.

As for the number of pumps needed, Table 27 details the required pumps.

Table 27. The pump that would be used in the water transportation and how many to be used for each process.

Process	Intake	Campus delivery
Pump	PACER SE2HL	
Flow rate [l/m]	433	388
Working head [m]	8	10
Number of pumps	2 in parallel	11 in series

5.3 Reverse Osmosis Plant's Energy Consumption

Combining the energy consumption of all these processes that happen before and after the RO process, one can obtain the overall permeate's SEC. Using the SEC, the annual energy consumption can be calculated. The total SEC of each of the processes can be seen in Table 28 and Table 29, for the double pass configuration and single pass configuration respectively. The pretreatment's energy consumption was assumed to be 0.16 kWh per m^3 of effluent [118].

Table 28. The SEC of different processes of the double pass configuration.

	W/ ERD		W/o ERD	
	$SEC_{effluent}$ [kWh/ m^3]	SEC [kWh/ m^3]	$SEC_{effluent}$ [kWh/ m^3]	SEC [kWh/ m^3]
Pretreatment	0.16	0.36	0.16	0.36
Intake	0.014	0.031	0.014	0.031
RO		2.55		4.64
Campus delivery		0.4		0.4
Total		3.34		5.41

Table 29. The SEC of different processes of the single pass configuration.

	W/ ERD		W/o ERD	
	$SEC_{effluent}$ [kWh/ m^3]	SEC [kWh/ m^3]	$SEC_{effluent}$ [kWh/ m^3]	SEC [kWh/ m^3]
Pretreatment	0.16	0.4	0.16	0.4
Intake	0.013	0.033	0.013	0.033
RO		2.25		4.8
Campus delivery		0.4		0.4
Total		3.08		5.66

A comparison of the breakdown of SEC between the two configurations can be seen in Figure 44.

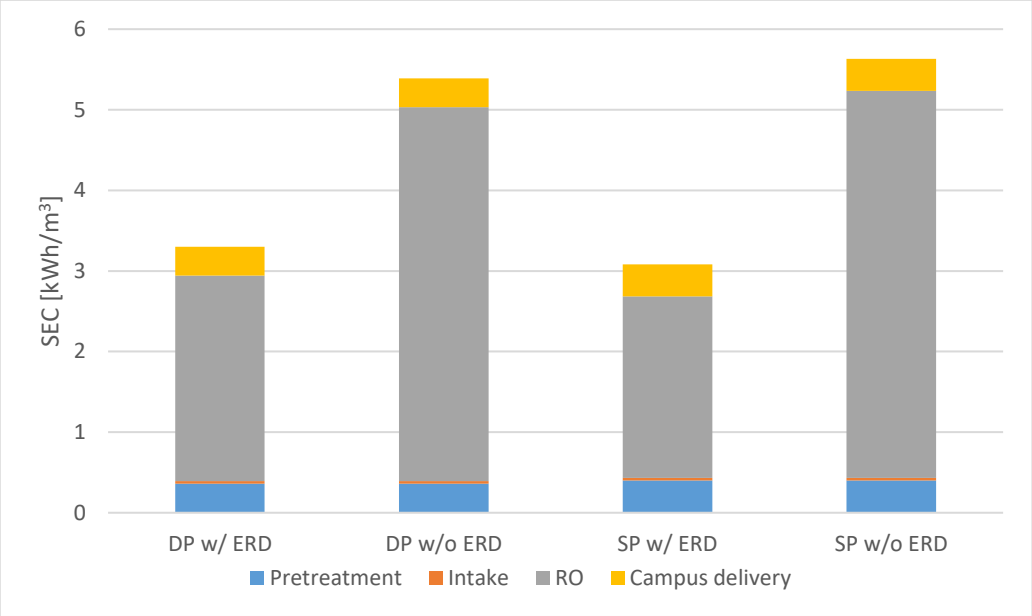

Figure 44. The SEC breakdown of the two configurations, with taking ERD into consideration, DP is double pass configuration, SP is single pass configuration.

As seen in Figure 44, the SEC of the intake barely makes an impact into the total SEC of any of the configurations. While for both single and double pass configurations, having an ERD reduces the SEC significantly. But that effect of reducing the SEC with ERD is more evident in the single pass configuration.

5.4 PV Performance

According to the RO performance for both configurations, the required energy per year is shown in Table 30.

Table 30. The required annual energy for the two configurations and ERD availability.

Configuration	Double pass		Single pass	
ERD availability	W/ ERD	W/o ERD	W/ ERD	W/o ERD
Annual Energy required [kWh]	683,147	1,105,801	630,178	1,157,631

Using the annual energy required to run the RO plant, the number of panels and inverters needed can be calculated. The amount of PV panels needed along with inverters are shown in Table 31.

Table 31. The amount of PV panels and inverters needed for both configurations.

Configuration	Double pass		Single pass	
ERD availability	W/ ERD	W/o ERD	W/ ERD	W/o ERD
Energy that can be supplied annually by 1 kW of capacity [kWh]*	1548.17			
PV plant capacity needed [kW]	442	715	407	748
PV panels needed	1118	1809	1031	1894
50k Inverters needed	7	12	6	12
25k Inverters needed	0	0	1	0

*Per 1 kW of power by using CWT396-72PM panels in METU NCC's weather conditions.

A more detailed energy production of the proposed PV plants can be seen below. For the double pass configuration, the proposed PV plants are 442 kW and 715 kW for with ERD and without ERD respectively. While for the single pass configuration, the proposed PV plants are 407kW and 748 kW for with ERD and without ERD respectively. The estimated monthly energy produced for both configurations can be seen in Figure 45.

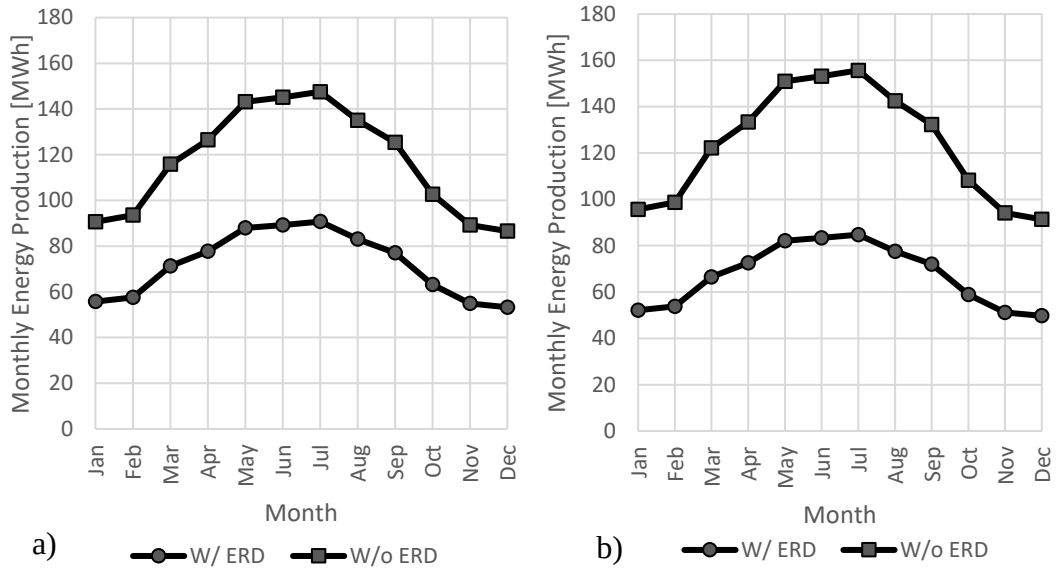

Figure 45. The monthly energy production of the proposed PV plants in MWh, where a) Double pass configuration, and b) Single pass configuration.

As can be seen from Figure 45, the energy production peaks in the summer months. This may be a problem where most of the energy comes in the summer months, while the water is needed the most in the months where the energy is produced the least as can be seen from Figure 46 and Figure 47 for double pass configuration and single pass configuration respectively. The year used was the year 2019, which had the highest energy consumption of the previous 7 years. Along with an additional 80% for unexpected peaks.

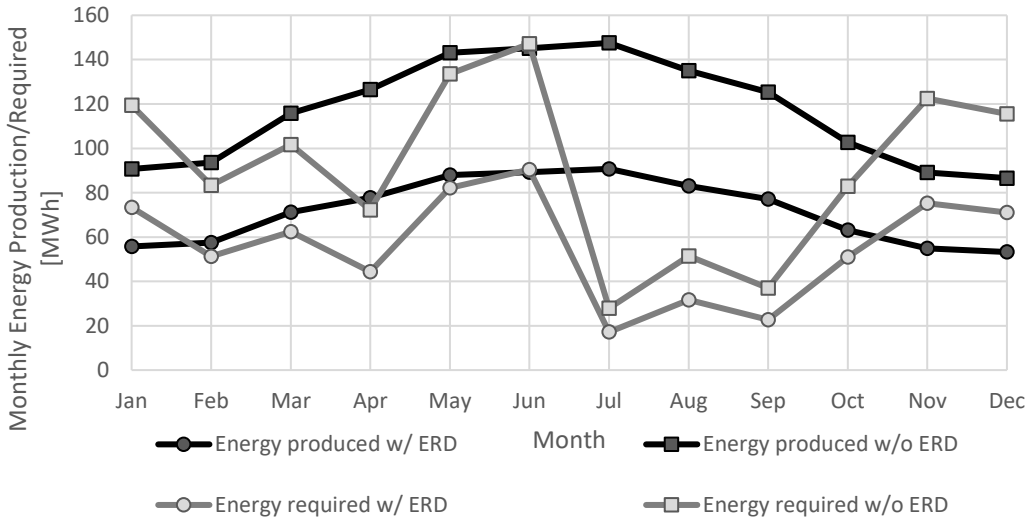

Figure 46. The monthly energy produced by the PV plant and the monthly energy required to produce water for the double pass configuration.

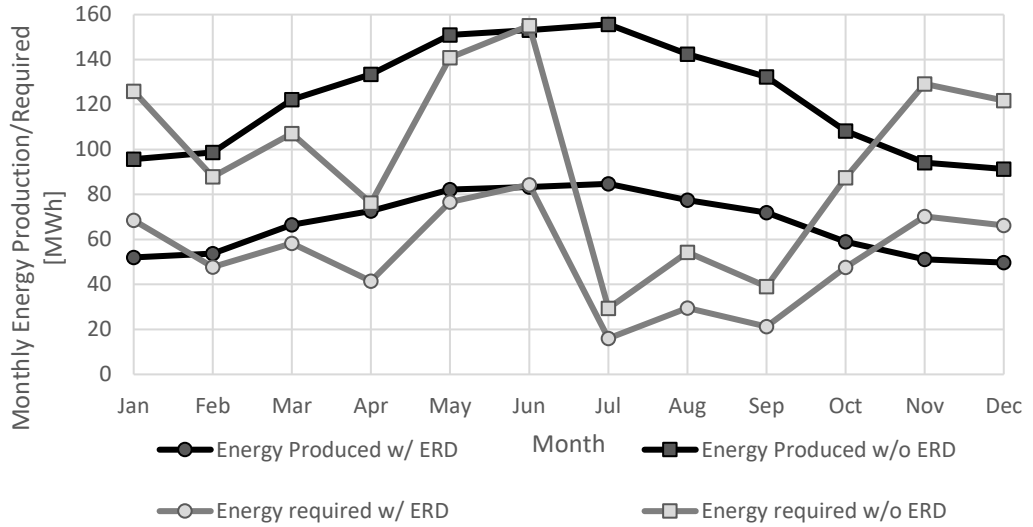

Figure 47. The monthly energy produced by the PV plant and the monthly energy required to produce water for the single pass configuration.

However, since the proposed PV-RO system in this study would rely on giving the grid and taking back the energy when needed, this peak at the summer will not cause any problems.

5.5 Economic Analysis

- **Double Pass Configuration**

Taking all the costs and number of components needed, the total price of the PV plant, RO plant, and the water transportation system was obtained as shown in Table 32. For the prices and number of components used, please refer to Appendix.

Table 32. The overall CAPEX of the PV-RO system of the double pass configuration.

CAPEX	W/ ERD		W/o ERD	
	%	Total USD	%	Total USD
PV plant	10.57	283,505.57	16.40	462,166.68
Water transport	1.18	31,688.92	1.12	31,688.92
RO plant	88.25	2,368,201.00	82.47	2,323,487.00
Total cost	***100.00***	***2,683,395.48***	***100.00***	***2,817,342.60***

While the annual operating costs are shown in Table 33.

Table 33. The overall OPEX of the PV-RO system of the double pass configuration.

OPEX	W/ ERD		W/o ERD	
	%	Total USD	%	Total USD
Chemicals	33.88	20,012.15	31.88	20,012.15
Replacements	57.15	33,753.75	54.46	34,186.65
PV maintenance	8.97	5,299.32	13.66	8,574.66
Total annual cost	***100.00***	***59,065.22***	***100.00***	***62,773.46***

As for the overall LCOE of the PV plant and the LCOW of the PV-RO plant, Table 34 clarifies these numbers.

Table 34. The LCOE nad LCOW of the PV and PV+RO plant respectively of the double pass configuration.

	W/ ERD	W/o ERD
LCOE [$/kWh]	0.0446	0.0449
LCOW [$/m^3]	1.455	1.531

- **Single Pass Configuration**

As for the single pass configuration, the price of the RO plant is expected to be around 85% of the price of a double pass configuration RO plant. The CAPEX breakdown is shown in Table 35.

Table 35. The overall CAPEX of the PV-RO system of the single pass configuration.

CAPEX	W/ ERD		W/o ERD	
	%	Total USD	%	Total USD
PV plant	11.42	264,546.39	19.37	480,651.05
Water transport	1.37	31,740.44	1.28	31,740.44
RO plant	87.21	2,019,575.00	79.35	1968575.00
Total cost	***100.00***	***2,315,861.83***	***100.00***	***2,480,966.49***

As for the single pass configuration's operational and maintenance costs, they are listed in Table 36.

Table 36. The overall OPEX of the PV-RO system of the single pass configuration.

OPEX	W/ ERD		W/o ERD	
	%	Total USD	%	Total USD
Chemicals	32.94	17,154.41	30.82	17,154.41
Replacements	57.68	30,039.43	53.05	29,529.43
PV maintenance	9.38	4,886.94	16.13	8,977.56
Total annual cost	***100.00***	***52,080.78***	***100.00***	***55,661.40***

As for the overall LCOE of the PV plant and the LCOW of the PV-RO plant, Table 37 clarifies these numbers.

Table 37. The LCOE and LCOW of the PV and PV+RO plant respectively of the single pass configuration.

	W/ ERD	W/o ERD
LCOE [$/kWh]	0.0450	0.0446
LCOW [$/m^3]	1.261	1.331

To better compare the two configurations' LCOE and LCOW, Table 38 shows the LCOE and LCOW of the two configurations.

Table 38. The LCOE and LCOW of the PV and PV+RO plant respectively of both configurations.

Configuration	Double pass		Single pass	
	W/ ERD	W/o ERD	W/ ERD	W/o ERD
LCOE [$/kWh]	0.0446	0.0449	0.0450	0.0446
LCOW [$/m^3]	1.455	1.531	1.261	1.351

For both the configurations, all cases end up having a payback period of infinity. What that means, is that with the assumed CAPEX and OPEX, the PV-RO plant would be unfeasible. Another way to look at it is by comparing the LCOW with the water price in the market. And since the market price 0.75$, is lower than all the LCOW obtained from the different cases, none of the cases would be feasible.

Having an ERD in both configurations increased the CAPEX of the RO plant. However, since it decreases the SEC, the overall CAPEX was lower because the energy needed is lower, therefore less PV modules are needed. Table 39 shows the effect of installing an ERD on the CAPEX of the PV plant.

Table 39. The CAPEX savings that occur when employing an ERD.

Configuration	PV CAPEX w/o ERD [USD]	PV CAPEX w/ ERD [USD]	Savings [%]
Double pass	462167	283506	38.66%
Single pass	480651	264546	44.96%

- **CO_2 Emission Avoided**

Since the energy used to run the RO plant is produced by a PV plant, there will be no CO_2 emission during the operation of that PV plant. Currently, the electricity production company in TRNC, KIBTEK, uses diesel generators to produce electricity. If KIBTEK's diesel generators has an assumed efficiency of 35% of converting thermal energy to electricity. And the specific CO_2 emission of diesel is 74 kg CO_2/GJ or 0.2664 kg CO_2/kWh [119]. Subsequently, the CO_2 emission that was avoided by using PV instead of grid electricity is shown in Table 40 for both configurations. CO_2 is assumed to have 50 USD worth of society related damages per ton [120]. Where society related damage can include the effect of CO_2 on healthcare damages and climate change damages.

Table 40. CO_2 emission and damages avoided by employing a PV plant instead of using electricity from the grid.

Configuration	Annual CO_2 emission avoided [t CO_2]	Lifetime CO_2 emission avoided [t CO_2]	Annual damages from CO_2 avoided [USD]
DP w/ ERD	179.9	5391	8995
DP w/o ERD	292.3	8769	14615
SP w/ ERD	167.9	5037	8395
SP w/o ERD	308.4	9252	15420

As can be seen from Table 40, the minimum avoided tons of carbon emission were 167.9 tons CO_2 per year, which corresponds to about 8395 USD of societal damages avoided per year. This cost of society related damages can be reduced from the total annual OPEX of the PV-RO plant for an environmental-economic analysis. However, this was not done in this paper because there is no carbon tax implemented in TRNC.

- **Further Discussion**

Looking at the LCOE of all the cases, it can be seen that there is barely any difference in the LCOE between the four cases. The LCOE is considered cheap, comparing it to the electricity price that is bought from the energy generation company of TRNC, KIBTEK. As of August 2021, the average price of a kWh from KIBTEK costs around 0.11 USD, while the LCOE obtained from the PV plants in the four cases is between 0.0446 and 0.0450 USD [121].

As can be seen from Table 38, the LCOW of the single pass with an ERD has the lowest cost of water at 1.261 USD. The reason for the difference in the LCOW is that the single pass configuration has a lower capital cost compared to the double pass configuration. This can be deduced by looking at the energy consumption of the single pass configuration without an ERD. Compared to all the other cases, it has the higher SEC of 5.66 kWh/ m^3. Nonetheless, it has a lower LCOW compared to both cases of the double pass configuration.

For both configurations, looking at Table 32 and Table 35, it can be seen that the RO plant costs the most in the PV-RO system. It is always above 79% of the total PV-RO system's price.

The assumption of the price of the RO plant may have been toward the higher end for a 560 m^3/day capacity RO plant. There are many studies that tackled the price estimation of the CAPEX and OPEX of an RO plant. Therefore, it would be interesting to try these methods in order to find the CAPEX and OPEX of this particular project's configurations. A comparison between different studies' cost estimation, along with the final LCOW according to the configurations with ERD of the proposed PV-RO plant in this thesis was done in Table 41.

Table 41. The estimated CAPEX, OPEX and LCOW of the proposed PV-RO plant by using different studies.

Study	Ref. Cap. [m^3/d]	Double pass w/ ERD			Single pass w/ ERD		
		CAPEX	OPEX	LCOW	CAPEX	OPEX	LCOW
This paper	560	2683395	59065	**1.43**	2315861	52080	**1.24**
Kayaci et al. (2006) [122]	10000	1072289	56844	**0.72**	1123373	56000	**0.738**
Kim et al. (2006) [123]	10000	957923	46299	**0.617**	920448	40023	**0.58**
Alabduljalil et al. (2010) [117]	200	1693623	58530	**1.02**	1463466	56471	**1.04**
Elfaqih et al. (2021) [124]	500	-	-	-	587839	34200	**0.423**
Rahimi et al. (2021) [125]	1000	-	-	-	861840	44800	**0.747**

Looking at Table 41, it can be seen that by using different methods in obtaining the costs of the system, the RO plant may actually become economically feasible. However, it should be mentioned that in some studies, the reference capacity of the RO plant was high in the studies done by Kayaci et al. and Kim et al. at 10000 m^3/day. There is a noticeable difference between the cost estimations of this paper and the other studies. But also, each study had a significant difference in LCOW to other studies. However, all the studies' cost estimations are lower than ours. Using Table 41, a comparison between these cases is made in Table 42 for different economic parameters of the single pass configuration.

Table 42. The LCOW, discounted payback period (DPBP), return on investment (ROI) and feasibility of the cases mentioned in Table 41.

Study	LCOW	DPBP	ROI	Feasible
This thesis	1.24	-	-45.53%	No
Kayaci et al. [122]	0.738	*34 years*	6.17%	No
Kim et al.[123]	0.58	14 years	50.85%	Yes
Alabduljalil et al. [117]	1.04	-	-18.90%	No
Elfaqih et al. [124]	0.423	7 years	148.35%	Yes
Rahimi et al. [125]	0.747	14 years	54.32%	Yes

Looking at Table 42, the estimated CAPEX and OPEX from Kayaci et al. study has an LCOW of lower than 0.75$, and the ROI is a positive number. However, these parameters are not enough to justify the feasibility of the proposed plant. Because the DPBP is above the proposed lifetime of the plant which was 30 years.

The current assumption of the single pass configuration has a negative ROI. Which means that the money invested in the project will not be fruitful. Over the 30 years of the plant's life, the total cashflow would be around -1.16 million USD. Which means there is a net money loss for the proposed project with the current economical assumption of this thesis. However, considering the ongoing droughts due to decreasing rainfall and drying aquifers, our found LCOW should still be considered, especially in the upcoming future years.

CHAPTER 5

CONCLUSION

In this study, an RO plant was designed to produce 560 m^3/day of potable water that would meet the demand of METU NCC throughout the year. Two different configurations were considered, i.e. double pass and single pass configurations. Within these two configurations, installing an ERD was also considered. The pretreatment, intake and produced water transportation energy requirements were also considered. For all the four cases, a PV plant was sized to fullfil the electrical energy need of the RO plant, pretreatment, intake and water transportation of the system. Finally, an economic analysis was done for the PV-RO system to determine the feasibility of the system.

It was found that with the installation of an ERD, there would be a reduction in the PV plant's size and therefore a reduction in PV plant's CAPEX by 39% and 45%, for double pass configuration and single pass configuration, respectively. As for the SEC of the RO plant with an ERD altogether with pretreatment, intake, and water transportation, it was found to be 3.08 kWh/m^3 and 3.30 kWh/m^3 for single pass and double pass configuration respectively. The PV plant was sized for 407 kW and 442 kW for the single pass and double pass configurations with ERD, respectively. The LCOE of the PV plant was found to be around 0.045 USD/kWh for the four cases.

After the economic analysis on the PV-RO cases, it was found that the single pass configuration had the lowest LCOW at 1.26 USD/m^3 and 1.33 USD/m^3 for ERD operated and ERD absent PV-RO plants respectively. As for the LCOW of the double pass configuration it was found to be 1.46 USD/m^3 and 1.53 USD/m^3 for ERD operated and ERD absent PV-RO plants, respectively. The reason that even the lower SEC ERD operated double pass configuration plant had a higher LCOW is

that the RO plant's CAPEX was high that it overpowered the CAPEX of the bigger PV plant needed for the single pass ERD absent configuration.

This paper investigated the amount of CO_2 emissions avoided by using PV plants, and it was found to range between 5037 and 9252 tons of CO_2 over the life of the PV-RO system, depending on the configuration case.

Different studies' cost estimation methods were taken into account to look into the feasibility of the proposed PV-RO plant in this paper. While all five of the cost estimations were lower than this paper's cost estimation, only three of the five were economically feasible. But the LCOW we found should still be considered due to the increasing water risk in the country.

While this study focuses on METU NCC's weather conditions and seawater composition of Akdeniz, it can also be done for other locations throughout TRNC or the world. To do that, the TMY data and the seawater composition of the suggested location should be considered and optimized accordingly.

For future works, off-grid PV-RO system shall be considered, where an economical comparison between the usage of batteries or water storage should be considered. Moreover, membrane-based pretreatment should be considered to evaluate the effect it has on the economy and performance of the PV-RO plant. Finally, other renewable energy sources should be considered e.g., wind turbines and concentrated solar power.

REFERENCES

[1] G. Elkiran, F. Aslanova, and S. Hiziroglu, “Effluent Water Reuse Possibilities in Northern Cyprus,” *Water*, vol. 11, no. 2, Art. no. 191, Jan. 2019.

[2] H. Gökçekuş, S. Gucel, and U. Türker, “Effects of climate change on North Cyprus forests,” presented at the International Conference of Ecology and Forests For Public Health, Oslo, Norway, 2009.

[3] M. Ergil, “The salination problem of the Guzelyurt aquifer, Cyprus,” *Water Research*, vol. 34, no. 4, pp. 1201–1214, 2000.

[4] H. Gökçekuş, D. Orhon, G. Oğuz, A. Yücel, and S. Sözen, “Integrated water and wastewater management strategy in North Cyprus – basis for an action plan,” *Desalination and Water Treatment*, vol. 177, pp. 384–392, 2020.

[5] Agri-food Canada, “Irrigation and Salinity.” 2000, [Online]. Available: https://www1.agric.gov.ab.ca/$department/deptdocs.nsf/ba3468a2a8681f69872569d60073fde1/42131e74693dcd01872572df00629626/$file/irrsalin.pdf

[6] I. Ozturk, N. Ağıralioğlu, O. Ozdemir, and N. Akinci, “Water Supply from Turkey to Cyprus Island with Suspended Marine Pipeline,” presented at the International Conference on Civil Infrastructure and Construction, Doha, Qatar, February 2-5, 2020.

[7] D. Manolakos, “On site experimental evaluation of a low-temperature solar organic Rankine cycle system for RO desalination,” *Solar Energy*, vol. 83, no. 5, pp. 646–656, 2009.

[8] J. Eke, A. Yusuf, A. Giwa, and A. Sodiq, “The global status of desalination: An assessment of current desalination technologies, plants and capacity,” *Desalination*, vol. 495, Art no. 114633, 2020.

[9] E. Chiavazzo, M. Morciano, F. Viglino, M. Fasano, and P. Asinari, “Passive solar high-yield seawater desalination by modular and low-cost distillation,” *Nature Sustainability*, vol. 1, no. 12, pp. 763–772, 2018.

[10] J. Kucera, *Desalination: Water from Water*, 2nd ed. Beverly, MA: Scrivener Publishing, 2019.

[11] A. Al-Karaghouli and L. L. Kazmerski, “Energy consumption and water production cost of conventional and renewable-energy-powered desalination processes,” *Renewable and Sustainable Energy Reviews*, vol. 24, pp. 343–356, 2013.

[12] D. T. Haynie, *Biological thermodynamics*. Cambridge University Press, 2001.

[13] H. T. El-Dessouky and H. M. Ettouney, *Fundamentals of salt water desalination*. Elsevier Science, 2002.

[14] A. Ruiz-García, N. Melián-Martel, and I. Nuez, “Short review on predicting fouling in RO desalination,” *Membranes*, vol. 7, no. 4, Art. no. 62, 2017.

[15] T. Hasani, S. M. F., A. S. Sowayan, and M. Shakaib, “The effect of spacer orientations on temperature polarization in a direct contact membrane distillation process using 3-d CFD modeling,” *Arabian Journal for Science and Engineering*, vol. 44, no. 12, pp. 10269–10284, 2019.

[16] A. Altaee, “Theoretical study on feed water designs to reverse osmosis pressure vessel,” *Desalination*, vol. 326, pp. 1–9, 2013.

[17] K. P. Lee, T. C. Arnot, and D. Mattia, “A review of reverse osmosis membrane materials for desalination—Development to date and future potential,” *Journal of Membrane Science*, vol. 370, no. 1–2, pp. 1–22, 2011.

[18] L. F. Greenlee, D. F. Lawler, B. D. Freeman, B. Marrot, and P. Moulin, “Reverse osmosis desalination: water sources, technology, and today’s challenges,” *Water research*, vol. 43, no. 9, pp. 2317–2348, 2009.

[19] P. Côté, S. Siverns, and S. Monti, “Comparison of membrane-based solutions for water reclamation and desalination,” *Desalination*, vol. 182, no. 1–3, pp. 251–257, 2005.

[20] Lenntech, “Reverse osmosis stage vs pass.” [Online]. Available: https://www.lenntech.com/processes/reverse-osmosis-stage-vs-pass.htm.

[21] V. S. Freger, H. Shemer, A. A. Sagiv, and R. R. Semiat, “Boron Removal Using Membranes,” in *Boron Separation Processes*, Elsevier Inc., 2015, pp. 199–217. doi: 10.1016/B978-0-444-63454-2.00008-3.

[22] C. P. Koutsou, E. Kritikos, A. J. Karabelas, and M. Kostoglou, “Analysis of temperature effects on the specific energy consumption in reverse osmosis desalination processes,” *Desalination*, vol. 476, Art no. 114213, 2020.

[23] M. F. A. Goosen, S. S. Sablani, and R. Roque-Malherbe, “Membrane fouling: recent strategies and methodologies for its minimization,” in *Handbook of membrane separations: Chemical, pharmaceuticals, food and biotechnological applications*, CRC press, Taylor and Francis, 2008, pp. 325–341.

[24] Lenntech, “Desalination Pretreatment: Seawater chlorination.” https://www.lenntech.com/processes/desalination/pretreatment/pretreatment/seawater-chlorination.htm (accessed Aug. 28, 2021).

[25] J. Kucera, “Reverse osmosis.” Scrivener Pub, 2010. [Online]. Available: https://www.lenntech.com/processes/desalination/pretreatment/pretreatment/seawater-chlorination.htm (accessed Aug. 28, 2021).

[26] N. Voutchkov, *Pretreatment technologies for membrane seawater desalination.* Australian Water Association, 2008.

[27] A. F. Ismail and W. J. Lau, “The effects of structural and electrical properties of hollow fiber nanofiltration membranes on salt and dye removal

under different solution properties," *Jurnal Teknologi*, vol. 49, pp. 103–113, 2008.

[28] X. Sun, C. Wang, Y. Li, W. Wang, and J. Wei, "Treatment of phenolic wastewater by combined UF and NF/RO processes," *Desalination*, vol. 355, pp. 68–74, 2015.

[29] S. A. A. Tabatabai, *Coagulation and ultrafiltration in seawater reverse osmosis pretreatment*. CRC Press, 2014.

[30] E. Cardona, A. Piacentino, and F. Marchese, "Energy saving in two-stage reverse osmosis systems coupled with ultrafiltration processes," *Desalination*, vol. 184, no. 1–3, pp. 125–137, 2005.

[31] J. J. Feria-Díaz, F. Correa-Mahecha, M. C. López-Méndez, J. P. Rodríguez-Miranda, and J. Barrera-Rojas, "Recent Desalination Technologies by Hybridization and Integration with Reverse Osmosis: A Review," *Water*, vol. 13, no. 10, Art no. 1369, 2021.

[32] J. Kim, K. Park, D. R. Yang, and S. Hong, "A comprehensive review of energy consumption of seawater reverse osmosis desalination plants," *Applied Energy*, vol. 254, Art. No. 113652, 2019.

[33] N. M. Mazlan, D. Peshev, and A. G. Livingston, "Energy consumption for desalination—A comparison of forward osmosis with reverse osmosis, and the potential for perfect membranes," *Desalination*, vol. 377, pp. 138–151, 2016.

[34] T. Singh, M. A. Atieh, T. Al-Ansari, A. W. Mohammad, and G. McKay, "The role of nanofluids and renewable energy in the development of sustainable desalination systems: a review," *Water*, vol. 12, no. 7, 2020.

[35] P. M. G. Olabarria, *Constructive Engineering of Large Reverse Osmosis Desalination Plants*. Chemical Publishing Company, 2015.

[36] U. Ezzeghni, M. Mosbah, A. Almabrouk, “Optimization study of Alwaha BWRO desalination plant for minimum water cost prediction,” B.S Thesis, Dept. Of Chemical Engineering, Janzour College of Engineering Technology, Tripoli, Libya 2017.

[37] K. Liang, Q. Ma, H. Lu, H. Fang, P. Yang, and J. Fan, “The research and application progress of the isobaric ERD technique for SWRO desalination plant,” *Desalination and Water Treatment*, vol. 202, pp. 14–26, 2020.

[38] “Minimizing RO energy consumption under variable conditions of operation,” *Desalination*, vol. 157, no. 1–3, pp. 9–21, 2003.

[39] J. Zhou, Y. Wang, Y. Duan, J. Tian, and S. Xu, “Capacity flexibility evaluation of a reciprocating-switcher energy recovery device for SWRO desalination system,” *Desalination*, vol. 416, pp. 45–53, 2017.

[40] B. Ladewig and B. Asquith, *Desalination concentrate management*. Springer Science & Business Media, 2011.

[41] M. F. Keyes Jr Conrad G. and eds. Berrin Tansel, Eds., *Concentrate Management in Desalination: Case Studies*. American Society of Civil Engineers, 2012.

[42] Y. Fernández-Torquemada and J. L. Sánchez-Lizaso, “Effects of salinity on leaf growth and survival of the Mediterranean seagrass Posidonia oceanica (L.) Delile,” *Journal of Experimental Marine Biology and Ecology*, vol. 320, no. 1, pp. 57–63, Jun. 2005, doi: 10.1016/j.jembe.2004.12.019.

[43] N. Delion, G. Mauguin, and P. Corsin, “Importance and impact of post treatments on design and operation of SWRO plants,” *Desalination*, vol. 165, pp. 323–334, 2004, doi: https://doi.org/10.1016/j.desal.2004.06.037.

[44] F. Edition, “Guidelines for drinking-water quality,” *WHO chronicle*, vol. 38, no. 4, pp. 104–108, 2011.

[45] I.R.E.N.A., “Renewable Capacity Statistics 2021,” in *International Renewable Energy Agency (IRENA)*. Abu Dhabi, UAE, 2020.

[46] F. L. Camera, “Renewable Power Generation Costs in 2019,” in *International Renewable Energy Agency (IRENA)*. Abu Dhabi, UAE, 2020.

[47] Power-technologycom, “Pavagada Solar Park, Karnataka.” Aug. 2021. [Online]. Available: https://www.power-technology.com/projects/pavagada-solar-park-karnataka/

[48] P. Hersch, K. Zweibel, “Basic photovoltaic principles and methods,” Golden, Colo: Technical Information Office, Solar Energy Research Institute, 1982.

[49] R. K. Satpathy and V. Pamuru, *Solar PV Power: Design, Manufacturing and Applications from Sand to Systems*. Academic Press, 2020.

[50] ITACA, “Part 1: Photovoltaic (PV) Cells ITACA,” *Itacanet.org*, 2019, [Online]. Available: https://www.itacanet.org/a-guide-to-photovoltaic-panels/photovoltaic-pv-cells/.

[51] T. Pavlovic, *The Sun and Photovoltaic Technologies*. Springer Nature, 2019.

[52] S. Gorjian and A. Shukla, *Photovoltaic Solar Energy Conversion: Technologies, Applications and Environmental Impacts*. Academic Press, 2020.

[53] A. H. El-din, C. F. Gabra, and A. H. Ali, “A comparative analysis between the performances of monocrystalline, polycrystalline and amorphous thin film in different temperatures at different locations in Egypt,” presented at the Africa Photovoltaic Solar Energy Conference, Durban, South Africa, Mar. 2014.

[54] J. Y. Ye, T. Reindl, A. G. Aberle, and T. M. Walsh, “Performance degradation of various PV module technologies in tropical Singapore,” *IEEE Journal of Photovoltaics*, vol. 4, no. 5, pp. 1288–1294, 2014.

[55] D. A. Quansah, M. S. Adaramola, G. Takyi, and I. A. Edwin, “Reliability and degradation of solar PV modules—case study of 19-year-old polycrystalline modules in Ghana,” *Technologies*, vol. 5, no. 2, Art. no. 22, 2017.

[56] S. Ekici and M. A. Kopru, “Investigation of PV system cable losses,” *International Journal of Renewable Energy Research (IJRER*, vol. 7, no. 2, pp. 807–815, 2017.

[57] K. D. Papastergiou, S. Norrga, P. Bakas, and B. Stridth, “Power loss calculations in Large Solar Parks,” presented at the *Distributed Renewable Energy Sources in the Mediterranean-DISTRESS*, Nicosia, Cyprus, 2009.

[58] H. K. Salim, R. A. Stewart, O. Sahin, and M. Dudley, “Drivers, barriers and enablers to end-of-life management of solar photovoltaic and battery energy storage systems: A systematic literature review,” *Journal of cleaner production*, vol. 211, pp. 537–554, 2019.

[59] DuPont, “System Operation RO & NF Systems Shut-down,” *Dupont*, [Online]. Available: https://www.dupont.com/content/dam/dupont/amer/us/en/water-solutions/public/documents/en/45-D01613-en.pdf

[60] EIA, “Total energy production from petroleum and other liquids 2019,” *EIA*, [Online]. Available: https://www.eia.gov/international/rankings/world?pa=288&u=0&f=A&v=none&y=01%2F01%2F2019 (accessed Aug. 28, 2021).

[61] UN, “Desalination through Sustainable Water and Energy Solutions in West Asia,” *Un.org*, 2021, [Online]. Available: https://www.un.org/sites/un2.un.org/files/case_study_7_-_desalination_through_sustainable_water_and_energy_solutions_in_west_asia.pdf.

[62] AWT, “Al Khafji SWRO Desalination Plant Powered by Solar Advanced Water Technology.” Advanced Water Technology, 2021. [Online]. Available: http://awatertech.com/en/projects/al-khafji-swro-powered-by-solar/.

[63] Water Technology, “Al Khafji Solar Saline Water Reverse Osmosis (Solar SWRO) Desalination Plant - Water Technology,” *Water-technology.net*, 2021, [Online]. Available: https://www.water-technology.net/projects/al-khafji-solar-saline-water-reverse-osmosis-solar-swro-desalination-plant/.

[64] TYPSA, “AL KHAFJI DESALINATION PLANT – Grupo TYPSA,” *Typsa.com*, 2021, [Online]. Available: https://www.typsa.com/en/proyectos/al-khafji-desalination-plant/.

[65] A. Alsheghri, “Design and cost analysis of a solar photovoltaic powered reverse osmosis plant for Masdar Institute,” *Energy Procedia*, vol. 75, pp. 319–324, 2015.

[66] M. A. Dawoud, “Environmental impacts of seawater desalination: Arabian Gulf case study,” *International Journal of Environment and Sustainability*, vol. 1, no. 3, 2012.

[67] D. Manolakos, E. S. Mohamed, I. Karagiannis, and G. Papadakis, “Technical and economic comparison between PV-RO system and RO-Solar Rankine system,” *Case study: Thirasia island. Desalination*, vol. 221, no. 1–3, pp. 37–46, 2008.

[68] M. A. Jones, I. Odeh, M. Haddad, A. H. Mohammad, and J. C. Quinn, “Economic analysis of photovoltaic (PV) powered water pumping and desalination without energy storage for agriculture,” *Desalination*, vol. 387, pp. 35–45, 2016.

[69] Our World in Data, “Solar PV module prices vs. cumulative capacity,” *Our World in Data*, 2020, [Online]. Available:

https://ourworldindata.org/grapher/solar-pv-prices-vs-cumulative-capacity?tab=table&time=2010..latest.

[70] E. Gozen and A. Turkman, “Water Scarcity Impacts On Northern Cyprus And Alternative Mitigation Strategies,” 2009, pp. 241–250. doi: 10.1007/978-1-4020-8960-2_17.

[71] S. T. Başaran, H. Gökçekuş, D. Orhon, and S. Sözen, “Autonomous desalination for improving resilience and sustainability of water management in North Cyprus,” *Desalination and Water Treatment*, vol. 177, pp. 283–289, Feb. 2020, doi: 10.5004/dwt.2020.25090.

[72] Y. Kassem, H. Çamur, and S. Alhuoti, “Solar Energy Technology for Northern Cyprus: Assessment, Statistical Analysis, and Feasibility Study,” *Energies*, vol. 13, no. 4, Art. no. 940, 2020.

[73] J. Beták, “Solar resource and photovoltaic electricity potential in EU-MENA region,” 2012, pp. 4623-4626. doi: 10.4229/27thEUPVSEC2012-6CV.3.51.

[74] SeaTemperature, “Water temperature in Guzelyurt in Mediterranean Sea,” seatemperature.net, [Online]. Available: https://seatemperature.net/current/northen-cyprus/guzelyurt-sea-temperature.

[75] S. D. Lin, *Water and wastewater calculations manual*. McGraw-Hill Education, 2014.

[76] T. Khediya, “Quantity of Water Required for Designing a Water,” *International Journal of Engineering Development and Research (IJEDR)*, vol. 4, no. 4, pp. 363-366, 2016.

[77] Lenntech, “Improving the Reverse Osmosis Recovery Rate.” [Online]. Available: https://www.lenntech.com/systems/reverse-osmosis/ro/reverse-osmosis-recovery-rate.htm

[78] M. Wilf and P. Aerts, *The guidebook to membrane technology for wastewater reclamation*. Hopkinton, Massachusetts: Balaban Desalination Publications, 2010.

[79] Hydranautics, “Terms and Equations of Reverse Osmosis.” [Online]. Available: https://membranes.com/docs/trc/termsequ.pdf

[80] DuPont, “System Design: System Performance Projection,” *Dupont.com*, 2021, [Online]. Available: https://www.dupont.com/content/dam/dupont/amer/us/en/water-solutions/public/documents/en/45-D01591-en.pdf.

[81] B. Huang, K. Pu, P. Wu, D. Wu, and J. Leng, “Design, selection and application of energy recovery device in seawater desalination: a review,” *Energies*, vol. 13, no. 6. MDPI AG, Aug. 01, 2020. doi: 10.3390/en13164150.

[82] J. A. Duffie, W. A. Beckman, and Nate. Blair, *Solar engineering of thermal processes, photovoltaics and wind*. John Wiley & Sons, Inc., 2020.

[83] H. Cho, A. Smith, R. Luck, and P. Mago, “Transient Uncertainty Analysis in Solar Thermal System Modeling,” *Journal of Uncertainty Analysis and Applications*, vol. 5, no. 1, 2017.

[84] J. Ehnberg, “Generation Reliability for Isolated Power Systems with Solar, Wind and Hydro Generation Exploring and mitigating the environmental risk of marine renewable energy installations View project Cross-Sectoral Energy Control through Interconnected Microgrids by Multiport Converter View project.” [Online]. Available: https://www.researchgate.net/publication/239558857

[85] ITACA, “Part 1: Solar Astronomy ITACA,” *Itacanet.org*, 2019, [Online]. Available: https://www.itacanet.org/the-Sun-as-a-source-of-energy/part-1-solar-astronomy/.

[86] J. Widén, “System Studies and Simulations of Distributed Photovoltaics in Sweden,” *ResearchGate,* 2019, [Online]. Available: https://www.researchgate.net/publication/271135303_System_Studies_and_Simulations_of_Distributed_Photovoltaics_in_Sweden.

[87] I. Daut, F. Zainuddin, Y. Irwan, and A. Razliana, “Analysis of Solar Irradiance and Solar Energy in Perlis, Northern of Peninsular Malaysia,” *Energy Procedia*, vol. 18, pp. 1421–1427, 2012.

[88] T. A. Olukan and M. Emziane, “A comparative analysis of PV module temperature models,” in *Energy Procedia*, 2014, vol. 62, pp. 694–703. doi: 10.1016/j.egypro.2014.12.433.

[89] F. A. Tiano and G. Rizzo, “A Thermal Model for Photovoltaic Panels Installed on a Vehicle Body,” presented at the International Symposium on Advanced Vehicle Control, Beijing, China, July 16-20, 2018.

[90] IRENA, “Session 2a: Solar power spatial planning techniques,” in IRENA Global Atlas Spatial Planning Techniques Seminar, 2014. [Online]. Available: https://www.irena.org/-/media/Files/IRENA/Agency/Events/2014/Jul/15/9_Solar_power_spatial_planning_techniques_Arusha_Tanzania.pdf?la=en%26hash=F98313D5ADB4702FC910B94586C73AD60FA45FDE

[91] SMA Solar Technology, *Central Inverter Planning of a PV Generator Planning Guidelines.* 2013, [Online]. Available: https://files.sma.de/downloads/DC-PL-en-11.pdf

[92] R. S. Subramanian, “Engineering Bernoulli Equation.” [Online]. Available: https://web2.clarkson.edu/projects/subramanian/ch330/notes/Engineering%20Bernoulli%20Equation.pdf

[93] Fristam, “Pump technology terms.” 2016, [Online]. Available: https://www.fristam.de/wp-content/uploads/2016/03/pump_technology.pdf

[94] J. P. Powers, A. B. Corwin, P. C. Schmall, and W. E. Kaeck, “Appendix A: Friction Losses for Water Flow Through Pipe.” 2007. doi: 10.1002/9780470168103.app1.

[95] L. Szychta, “Energy Consumption of Water Pumping for Selected Control Systems,” Electrical Power Quality and Utilisation, 2006, vol. 12, no. 1, pp 67-73.

[96] A. Collins and G., “Properties of produced waters,” in *Petroleum Engineering Handbook: Dallas, SPE*, H. Bradley and B., Eds. 1987, pp. 24–1–24–23.

[97] Google, “Cyprus.” Accessed: Aug. 28, 2021. [Online]. Available: https://www.google.com/maps/@35.2606139,32.9347782,576m/data=!3m1!1e3

[98] Topographic-mapcom, “Cyprus.” [Online]. Available: https://en-gb.topographic-map.com/maps/d9j/Cyprus/

[99] J. Hernández-Moro and J. M. Martínez-Duart, “Analytical model for solar PV and CSP electricity costs: Present LCOE values and their future evolution,” *Renewable and Sustainable Energy Reviews*, vol. 20. pp. 119–132, 2013. doi: 10.1016/j.rser.2012.11.082.

[100] J. Li, H. Sun, X. Ye, S. Gao, and J. Yang, “Economic evaluation of 20,000 M3/Day seawater desalination coupling with floating reactor nuclear power plant,” in *IOP Conference Series: Earth and Environmental Science*, Aug. 2019, vol. 300, no. 4. doi: 10.1088/1755-1315/300/4/042053.

[101] T. Jenkin, D. Feldman, A. Kwan, and B. J. Walker, “Estimating the Impact of Residual Value for Electricity Generation Plants on Capital Recovery, Levelized Cost of Energy, and Cost to Consumers,” 2019. [Online]. Available: www.nrel.gov/publications.

[102] SolarEvi, “Güneş Paneli PERC Monokristal 395Wp CWT Marka,” *SolarEvi*, [Online]. Available: https://solarevi.com/gunes-paneli/gunes-paneli-perc-monokristal-395-wp-cwt-marka.

[103] SolarEvi, “GOODWE GW25K-DT INVERTÖR,” *SolarEvi*, Aug. 2021. [Online]. Available: https://solarevi.com/inverter/goodwe-25k-dt-trifaze-invertor-25-000w-ac-260v-850v

[104] SolarEvi, “GOODWE GW50K-AC INVERTÖR,” *SolarEvi*, Aug. 2021. [Online]. Available: https://solarevi.com/inverter/goodwe-50k-dt-trifaze-invertor-50-000w-ac-260v-850v

[105] SolarDolap, “Güneş Paneli Montaj Profili,” *SolarDolap*, Aug. 2021. [Online]. Available: https://www.solardolap.com/solar-montaj-malzemeleri/gunes-paneli-montaj-profili/

[106] KuzeyBoru, “HDPE Pipe Price List 2021,” *Kuzey Boru*, [Online]. Available: https://www.kuzeyborugroup.com/Data/EditorFiles/price-list/2021/Hdpe_Pipe_Price_List_2021-2.pdf

[107] AW Pumps, “Pacer Self-Priming Centrifugal Electric Water Pump - SE2HL,” *Absolute Water Pumps*, [Online]. Available: https://www.absolutewaterpumps.com/pacer-self-priming-centrifugal-electric-water-pump-se2hl-d3-0c-3-phase-230-460-volt-2-180-gpm-female-npt

[108] AquaQuote, *private communication*, in Aug. 2021.

[109] ForeverPure, “Pentair CodeLine 80H100-7,” *ForeverPure*, Aug. 2021. [Online]. Available: https://www.foreverpureplace.com/GA90190-27-p/ga90190-27.htm

[110] ForeverPure, “Pentair CodeLine 80S30-6,” *ForeverPure*, Aug. 2021. [Online]. Available: https://www.foreverpureplace.com/GA90126-91-p/ga90126-91.htm

[111] BB Water, “Danfoss 904L Sea Water Pump APP30,” *Big Brand Water*, [Online]. Available: https://www.bigbrandwater.com/danfoss25.html

[112] K. H. Mistry and J. H. Lienhard, “An economics-based second law efficiency,” *Entropy*, vol. 15, no. 7, pp. 2736–2765, 2013.

[113] R. Huehmer *et al.*, “Evaluation and Optimization of Emerging and Existing Energy Recovery Devices for Desalination and Wastewater Membrane Treatment Plants,” WaterReuse Research Foundation, CA, USA. 2013.

[114] G. Blandin, A. R. Verliefde, C. Y. Tang, and P. Le-Clech, “Opportunities to reach economic sustainability in forward osmosis–reverse osmosis hybrids for seawater desalination,” *Desalination*, vol. 363, pp. 26–36, 2015.

[115] S. J. Im, S. Jeong, S. Jeong, and A. Jang, “Techno-economic evaluation of an element-scale forward osmosis-reverse osmosis hybrid process for seawater desalination,” *Desalination*, vol. 476, Art. no. 114240, 2020.

[116] P. Glueckstern and M. Priel, “Comparative cost of UF vs conventional pretreatment for SWRO systems,” *International Desalination and Water Reuse Quarterly*, vol. 13, no. 1, pp. 34–39, 2003.

[117] Alibaba, “Zhongtai chemical manufacturer sodium hydroxide naoh 99% caustic soda pearls/flakes 99%,” *Alibaba*, [Online]. Available: https://www.alibaba.com/product-detail/Naoh-Naoh-Naoh-Zhongtai-Chemical-Manufacturer_1600113670551.html?spm=a2700.galleryofferlist.normal_offer.d_title.6cf6125bfYt3Fj&s=p

[118] Alibaba, “Hydrochloric acid HCl 7647-01-0 factory price,” *Alibaba*, [Online]. Available: https://www.alibaba.com/product-detail/Hydrochloric-acid-HCl-7647-01-0_60439085052.html?spm=a2700.7724857.normal_offer.d_title.464b1e77xLrGhr

[119] S. Alabduljalila, S. Alotaibia, and H. Abdulrahimb, “Techno-economic evaluation of different seawater reverse osmosis configurations for efficient boron removal,” *Desalination and Water Treatment*, vol. 168, pp. 65–76, 2019.

[120] H. Ludwig, “Energy consumption of reverse osmosis seawater desalination-possibilities for its optimisation in design and operation of SWRO plants,” *Desalination and Water Treatment*, vol. 13, no. 1–3, pp. 13–25, 2010.

[121] K. Juhrich, *CO2 Emission Factors for Fossil Fuels*. Federal Environment Agency, 2016.

[122] H. Peter and S. Derek, “Expert consensus on the economics of climate change.” Institute for Policy Integrity, New York University School of Law, 2015.

[123] K.I.B.T.E.K., “Üç Zamanlı Tarife,” *KIBTEK*, Aug. 2021. [Online]. Available: https://www.kibtek.com/uc-zamanli-tarife/

[124] S. Kayaci, S. B. Tantekin-Ersolmaz, M. G. Ahunbay, and W. B. Krantz, “Technical and economic feasibility of the concurrent desalination and boron removal (CDBR) process,” *Desalination*, vol. 486, Art. no. 114474, 2020.

[125] J. Kim, M. Wilf, J. S. Park, and J. Brown, *Boron rejection by reverse osmosis membranes: national reconnaissance and mechanism study-phase 1*. Georgia Institute of Technology, 2006.

[126] A. K. Elfaqih and S. O. Belhaj, “Economic evaluation of SWRO desalination plants using ERD powered by Off-Grid PV system,” in *2021 IEEE 1st International Maghreb Meeting of the Conference on Sciences and Techniques of Automatic Control and Computer Engineering MI-STA*, May 2021, pp. 458–462.

[127] B. Rahimi, H. Shirvani, A. A. Alamolhoda, F. Farhadi, and M. Karimi, “A feasibility study of solar-powered reverse osmosis processes,” *Desalination*, vol. 500, Art. no. 114885, 2021.

[128] AW Pumps, “‘S’ PUMP FLOW CURVES,” *Absolute Water Pumps*, [Online]. Available: https://www.absolutewaterpumps.com/media/blfa_files/Pacer_Pumps_S_Series_Pump_Curves.pdf

APPENDICES

APPENDIX A. PV Data

Table 43: Estimated annual energy generation for 748 kW PV capacity in kWh.

Month	Days	E_{gen} [kWh]
1	31	95663.27211
2	28	98735.62394
3	31	122200.1135
4	30	133425.3073
5	31	150978.2924
6	30	153119.6142
7	31	155677.7538
8	31	142450.2092
9	30	132253.4372
10	31	108306.6688
11	30	94094.27046
12	31	91351.67568

APPENDIX B. Specifications

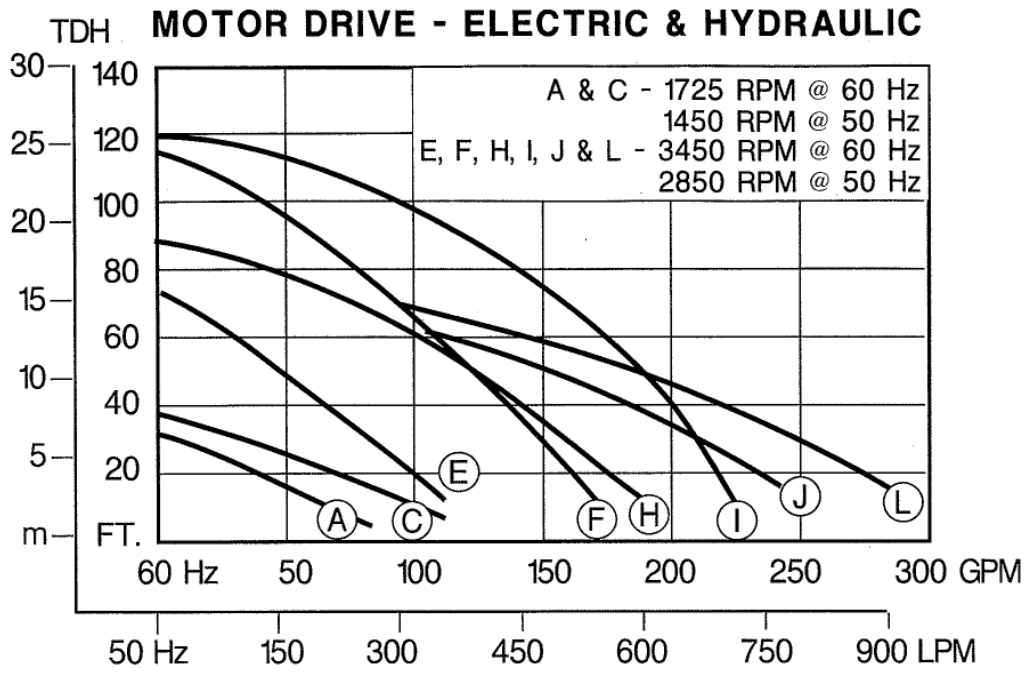

Figure 48. The pump curve of the PACER SE2HL electric pump, where H is the appropriate pump curve [126].

Model Tipi	CWT375 72PM	CWT380 72PM	CWT385 72PM	CWT390 72PM	CWT395 72PM	CWT400 72PM
Maksimum Güç (P_{max})	375 Wp	380 Wp	385 Wp	390 Wp	395 Wp	400 Wp
Modül Verimliliği	18,79	19,04	19,29	19,54	19,78	20,06
Maksimum Güç Gerilimi (V_{mp})	40,14	40,52	40,70	40,88	41,07	41,10
Maksimum Güç Akımı (I_{mp})	9,35	9,39	9,47	9,55	9,62	9,75
Açık Devre Gerilimi (V_{oc})	48,67	48,91	49,12	49,32	49,54	49,83
Kısa Devre Akımı (I_{sc})	9,94	9,97	10,05	10,13	10,24	10,38
Güç Toleransı	0~+5W					
Maks. Sistem Anma Gerilimi	1000V DC / 1500V DC					
Çalışma Sıcaklık Aralığı	-40 ~ +85°C					
Güvenlik	C Sınıfı					
Maks. Seri Sigorta Akımı	15A / 20A					

MEKANİK ÖZELLİKLER

Hücre Boyutu	158,75 mm x 158,75 mm
Hücre Sayısı	72 (6X12)
Ağırlık	22
Panel Boyutu	1984x1007x40mm
Maks. Rüzgar/Kar Yükü Dayanımı	2400/5400 Pa
Bağlantı Kutusu	IP67

SICAKLIK KATSAYISI

Sıcaklık Katsayısı (I_{sc})	0.040%/°C
Sıcaklık Katsayısı (V_{oc})	-0.27%/°C
Sıcaklık Katsayısı (P_{max})	-0.36%/°C

AMBALAJ ŞEKLİ

Konteyner	20' GP	40' GP
Palet Başına Adet	27	27
Konteyner Başına Adet	270	696

FİZİKSEL ÖZELLİKLER

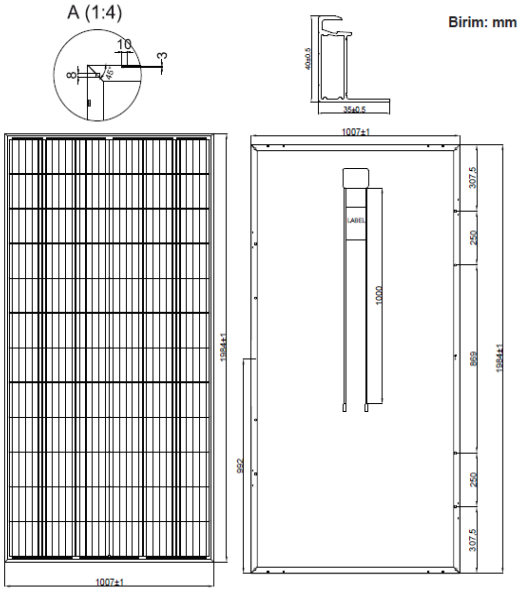

ELEKTRİKSEL ÖZELLİKLER

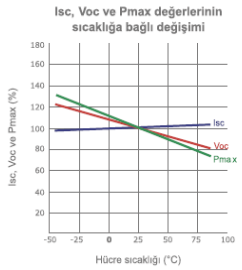

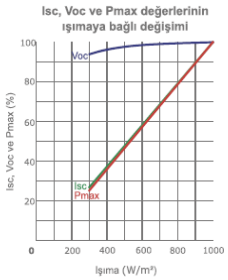

*Not: Elde edilen verilerin; Standart Test Koşulları: 1000 W/m² güneş ışınımı, (AM 1.5) ve hücre sıcaklığı 25°C. Nominal Test Koşulları: 800 W/m² güneş ışınımı, ortam sıcaklığı 20°C, rüzgar hızı 1m/s. Tüm paneller için ölçüm belirsizliği %3'dür. Gerçek veriler yapılan sözleşmelere tabi olacaktır. Bu parametreler sadece referans amaçlıdır ve bu sözleşmelerin bir parçası değildir. Teknik özellikler, önceden haber verilmeksizin değiştirilebilir.

Figure 49. The CWT395-72PM data sheet.

FilmTec™ Element	Active Area (ft^2)	Active Area (m^2)	Feed Spacer Thickness (mil)	Permeate Flowrate (gpd)	Permeate Flowrate (m^3/d)	Stabilized Boron Rejection (%)	Stabilized Salt Rejection (%)
SW30HRLE-440i	440	41	28	8,000	30.2	92	99.80

FilmTec™ Element	Active Area (ft^2)	Active Area (m^2)	Feed Spacer Thickness (mil)	Permeate Flowrate (gpd)	Permeate Flowrate (m^3/d)	Stabilized Boron Rejection (%)	Stabilized Salt Rejection (%)
Seamaxx™-440i	440	41	28	17,000	64.4	89	99.70

1. The above values are normalized from the 600-psi specification standard test to the following conditions: 32,000 ppm NaCl, 800 psi (5.5 MPa), 77°F (25°C), pH 8, 8% recovery. Due to the very high permeability of FilmTec™ Seamaxx™-440i Elements, they are not tested at the typical feed pressure for standard test conditions of 800 psi, but at a lower feed pressure of 600 psi. This allows to standard test the element within its operating guidelines.
2. Permeate flows for individual elements may vary ± 15%.
3. Minimum Salt Rejection is 99.58%.
4. Specific boron stabilized rejection based on the following normalization conditions: 32,000 ppm NaCl, 5 ppm boron, 800 psi (5.5 MPa), 77°F (25°C), pH 8, 8% recovery.

Element Dimensions

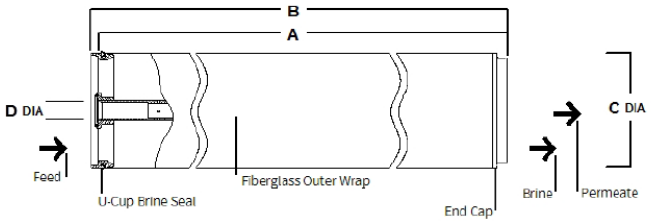

Dimensions – inches (mm)								1 inch = 25.4 mm
	A		B		C		D	
FilmTec™ Element	(in)	(mm)	(in)	(mm)	(in)	(mm)	(in)	(mm)
Seamaxx™-440i	40.0	1,016	40.5	1,029	7.9	201	1.125 ID	29 ID

Figure 50. The data sheet of both SW30HRLE-440i™ and Seamaxx-440i™.

APPENDIX C. Raw Water Ion Composition

Table 44. The ionic composition of the raw water with TDS and pH before being treated.

Ion	mg/l
K^{+}	450.9
Na^{+}	12505
Mg^{+}	1455
Ca^{+2}	450.9
Sr^{+2}	9.32
HCO_3^{-}	136
Cl^{-}	22055
Br^{-1}	155
SO_4^{-2}	3399
SiO_2	1.14
Boron	4.48
CO_2	155.5
TDS	40667
pH	8.2

APPENDIX D. PV-RO CAPEX and OPEX

Table 45. The detailed CAPEX of the double pass configuration with ERD

	%	TL	USD	Amount	Total USD
		PV plant w/ ERD			
PV panels	81.91	1764.36	207.72	1118.00	232230.96
inverter 25k	0.00	21941.60	4279.15	0.00	0.00
inverter 50k	6.38	36330.00	2584.40	7.00	18090.80
Mounts	11.70	120.00	14.13	2347.80	33183.81
Total	***100.00***				***283505.57***
		Water transport			
HDPE 140	0.00	45.74	5.39	0.00	0.00
HDPE 125	0.60	36.02	4.24	545.00	190.92
HDPE 110	65.35	28.35	3.34	6200.00	20708.00
Intake Pump	5.24		830.00	2.00	1660.00
To campus pump	28.81		830.00	11.00	9130.00
Total	***100.00***				***31688.92***
		RO plant			
SW30HRLE-440i	0.58		649.00	21.00	13629.00
Seamaxx-440i	1.60		677.00	56.00	37912.00
XLE-440i	0.15		600.00	6.00	3600.00
SW pressure vessel	0.93		2000.00	11.00	22000.00
BW pressure vessel	0.04		1000.00	1.00	1000.00
HPP	2.41		57000.00	1.00	57000.00
HPP motor	0.51		12000.00	1.00	12000.00
Booster pump	0.72		17000.00	1.00	17000.00
Booster pump motor	0.17		4000.00	1.00	4000.00
ERD	2.15		51000.00	1.00	51000.00
Piping	14.36		340000.00	1.00	340000.00
Equipment and materials	25.76		610000.00	1.00	610000.00
Construction	18.16		430000.00	1.00	430000.00
Installation	8.02		190000.00	1.00	190000.00
Design	6.33		150000.00	1.00	150000.00
Legal	1.06		25000.00	1.00	25000.00
Pretreatment	16.89		400000.00	1.00	400000.00
Posttreatment	0.17		4060.00	1.00	4060.00
Total	***100.00***				***2368201.00***

Table 46. The detailed CAPEX of the double pass configuration without ERD.

	%	TL	USD	Amount	Total USD
		PV plant w/o ERD			
PV panels	81.31	1764.36	207.72	1809.00	375765.48
inverter 25k	0.93	21941.60	4279.15	1.00	4279.15
inverter 50k	6.15	36330.00	2584.40	11.00	28428.40
Mounts	11.62	120.00	14.13	3798.90	53693.65
Total	***100.00***				***462166.68***
		Water transport			
HDPE 140	0.00	45.74	5.39	0.00	0.00
HDPE 125	0.60	36.02	4.24	545.00	190.92
HDPE 110	65.35	28.35	3.34	6200.00	20708.00
Intake Pump*	5.24		830.00	2.00	1660.00
To campus pump	28.81		830.00	11.00	9130.00
Total	***100.00***				***31688.92***
		RO plant			
SW30HRLE-440i	0.63		695.00	21.00	14595.00
Seamaxx-440i	1.86		772.00	56.00	43232.00
XLE-440i	0.15		600.00	6.00	3600.00
SW pressure vessel	0.95		2000.00	11.00	22000.00
BW pressure vessel	0.04		1000.00	1.00	1000.00
HPP	2.45		57000.00	1.00	57000.00
HPP motor	0.52		12000.00	1.00	12000.00
Booster pump	0.73		17000.00	1.00	17000.00
Booster pump motor	0.17		4000.00	1.00	4000.00
ERD	0.00		51000	0	0.00
Piping	14.63		340000.00	1.00	340000.00
Equipment and materials	26.25		610000.00	1.00	610000.00
Construction	18.51		430000.00	1.00	430000.00
Installation	8.18		190000.00	1.00	190000.00
Design	6.46		150000.00	1.00	150000.00
Legal	1.08		25000.00	1.00	25000.00
Pretreatment	17.22		400000.00	1.00	400000.00
Posttreatment	0.17		4060.00	1.00	4060.00
Total	***100.00***				***2323487.00***

Table 47. The detailed OPEX of the double pass configuration with ERD

	%	TL USD	Amount	Total USD
		Chemicals		
NaOH	6.70	0.27	4963.85	1340.24
HCl	38.30	0.40	19162.03	7664.81
pretreatment chemicals	45.49	0.02	455155.00	9103.10
RO cleaning chemicals	9.51	3.40	560.00	1904.00
Total cost	***100.00***			***20012.15***
		Replacement and Maintenance		
Granular media replacement	1.00	0.60	560.00	336.00
Cartridge filters	5.97	3.60	560.00	2016.00
SW30HRLE-440i replacement	5.65	90.86	21.00	1908.06
Seamaxx-440i replacement	15.72	94.78	56.00	5307.68
XLE-440i replacement	1.49	84.00	6.00	504.00
Maintenance	70.16	2368201.00	0.01	23682.01
Total cost	***100.00***			***33753.75***

Table 48. The detailed OPEX of the double pass configuration without ERD

	%	TL USD	Amount	Total USD
		Chemicals		
NaOH	6.70	0.27	4963.85	1340.24
HCl	38.30	0.40	19162.03	7664.81
pretreatment chemicals	45.49	0.02	455155.00	9103.10
RO cleaning chemicals	9.51	3.40	560.00	1904.00
Total cost	***100.00***			***20012.15***
		Replacements		
Granular media replacement	0.98	0.60	560.00	336.00
Cartridge filters	5.90	3.60	560.00	2016.00
SW30HRLE-440i replacement	5.98	97.30	21.00	2043.30
Seamaxx-440i replacement	17.70	108.08	56.00	6052.48
XLE-440i replacement	1.47	84.00	6.00	504.00
Maintenance	67.96	2323487.00	0.01	23234.87
Total cost	***100.00***			***34186.65***

Table 49. The detailed CAPEX of the single pass configuration with ERD

	%	TL	USD	Amount	Total USD
		PV plant w/ ERD			
PV panels	80.95	1764.36	207.72	1031.00	214159.32
inverter 25k	1.62	21941.60	4279.15	1.00	4279.15
inverter 50k	5.86	36330.00	2584.40	6.00	15506.40
Mounts	11.57	120.00	14.13	2165.10	30601.52
Total	***100.00***				***264546.39***
		Water transport			
HDPE 140	0.76	45.74	5.39	545.00	242.44
HDPE 125	0.00	36.02	4.24	0.00	0.00
HDPE 110	65.24	28.35	3.34	6200.00	20708.00
Intake Pump*	5.23		830.00	2.00	1660.00
To campus pump	28.76		830.00	11.00	9130.00
Total	***100.00***				***31740.44***
		RO plant			
SW30HRLE-440i	2.65		695.00	77.00	53515.00
Seamaxx-440i	0.00		772.00	0.00	0.00
XLE-440i	0.00		600.00	0.00	0.00
SW pressure vessel	1.09		2000.00	11.00	22000.00
BW pressure vessel	0.00		1000.00	0.00	0.00
HPP	2.82		57000.00	1.00	57000.00
HPP motor	0.59		12000.00	1.00	12000.00
Booster pump	0.84		17000.00	1.00	17000.00
Booster pump motor	0.20		4000.00	1.00	4000.00
ERD	2.53		51000.00	1.00	51000.00
Piping	13.47		272000.00	1.00	272000.00
Equipment and materials	24.26		490000.00	1.00	490000.00
Construction	17.08		345000.00	1.00	345000.00
Installation	7.53		152000.00	1.00	152000.00
Design	5.94		120000.00	1.00	120000.00
Legal	0.99		20000.00	1.00	20000.00
Pretreatment	19.81		400000.00	1.00	400000.00
Posttreatment	0.20		4060.00	1.00	4060.00
Total	***100.00***				***2019575.00***

Table 50. The detailed CAPEX of the single pass configuration without ERD

	%	TL	USD	Amount	Total USD
		PV plant w/o ERD			
PV panels	81.85	1764.36	207.72	1894.00	393421.68
inverter 25k	0.00	21941.60	4279.15	0.00	0.00
inverter 50k	6.45	36330.00	2584.40	12.00	31012.80
Mounts	11.70	120.00	14.13	3977.40	56216.57
Total	***100.00***				***480651.05***
		Water transport			
HDPE 140	0.76	45.74	5.39	545.00	242.44
HDPE 125	0.00	36.02	4.24	0.00	0.00
HDPE 110	65.24	28.35	3.34	6200.00	20708.00
Intake Pump*	5.23		830.00	2.00	1660.00
To campus pump	28.76		830.00	11.00	9130.00
Total	***100.00***				***31740.44***
		RO plant			
SW30HRLE-440i	2.72		695.00	77.00	53515.00
Seamaxx-440i	0.00		772.00	0.00	0.00
XLE-440i	0.00		600.00	0.00	0.00
SW pressure vessel	1.12		2000.00	11.00	22000.00
BW pressure vessel	0.00		1000.00	0.00	0.00
HPP	2.90		57000.00	1.00	57000.00
HPP motor	0.61		12000.00	1.00	12000.00
Booster pump	0.86		17000.00	1.00	17000.00
Booster pump motor	0.20		4000.00	1.00	4000.00
ERD	0.00		0.00	1.00	0.00
Piping	13.82		272000.00	1.00	272000.00
Equipment and materials	24.89		490000.00	1.00	490000.00
Construction	17.53		345000.00	1.00	345000.00
Installation	7.72		152000.00	1.00	152000.00
Design	6.10		120000.00	1.00	120000.00
Legal	1.02		20000.00	1.00	20000.00
Pretreatment	20.32		400000.00	1.00	400000.00
Posttreatment	0.21		4060.00	1.00	4060.00
Total	***100.00***				***1968575.00***

Table 51. The detailed OPEX of the single pass configuration with ERD

	%	TL USD	Amount	Total USD
		Chemicals		
NaOH	29.45	0.27	18713.51	5052.65
HCl	0.00	0.40	0.00	0.00
pretreatment chemicals	59.45	0.02	509905.00	10198.10
RO cleaning chemicals	11.10	3.40	559.90	1903.66
Total cost	***100.00***			***17154.41***
		Replacement and Maintenance		
Granular media replacement	1.12	0.60	559.90	335.94
Cartridge filters	6.71	3.60	559.90	2015.64
SW30HRLE-440i replacement	24.94	97.30	77.00	7492.10
Seamaxx-440i replacement	0.00	108.08	0.00	0.00
XLE-440i replacement	0.00	84.00	0.00	0.00
Maintenance	67.23	2019575.00	0.01	20195.75
Total cost	***100.00***			***30039.43***

Table 52. The detailed OPEX of the single pass configuration without ERD

	%	TL USD	Amount	Total USD
		Chemicals		
NaOH	29.45	0.27	18713.51	5052.65
HCl	0.00	0.40	0.00	0.00
pretreatment chemicals	59.45	0.02	509905.00	10198.10
RO cleaning chemicals	11.10	3.40	559.90	1903.66
Total cost	***100.00***			***17154.41***
		Replacements		
Granular media replacement	1.14	0.60	559.90	335.94
Cartridge filters	6.83	3.60	559.90	2015.64
SW30HRLE-440i replacement	25.37	97.30	77.00	7492.10
Seamaxx-440i replacement	0.00	108.08	0.00	0.00
XLE-440i replacement	0.00	84.00	0.00	0.00
Maintenance	66.66	1968575.00	0.01	19685.75
Total cost	***100.00***			***29529.43***

APPENDIX E. WAVE Software

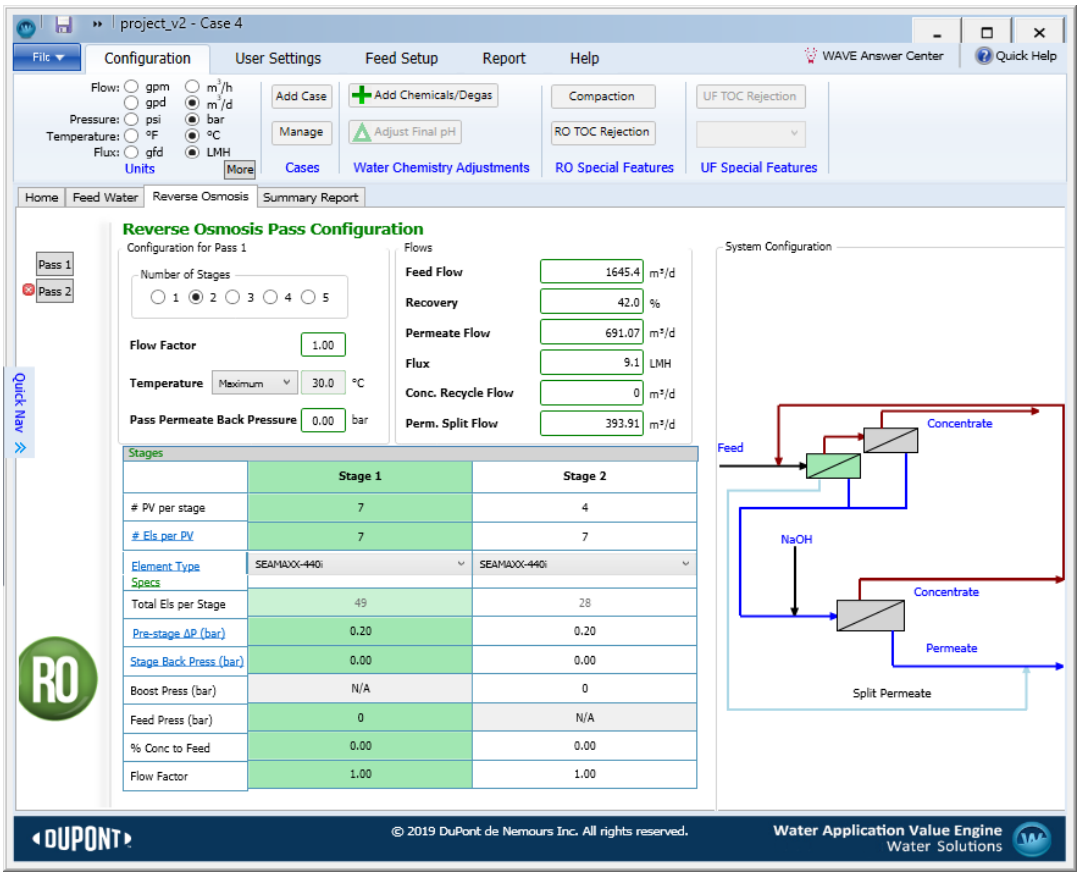

Figure 51. WAVE RO interface

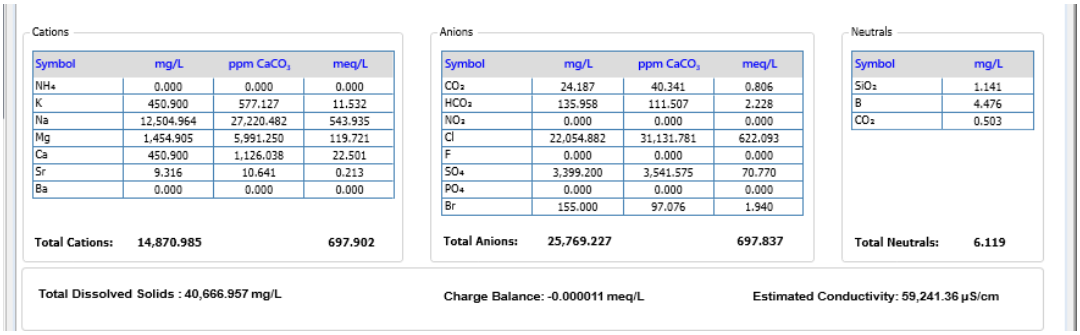

Figure 52. WAVE feedwater ion composition